Vulnerabilities of the three-leg moored TetraSpar floating offshore wind turbine

Are the risks of the TetraSpar mooring system ALARP?

Master Thesis

M.A. Huting

Delft University of Technology

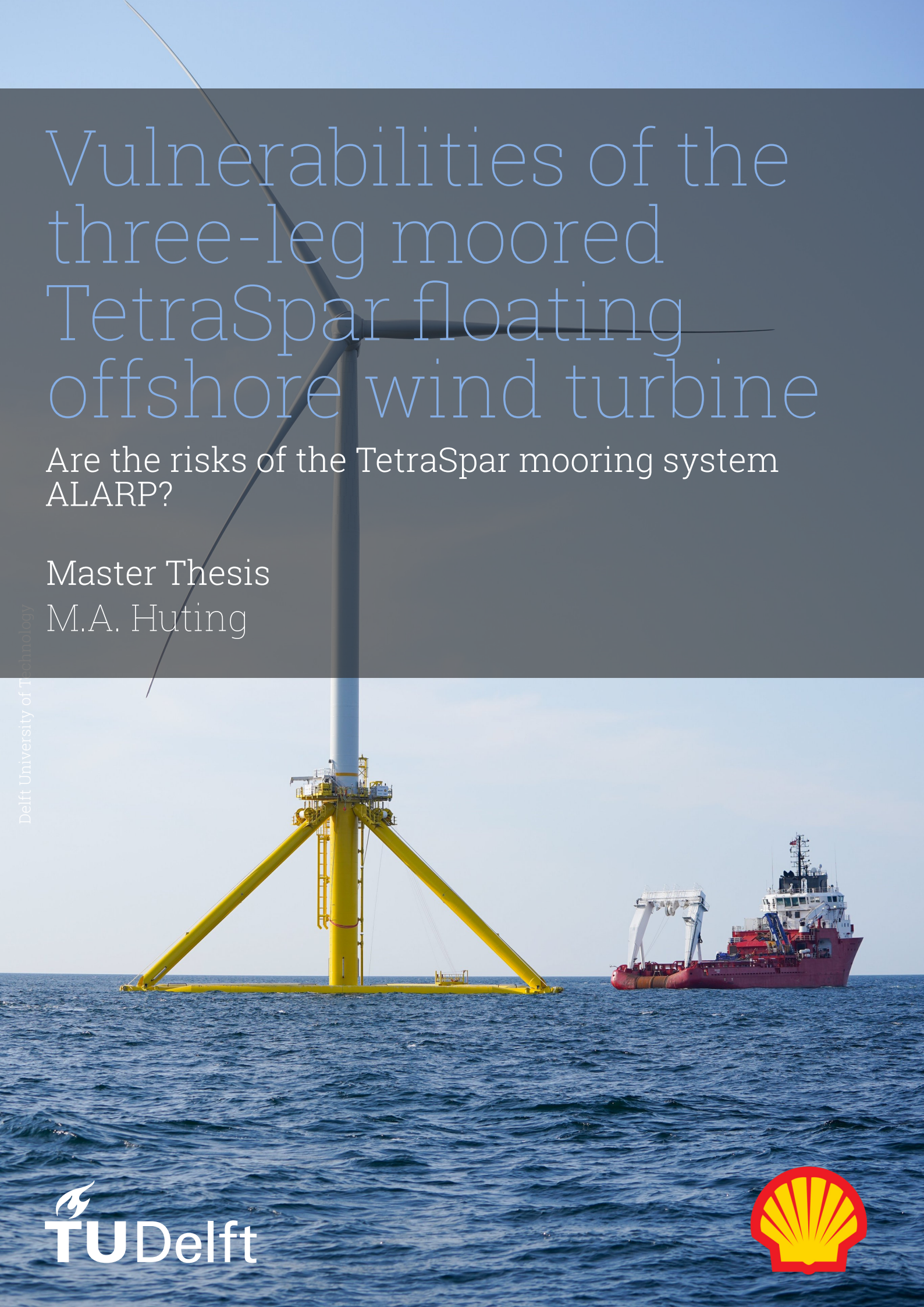

TU Delft

Vulnerabilities of the three-leg moored TetraSpar floating offshore wind turbine

Are the risks of the TetraSpar mooring system ALARP?

by

M.A. Huting

Student Name	Student Number
Max Huting	4463897

Chair graduation committee TU Delft:	ir. A. van der Stap
Supervisor Shell:	dr.ir. J. van Kessel
Supervisor TU Delft:	ir. F. Lange
Independent corrector TU Delft:	dr.ir. R. Lanzafame
Project Duration:	11, 2022 - 08, 2023
Faculty:	Mechanical, Maritime and Materials Engineering, Delft

TU Delft

Abstract

The increasing demand for renewable energy sources has brought about the need for innovative solutions to harness energy from the wind. One such solution is floating offshore wind turbines (FOWT), which offer several advantages over traditional onshore wind turbines and bottom-fixed offshore wind turbines. FOWTs present a challenge concerning overall cost, using fewer mooring lines than seen previously in the offshore industry. Statistically, these mooring line failures are expected to occur annually in large turbine fields and could result in untethered turbines causing extensive financial and reputational damage. It is, therefore, critical to understand whether a single mooring line failure could endanger the entire system, creating a risk that must be reduced to a level that is as low as reasonably practicable (ALARP). The Tetraspar demo FOWT off the coast of Norway is used as a model to investigate the influence of mooring line failure on the mooring system. This thesis investigates the potential risks associated with the three-leg mooring system of a FOWT following mooring line failure. The research employs a simulation-based methodology coupled with insights from previous studies and a fault tree analysis (FTA) to estimate the increase in failure probability of a complete mooring system in case of a single mooring line failure relative to an intact system. Specific assumptions underpin this investigation, including a six-month repair time bridging winter weather till the repair campaign and categorising two mooring line failures in a three-leg mooring system as a complete system failure. This thesis's research is divided into two categories: new failure modes specific to Tetraspar and altered failure modes, which are fatigue-related modes already included in the FTA, adopted from previous studies. Findings highlight the risk of Tetraspar capsizing after a mooring line failure and potential issues with slack line events and fibre sections of the mooring line touching the seafloor. Low-frequency second-order drift significantly increases fatigue in the mooring lines and fairleads, evidenced by an over 1200% fatigue increase in some instances. A FTA consolidates these findings, showing a total failure probability increase in broken line state of between 32% to 137% based on the assumptions made. The study reveals a notable increase in fatigue following a mooring line failure. However, this state will persist for only six months within the turbine's 20-year lifespan, accounting for 1/40th of its design life. With the implementation of a robust safety factor, these fatigue issues can be effectively mitigated. It is advocated that 'design for failure' is incorporated into a three-leg mooring system design to ensure the risks associated with TetraSpar are ALARP. Five recommendations are suggested for the design phase to ensure the TetraSpar and FOWTs achieve ALARP risk levels considering potential mooring line failure, offering solutions that do not necessitate on-site visits, and ideally creating a system that can endure for six months without intervention, allowing for repairs during the summer campaign for more cost-effective and safer operations.

Contents

List of Figures

List of Tables

Nomenclature

Abbreviations

Abbreviation	Definition
ALARP	As Low As Reasonably Practicable
ALS	Accidental Limit State
API	American Petroleum Institute
CoG	Center of Gravity
DEA	Drag Embedment Anchor
deg	Degree
DLC	Design Load Case
DNV	Det Norske Veritas
FEA	Finite Element Analysis
FLS	Fatigue Limit State
FOW	Floating Offshore Wind
FOWT	Floating Offshore Wind Turbine
FPU	Floating Production Unit
FTA	Fault Tree Analysis
GW	Giga Watt
IEC	International Electrotechnical Commission
JIP	Joint Industry Project
JONSWAP	Joint North Sea Wave Project
kN	kilo Newton
MBL	Minimum Breaking Load
ML	Mooring Line
MPa	Megapascal
MW	Mega Watt
MWL	Mean Water Level
NPD	Norwegian Petroleum Directorate
NREL	National Renewable Energy Laboratory
OC3	Offshore Code Comparison Collaboration
OC4	Offshore Code Comparison Collaboration Continuation
OPB	Out of Plane Bending
OTC	Offshore Technology Conference
QTF	Quadratic Transfer Function
RBS	Reference Breaking Strength
RNA	Rotor Nacelle Assembly
ROV	Remote Operated Vehicle
RP	Return Period
SCV	Scatter Case Value
UHC	Ultimate Holding Capacity
ULS	Ultimate Limit State

1 Introduction

The increasing demand for renewable energy sources has brought about the need for innovative solutions to harness energy from the wind. One such solution is floating offshore wind turbines, which offer several advantages over traditional onshore wind turbines and bottom-fixed offshore wind turbines.

Firstly, floating offshore wind turbines can be placed in deeper waters and thus further offshore, where wind speeds are generally higher and more consistent. Higher and more consistent wind allows for generating more electricity and obtaining higher efficiency, as rough terrain and other obstructions found on land do not hinder it. Deeper water will also open up renewable energy sources to countries surrounded by deeper waters where conventional offshore wind is not an option.

Secondly, offshore floating wind turbines do not require the construction of foundations on the seabed, which can be an environmentally damaging process. 70% of bottom-fixed wind turbines are installed using driven monopiles, emitting high dB levels damaging wildlife.[29] The German federal government specified the maximum sound exposure level allowed to 160 dB, which current installation methods easily surpass.[43] With this growing issue, other regulatory bodies are soon to follow. Floating offshore wind turbines can be anchored to the seabed using less environmental-taxing methods, like drag anchors and suction piles. Different installation methods make floating offshore wind a more environmentally flexible offshore energy generation option than bottom-fixed offshore wind.

Finally, offshore floating wind turbines can help reduce the visual impact of wind energy on the landscape, as floating offshore wind turbines can be located further offshore. Turbines further offshore make them a more acceptable option for communities that may oppose traditional onshore wind farms and offshore wind farms near shore.

Det Norske Veritas (DNV), a prominent classification society, predicts that by 2050, floating offshore wind will generate 264 GW or 15% of all offshore wind energy. To put this into context, this is equivalent to the development of more than 3,000 times the size of Hywind Tampen, the world's largest floating offshore wind farm currently under construction in Norway, or 15,000 individual turbines of 17.5 MW.[9]

One of the main challenges facing the evolving floating offshore wind industry is the higher cost of energy production, which has necessitated a focus on cost efficiency in response to market pressures. The expenditure on mooring lines and anchoring now represents a more significant proportion of installed costs for floating offshore wind turbines, around 20-30%, compared to 2-3% previously associated with floating oil structures.[22] Furthermore, environmental impact due to mooring loss is typically lower for floating offshore wind compared to floating production units, and since the wind platforms are primarily unmanned, the safety factor is reduced. Consequently, the reduced redundancy commonly found in floating oil and gas becomes less probable for FOW, leading to lower safety margins and possibly more mooring line failures.

Historically, mooring line failures have occurred more frequently than desired, with an annual rate of single line failure of 2.2E–3 per mooring line per year.[11] For a field of 151 turbines; statistically, at least one mooring line would fail every year. If floating wind develops as DNV predicts, floating wind farms will emerge worldwide, grouped in farms with more than 100 floating wind turbines in

proximity. Whether a mooring line failure will result in a complete system failure is still uncertain, but it poses a significant danger to FOW field safety. Unlike in the oil and gas industry, where immediate repairs are often necessary, a damaged mooring line in a FOW field, comprising hundreds of mooring lines, is favoured for repair until the summer repair campaign. This approach is favoured due to a FOW field's higher expected failure rate and the relatively lower financial and environmental consequences associated with FOWT mooring line failure compared to floating oil and gas production units. However, a rogue floating wind turbine, cut loose from its mooring system, is bound to wreak havoc in its own floating wind farm and surroundings. The financial loss will be significant, and the reputation of floating wind will be set back in the eye of the public. Understanding whether a mooring line failure results in complete system failure is crucial when such failures seem inevitable in the future.

1.1. TetraSpar

The introduction poses the relevance of FOWT, and the questions left unanswered. This thesis will focus on data and specific characteristics of the TetraSpar demo. However, problems on the TetraSpar FOWT could carry over to other FOWTs. The TetraSpar is introduced where after in chapter 2 the TetraSpar is described in more detail.

The TetraSpar is a spar-type floating platform which supports a 3.6 MW wind turbine. The foundation consists of a floating platform moored to the seabed with a catenary mooring system using Dyneema, chain and clump weight sections at 205-meter water depth, anchored using drag embedment anchors (DEA). The floating platform comprises a floater and a keel structure, suspended below the floater by suspension lines. The keel acts as the counterweight for the turbine, making this arrangement a spar. The arrangement is shown in Figure 2.4. The demonstrator is installed at the Marine Energy Test Centre in the North Sea off the island of Karmøy on the western coast of Norway. The model has been in place since the end of 2021 and aims to collect data and knowledge on a new floating offshore wind concept and floating wind in general.

1.2. Problem identification

FOWTs represent a new technology in the renewable energy sector. While initial models have been launched without severe accidents, this technology's infancy presents potential teething problems, with various concepts currently in the testing phase. Historically, mooring systems have been troubled with reliability issues, making mooring line failures a concerning prospect for the future of FOWTs. This research aims to identify potential problems, particularly focusing on mooring line failures. The cost of FOWTs remains high compared to onshore wind, piled offshore wind, and other renewable energies, increasing the stakes for this technology.[11] The critical question this research addresses is: What could cause a mooring line to break in a three-leg moored FOWT, and what would be the consequences of such a failure?

A bowtie analysis is used to visualise the problem. A 'bowtie analysis' is a visual tool used to identify and assess potential hazards and the measures in place to mitigate those hazards. A bowtie analysis consists of four main components:

1. The top event represents the undesirable event or hazard that the bowtie analysis is designed to prevent.
2. The threat(s) are the factors that can lead to the top event occurring.
3. The barrier(s) or mitigation(s) are the measures in place to prevent the threat(s) or mitigate the consequence(s). They can be physical, procedural, or organisational.
4. The consequence(s) are the potential consequences of the top event, including immediate and long-term effects.

The barriers and mitigation are not considered in figure 1.1 as this phase is about identifying problems and not solving the found problems. Threats and consequences have been categorised into brackets. These brackets are dissected further in the coming sections to identify the knowledge gap and most impactful research topics. Figure 1.1 shows a difference in scope between threats and consequences. While threats focus on the possible ways a mooring line could fail, the consequences focus on what the impact is when this mooring line has been broken or separated.

1.2.1. Threats

Fatigue

Fatigue accumulates damage in material over time due to fluctuating stresses and strains, and offshore floating structures are constantly moving, which will inevitably cause fatigue. Failure in a component often transpires after it has endured a specific number of load fluctuations, leading to cumulative damage that reaches a critical threshold. The number of cycles quantifies this process to failure, denoted as N_k, which serves as a measure for the lifetime of a structure. These cycles can be either directly measured or estimated based on the observed movements of the structure, thereby providing insights into its overall durability and integrity. When N cycles have occurred, the accumulated damage can be

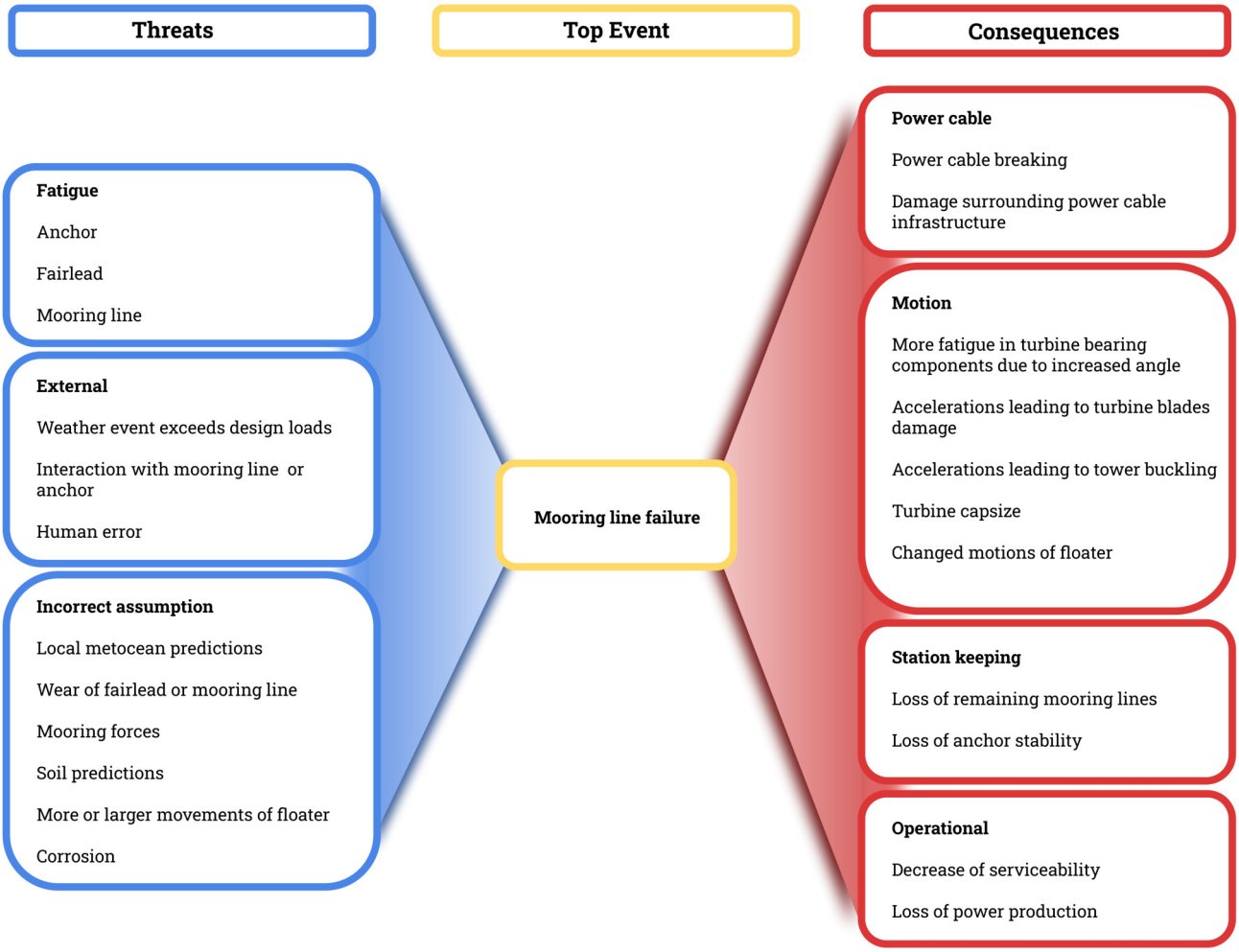

Figure 1.1: Bowtie model of mooring line failure top event

evaluated. Fatigue can occur and make parts fail with stresses lower than the tensile strength of the material used, sometimes causing unexpected failures. Possible failure points for the TetraSpar mooring system are the fairlead, the connection point between the offshore structure and the mooring line, which sees high loads and much movement, and the mooring line itself. It is hard to say where fatigue failure will occur. Further research would be necessary to determine this, but more information on historical failures will follow in the literature study.[4]

External

Accidents, though undesirable, must be anticipated and factored into calculations, as they cannot always be prevented. In the design process, considerations are made for 50-Year and 1000-Year conditions in the Ultimate Limit State (ULS) and Accidental Limit State (ALS) calculations, respectively. While estimations are carried out to forecast potential accidents stemming from weather conditions, it must be noted that severe weather events could inflict damage beyond these predictions during a 'perfect storm' with a return period not accounted for.

Next to weather conditions, humans always play a vital role in failing of well-designed systems. "The International Maritime Organization and the U.S. Coast Guard have independently estimated that human error is the direct cause of 80% of ship accidents and incidents. Chadwell et al. (1999) investigated the role of human error in petroleum system incidents. They found that in 47% of these incidents, human error was judged to be a causal or contributory factor."[42] Although FOWTs are generally unmanned, humans can cause damage by not following maintenance protocols, damaging the

mooring line or anchor, and improper installation.

Incorrect assumption
In the pursuit of profitability within an offshore project, efficiency in both planning and execution is vital. While every aspect should be examined, generalising issues can accelerate the process, saving time and money. For instance, hindcast models that build environmental conditions and generalise to wind and wave spectra can be adjusted with varying degrees of conservatism, influencing simulations and subsequent design modifications.

Soil properties, assessed through scanning and sampling, cannot be analysed down to every grain, resulting in unknown anomalies that might lead to unexpected anchor movements. Such changes in anchor position or depth may cause the anchoring forces to stray from the intended design.

Furthermore, incorrect assumptions made in the early stages of prospecting or design could lead to a cascade of increased motions and forces in the floater once the project is operational. These intricate interactions highlight the importance of careful consideration and accuracy in the preliminary phases of offshore development.

1.2.2. Consequences

Power cable
After mooring line failure, the FOWT will see a more extensive excursion than designed. The extent of the excursion will depend on environmental conditions and the possible failure of the remaining mooring lines. The excursion of FOWT could cause the cable to hit the keel of the TetraSpar, increasing wear on the power cable. If the excursion is large, the complete infrastructure of the inter-array cable from the seabed to the turbine will be damaged and eventually result in the power cable breaking. If tensile forces are not high enough to break the cable directly, the dynamic power cable could lose function due to a lack of bending radius and break internally. Figure 1.2 shows a simulation with an extreme design load condition, also called DLC, with extreme environmental conditions, which caused the largest mooring line tension and subsequent mooring line break. This DLC represents a 50-year storm in line with one mooring line. Figure 1.2 shows the event of a mooring line failure. Within the figure, the blue line represents the fairlead mooring line tension of a remaining mooring line after failure, while the red line depicts the offset of the TetraSpar concerning its static position. A line break causes an excursion that is ten times greater in broken line condition than what is expected for regular operation with three intact mooring lines concerning the static position. It may be reasonable to assume that similar forces are encountered in the power cable when the environmental conditions are directed so that the power cable bears the load as is seen in blue. Such an excursion would be too large for the dynamic power cable configuration to manage thus the power cable would bear the load. A specialist

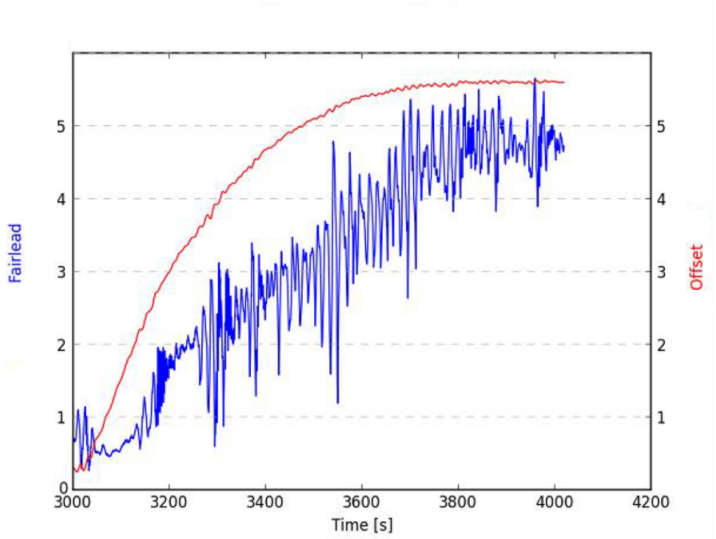

Figure 1.2: DLC with maximum excursion and corresponding Fairlead Tension after mooring line failure normalised

at Shell has estimated the minimum breaking load (MBL) of the dynamic power cable used by the

TetraSpar to be a fraction of the MBL of the mooring lines. However, no official MBL for the TetraSpar's power cables has been established. The MBL of the mooring lines is an order of magnitude higher than the MBL of the dynamic power cable. As mooring line tension after failure can become this high, a storm of half the storm's intensity presented in the figure 1.2 could therefore be more than enough to break the power cable. It would be unlikely that the power cable could be redundant, replacing a mooring line in case of failure. Research into the limits of dynamic power cables with possible strengthening and the consequences of a mooring line failure for the infrastructure could prove interesting for the future of FOW.

Motion

After the top event, a significant weight is released from one of the corners of the FOWT. The weight release from one corner will cause the FOWT to tilt and act like a catapult making the turbine and tower experience a larger acceleration than regular operation. These accelerations could be higher than designed for during operation. A result of these accelerations could be complete tower buckling or large deflections of the turbine blades. Assuming the turbine was in operation during the top event, large deflections of the turbine blades could damage or disintegrate the turbine blades from contact with the tower, resulting in material and environmental damage. However, the movements are dampened due to the Tetrapsar's considerable moment of inertia and hydrodynamic damping. Thus it is more likely that the floater will find its new equilibrium following the pitch natural frequency of the floater. Using the same DLC as used in figure 1.2 with 50-year storm conditions, the simulations show a large change in total pitch angle, measured from a negative to positive pitch angle. Documents on the TetraSpar conclude a strong increase in tower acceleration, leading to an significant increase in the tower base bending moment. Research into the maximum moment of the turbine tower and increased moment resulting from accelerations could be interesting for further research.

The acceleration resulting from the top event is a transient effect meaning it is only present in the transition from a complete mooring system to the new equilibrium of a broken system. The top event changes the mooring system significantly, and as a result, the motions and system response change. Changed motions affect the fatigue calculations, making the damage buildup after the top event unknown. How this system changes and how the floater responds should be investigated.

If the turbine blades and tower survive the larger accelerations, the turbine tilt could affect the internals of the turbine. An example of an effect of increased tilt is increased forces in the turbine bearings which could accelerate damage, something that should be looked into by turbine manufacturers.

Finally, when environmental forces align with the broken line, the two remaining mooring lines might undermine the turbine's stability in extreme scenarios. As the TetraSpar floats between the remaining anchors, forces apply nearer to or below the flotation centre than before the mooring line failure. This shift causes the mooring lines to decrease stability, contrary to their usual improving role. In an intact situation, the mooring lines help counter the wind-induced tilt of the turbine. However, with a broken line, this stabilising effect is diminished or could even exacerbate the tilt.

Station keeping

After the top event, the FOWT will drift to find a new equilibrium. The FOWT finds this new equilibrium as a combination of new mooring stiffness, wind, waves and current. This equilibrium changes as the environmental conditions do too. However, this does not put more tension on the mooring lines and anchors. A three-leg mooring is designed to take full environmental force in line with one mooring line. In this situation, the remaining mooring lines do not help to relieve tension on the stressed mooring line. Mooring lines are typically installed with a pretension of 10% to 20% of the MBL. Therefore, mooring lines add tension. A mooring line failure could consequently lower the pretension in the remaining mooring lines. A lower mean pretension could benefit the chain's fatigue life, as a paper by E. Lone et al. stated. However, other effects might take over to diminish this effect when a mooring line is lost completely.[25][31]

DEAs used for the TetraSpar are made for forces aligned with the anchor and naturally bury themselves. Drag anchors are, however, designed to be removed by pulling opposite to the installed direction. When force is applied out of line due to the top event, with the anchor pulled from the side or 180 degrees from the installed direction due to a shift in the wind, current or waves, anchor stability is not certain. This event could cause anchors to be dragged out, setting the FOWT a drift. This scenario should be investigated further.

Operational
After the top event, the FOWT will tilt, possibly making the boat landing or other access points unusable. Accessing the turbine's access points for inspection or repair of a broken mooring line could present challenges. Next to physical problems, the turbine should generate power which can be sold for a profit. After the top event, the power cable is expected to break and, therefore, no longer be able to carry electricity. This power cable failure may damage the infrastructure along the inter-array cable, connecting the different FOWTs in a FOW field, which will also lose power, decreasing profit further.

1.2.3. Scenario

To comprehend the sequence of events following a mooring line failure and decide on the most crucial research topic, the scenario is explained and illustrated in Figure 1.3.
The event does not state where the mooring line breaks, which is significant. If it breaks near the anchor, the FOWT remains upright with less tower lean. This break location also minimises tower acceleration, reducing potential tower and blade damage.

The FOWT will continually shift to new equilibrium positions, guided by environmental forces, as it responds to changes in these forces over time. According to industry professionals, the lead time for materials, vessel availability, and the maintenance weather window may extend to six months or more to conduct operations financially attractive and safe. Although the right environmental direction and conditions could allow the power cable to stay intact, it is unlikely to do so for six months as it has roughly one-tenth of the tensile strength of the mooring lines. Connecting power infrastructure will be damaged due to the tensile force before breaking. Depending on the position of the turbine within the field and its location along a particular 'string', which refers to a line of interconnected wind turbines linked by power cables, the power loss could differ. Damage incurred early in the string can lead to a power loss across the entire string, reducing overall power output. Ultimately, depending on the prevailing weather conditions, the cable could rupture.

The underlying problem causing the initial mooring line failure, like corrosion or fatigue, could be present in other mooring lines, triggering complete mooring system failure.

Following the initial failure of a mooring line, if the mooring system's stability is retained, it establishes a new equilibrium that could cause subsequent issues. The remaining mooring lines may lose tension and slacken, possibly leading to the fibre mooring line sections making contact with the seafloor. This 'fibre touchdown' could result in abrasion and particle ingress or snagging on seafloor objects, thereby reducing the MBL of the mooring line. Additionally, altered movements of the FOWT could introduce new fatigue-related failure modes within the entire mooring system. Changes in force distribution on the foundation from the mooring lines could further destabilise the turbine, potentially leading to capsizing. These three factors could lead to 'All MLs Fail', with ML standing for mooring line, which has been indicated with the dotted line.
The anchors will be subject to loads outside their installed direction, inducing uncertainty concerning anchor stability. Consequently, the anchors may release, turn following the new heading of the FOWT, or break due to unforeseen side loading. These problems with anchors could occur due to prolonged shifts in environmental conditions. In extreme environmental circumstances, the turbine loses stability.

In the unfortunate event of complete mooring system failure, the rogue turbine could collide with other turbines, or the remaining dragged mooring line could damage the seafloor power infrastructure, leading to large financial losses.

The prospect of a loose turbine within a field of FOWTs presents an outcome to be avoided at all costs. Ideally, the turbine should remain in place with two mooring lines intact until the summer service campaign can be carried out. Therefore, further research is required to prevent a complete mooring system failure resulting from a single-line failure. Failure modes leading to 'All MLs Fail', connected by a dotted line and 'Anchor Instability' as illustrated in figure 1.3 are explored further in the following literature study.

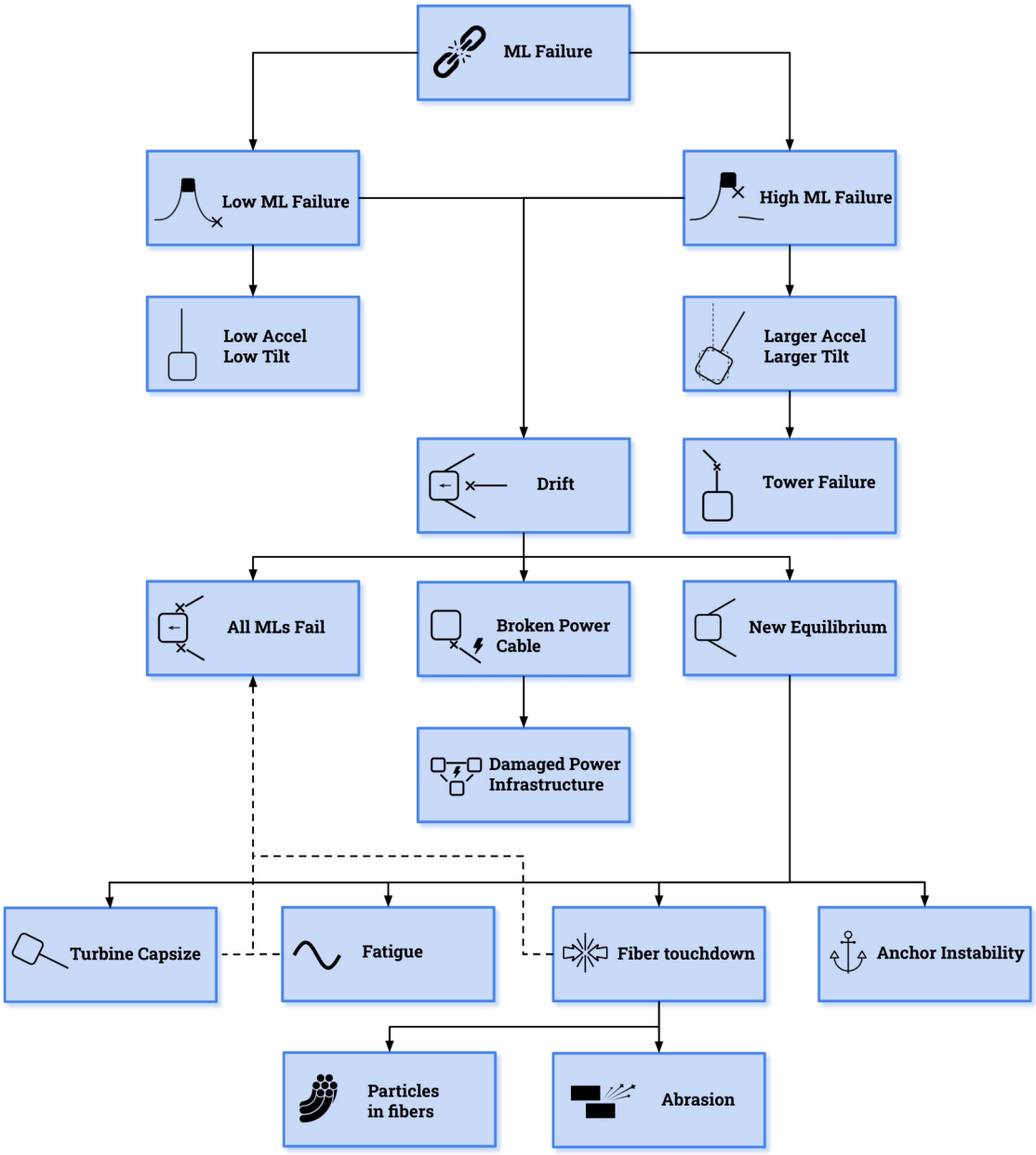

Figure 1.3: Failure flowchart

2

TetraSpar design basis

2.1. Location and metocean

The TetraSpar FOWT is situated at the Marine Energy Test Centre, located in the North Sea off the island of Karmøy on the western coast of Norway, as shown in Figure 2.1. The site is approximately 1500 m North-West of the Equinor Hywind Demo, another prominent full-scale FOWT. Conveniently, the site is also about 10 km from shore. There are a couple of advantages of selecting the Marine Energy Test

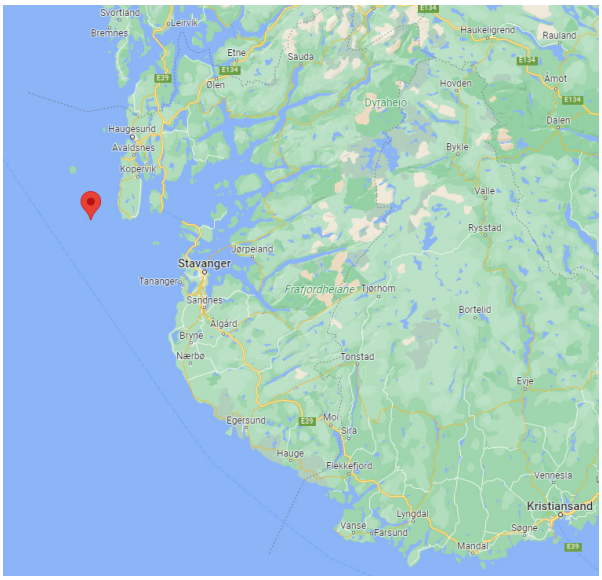

Figure 2.1: TetraSpar project location

Centre as the representative offshore site for the TetraSpar case study. Firstly, the site is home to the Hywind spar demonstrator. As such, metocean data has been collected over the years, which is used to develop the TetraSpar.

Secondly, the area of the North Sea where the Test Centre is located is known for its harsh conditions to offshore structures. If the structure can withstand these challenging conditions, it can be assumed that it will suffice for most locations worldwide.

Lastly, the pre-existing infrastructure of the Marine Energy Test Centre offers additional benefits. The power cable installed can be used for the TetraSpar, facilitating an economical means of transmitting generated power back to the mainland.

The design of the TetraSpar is fundamentally dependent on the probabilities, directionality and intensity of wind, wave, and current. These elements are individually represented through known three-parameter Weibull distributions. A notable observation from this data, as depicted in Figure

2.2, is the absence of wave activity from 0° to 120°, corresponding to the direction of the coast. This is contrary to wind and current activities, which are well correlated and originate from the same direction. The wave heading appears to shift by 30deg relative to the wind heading from 120deg to 180deg and from 240° to 330°; waves seem uncorrelated to other environments. The turbulent wind and

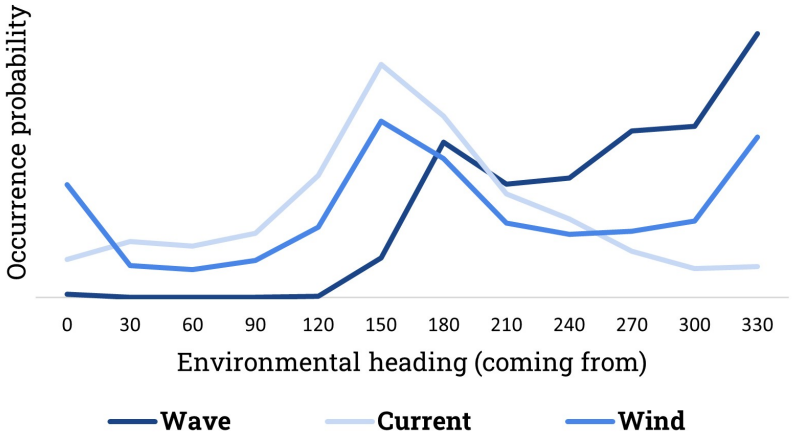

Figure 2.2: Environment occurrence probability vs heading

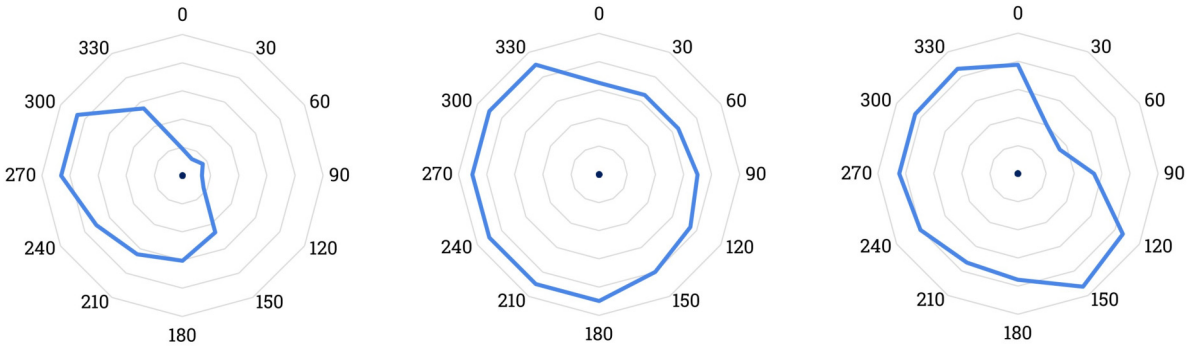

(a) Wave height **(b)** Current speed **(c)** Wind speed

Figure 2.3: Contour vs heading (coming from wrt North) without dimensions for a N return period storm

vertical wind speed variations are modelled using the NPD spectrum, while wave behaviour is captured via the Torsethaugen spectrum. Currents are treated as constant over time in the modelling process. Metocean data from the Hywind project has been used to develop the TetraSpar due to its proximity. Unfortunately, the joint probability of wind, wave, and current is not known, which presents a limitation in understanding environmental interactions. Due to the cost and sensitive nature of the environmental data, the presentation will be confined to descriptions, specific examples, and dimensionless graphs, rather than sharing the raw data itself.

2.2. Structure

The TetraSpar FOWT, as depicted in figure 2.4, brings forth several unique advantages that enable an efficient and cost-effective fabrication, assembly, and installation process, thus promoting the prospects of industrialisation. The steel structure and wind turbine can be quickly assembled on the quayside thanks to pin connections. The complete assembly is done in the quayside, installing the wind turbine while the structure floats near the dock. This process avoids the need for costly ships designed for offshore installation. Furthermore, the draft is minimised by holding the keel to the floater until the point of tow-out, offering significant advantages in terms of assembly, installation, and inspection.

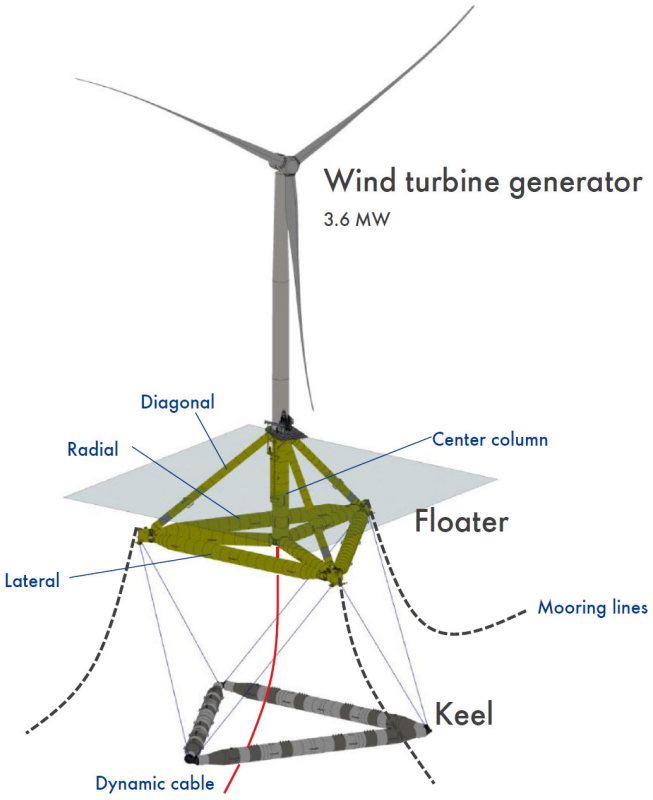

Figure 2.4: TetraSpar model

Apart from industrialisation, there are other benefits. The open structure of the floater minimises wave loads. The keel, used for ballasting, offers attractive dynamic properties. Decommissioning is straightforward, requiring the reversal of the installation process.

The TetraSpar concept comprises four main components: the wind turbine, the floater, the keel, and the mooring system. This thesis mainly focuses on the mooring system. The wind turbine used on the

Table 2.1: TetraSpar characteristics

Item	Value	Unit
Power	3.6	MW
Rotor Diameter	130	m
RNA mass	2.0×10^5	kg
Total mass incl. ballast	5.5×10^6	kg
Vertical center of gravity below MWL	40	m
Draft	66	m
Center column diameter	4.3	m
Radial brace diameter	3.5	m
Diagonal brace diamter	2.2	m
Lateral brace diameter	4.0	m

floater prototype is the Siemens Gamesa 3.6 MW, with rotor diameter and rotor nacelle assembly mass (RNA) displayed in table 2.1.

The floater, illustrated in 2.4, comprises steel members of varying lengths, diameters, and wall thicknesses. It features a vertical centre column with three radial members attached, making an angle of 120° with each other. These radial members are interconnected with lateral elements, providing the major part of the buoyancy. The structure forms a rigid body thanks to the diagonal elements attached to the radial elements. A transition piece, which connects the wind turbine and the floater, sits atop the floater.

The keel is affixed to the floater with six Dyneema suspension lines. The keel, which is ballasted and filled with concrete, provides dynamic stability to the structure.

The system is anchored to the seabed using three catenary mooring lines with drag embedment anchors.

In effect, this configuration bestows the TetraSpar with the characteristics of a spar, as it possesses significant buoyancy and derives its stability from the ballasted keel. Variations in the keel mass and depth allow the system's properties to be tuned to match the desired response of any location.

2.3. Mooring system

The TetraSpar demonstrator employs a three-leg spread mooring system for station-keeping. Table 2.2 provides a general description of the mooring system and details the mechanical properties of the lines. The mooring lines are distributed unevenly across azimuth angles to align with the dominant environmental load directions, positioning the lines towards headings with greater intensity. Figure 2.5 illustrates the mooring line catenary's static state.

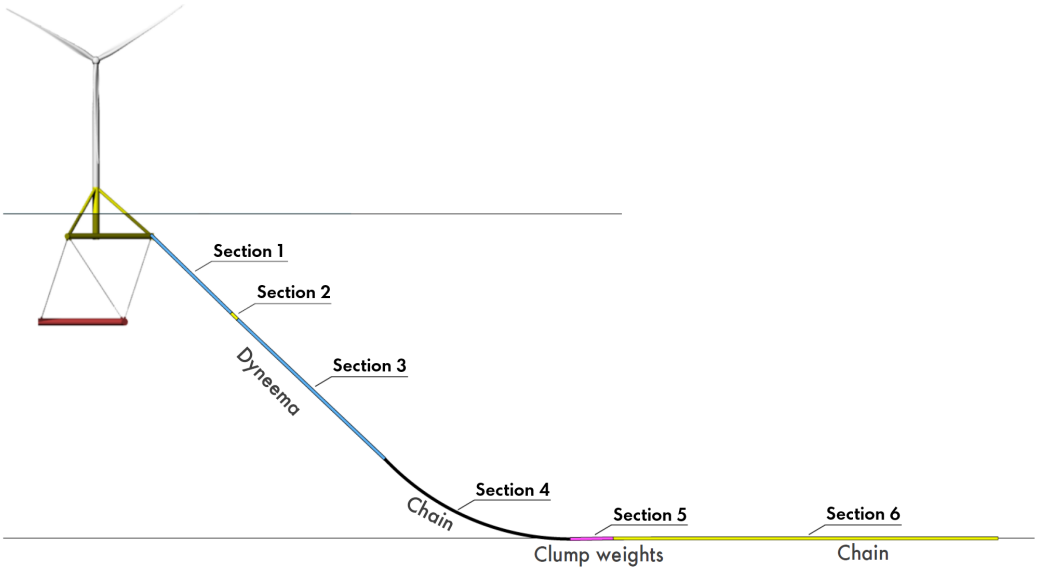

Figure 2.5: Linetypes TetraSpar

Table 2.2: Mooring sections of TetraSpar mooring system [6]

Section	Length [m]	Material	Submerged weight [N/m]
Section 1	80	150mm - Dyneema	2.2
Section 2	6	107mm - R4 studlink	2139.6
Section 3	140	150mm - Dyneema	2.2
Section 4	145.5	124mm - R3 studlink	2872
Section 5	30	117mm - R3s studless + clump weight	19515
Section 6	270	107mm - R4 studlink	2139.6
Total	671.5		

The TetraSpar's mooring system combines different line types, detailed in Table 2.2 and Figure 2.5, with all mooring sections having roughly the same MBL at 11 MN. Clump weights, Dyneema, and regular stud link chains characterise the TetraSpar mooring system. The clump weights, which substantially outweigh the submerged weight of the R4 stud link chain and Dyneema fibre by roughly 10 and 1000 times, are implemented to stabilise the system, maintain tension in the mooring lines, and limit excursion. Overall the mooring system is a complex design with many sections and, thus, connection points.

The mooring layout comprises three identical mooring lines (ML1, ML2, ML3) numbered clockwise viewed from above. The angular spacing of the mooring lines is slightly uneven to reduce the load from directions with the highest intensity.

3

Literature study

3.1. Anchor

3.1.1. Anchor systems

FOWTs are most commonly designed using a catenary mooring system, although concepts have been presented using taught mooring lines.[18] This could be because most floating wind projects are tested in 'shallow' water, where a catenary mooring system is cost-effective. Figure 3.1 shows the typical mooring systems ranging from shallow to deep and hard to soft soils, seen from left to right, and the different anchor systems are explained.

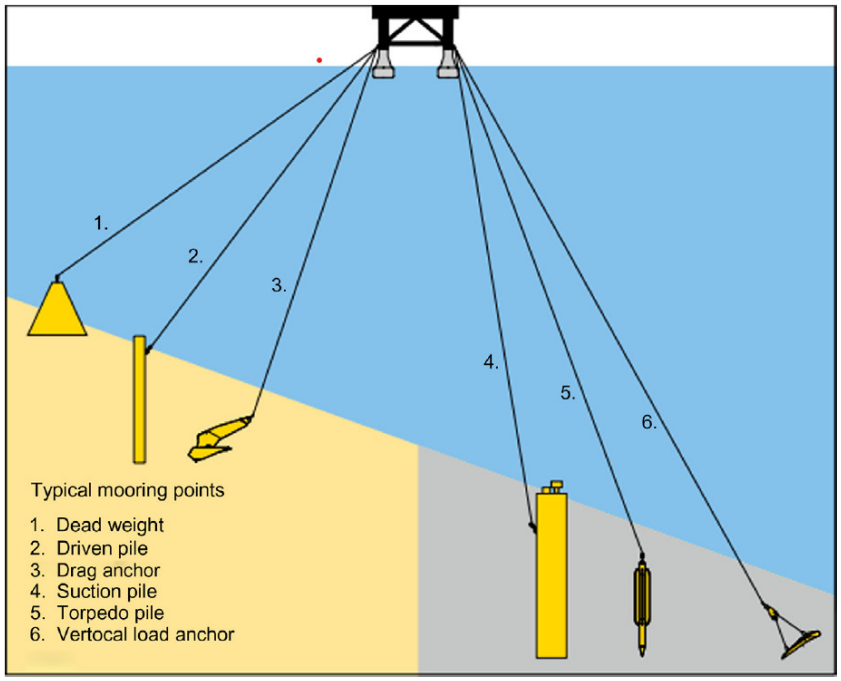

Figure 3.1: Anchor types[18]

- Drag embedment anchor: The DEA has been designed to penetrate the seabed, partly or fully. The soil resistance in front of the anchor generates the holding capacity of the DEA. The DEA is well suited for resisting large horizontal loads but not large vertical loads. However, some DEAs available today can resist significant vertical loads.
- Driven pile: The pile is a hollow steel pipe installed into the seabed by a piling hammer or vibro-hammer. A combination of the friction of the soil along the pile and lateral soil resistance generates the holding capacity of the pile. Generally, the pile has to be installed at 3 to 6 times the

diameter of the pile resulting in a depth of 10 to 30-meter penetration depth to obtain the required holding capacity.[34] The pile can resist horizontal and vertical loads.

- Gravity Anchor: The dead weight is probably the oldest anchor. The holding capacity is generated by the weight of the material used and partly by the friction between the dead weight and the seabed. Common materials in use today for dead weights are steel and concrete.
- Suction anchor: Like the pile, the suction anchor is a hollow steel pipe. However, unlike the pile, the suction anchor is closed at the top and generally has a much larger diameter than the pile. The suction anchor is forced into the seabed using a pump connected to the top of the pipe. When the water is pumped out of the suction anchor, a pressure difference is created between the outside of the pipe and the inside forcing the anchor into the seabed. After installation, the pump is removed. A combination of the friction of the soil along the suction anchor and lateral soil resistance generates the holding capacity of the suction anchor. The suction anchor is capable of withstanding both horizontal and vertical loads.
- Gravity-installed anchor: This anchor type is shaped like a torpedo and dropped from a water depth of 30 to 150 meters. Due to its drop weight, it installs itself and requires no external energy or mechanical handling. Kinetic energy acquired by gaining speed from the drop is used to bury itself into the ground like a driven pile. Therefore it is ultimately suited for deepwater moorings. The depth of the anchor can, however, not be accurately controlled.[24]
- Vertical load anchor: The vertical load anchor can be installed using a suction anchor, driven or using the same method as the DEA. When the anchor mode is changed from the installation mode to the vertical (normal) loading mode, the anchor can withstand both horizontal and vertical loads. Although designed to suit deep water mooring applications, its omnidirectional load capacity allows mooring objects in confined subsea infrastructures such as close to pipelines and cables.[18]

Table 3.1: Relative installation cost of anchor systems [23]

DEA	Driven Pile	Gravity	Suction	Gravity-installed	Vertical
Low	High	Low*	Medium	Low	Medium**

*Not provided but guessed

**Depending on the installation method of vertical anchor

3.1.2. Drag Embedment Anchor

As DEAs have been chosen as the anchor system for the Tetraspar project and are seemingly the preferred installation method for FOWTs, further research will be conducted.[20] A DEA is a bearing plate, also called the fluke, that is dragged into the seafloor by a wire rope or chain. A shank of one or more plates secures the fluke to the anchor line, as shown in figure 3.2. The angle between the fluke and shank of drag embedment anchors is designed to make the soil break roughly in line with the fluke. This design ensures that when the anchor is pulled, it moves downward instead of simply sliding across the surface.

DEAs are typically constructed for various fluke-shank angle setups depending on the soil type. The fluke-shank angle is around 30 degrees for stiff clays and sands and 50 degrees for soft clays.

The new generation of fixed fluke DEAs develop a higher retention capacity than the self-weight would assume, thanks to significant advancements in DEA technology, under diverse soft soil situations. They are simple to install and have a track record of effectiveness. Prior to the arrival of the floating vessel at the destination, the anchor piece of a mooring line can be pre-installed and proof loaded. This reduces scheduling risk as multiple installations can be done in one go and fast before the arrival of the FOWT.[26]

Advantages and limitations of drag embedment anchors

DEAs offer a higher load capacity-to-anchor weight ratio than suction and driven piles and are less expensive to install. High-efficiency DEA can hold multiple times its weight, depending on the soil type, as shown in figure 3.3. However, unlike suction and driven piles, DEAs cannot achieve precise positioning. Their load capacity is determined by the depth of anchor penetration and soil properties, which cannot be predicted accurately.

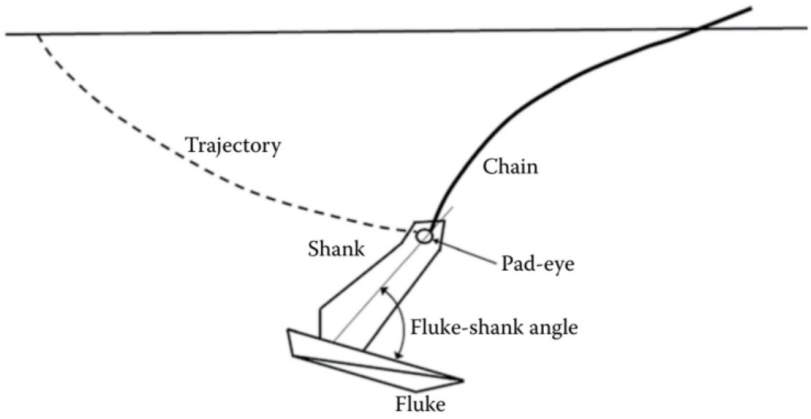

Figure 3.2: Drag Embedment Anchor[2]

Proof load testing of DEAs after installation can greatly reduce the uncertainty in their load capacity. However, this requires anchor-handling vessels with specific bollard pull capabilities or onboard tensioning equipment. In sands and stiff clays, DEA penetration into the seafloor is typically less than 1-2 fluke lengths, limiting their use to catenary systems and reducing their vertical load capacity. The anchor mainly resists horizontal loads, while the anchor and chain's dead weight bear the vertical loads. Soft clays allow for much deeper DEA penetration in contrast to sands and hard clays. With proper construction, DEAs can penetrate hard soils, cemented layers, and soft rocks like chalk, calcarenite, corals, and limestone. A serrated shank, cutter teeth, and strong structural support must withstand concentrated stresses to achieve this soil penetration.[26]

Holding capacity of drag embedment anchors

One of the simplest methods is to use charts that estimate holding capacity, drag distance, and penetration depth based on the anchor's weight and the type of soil to determine the capacity of a drag anchor. These charts are typically derived from full-scale model testing or field experience. However, it is essential to note that suppliers' standard Ultimate Holding Capacity (UHC) charts are general guides for selecting an appropriate anchor size rather than design guidelines. These charts only apply to uniform, generic soil types with unlimited thickness. Figure 3.3 shows such a chart for anchors from new to old. Stockless anchors are familiar from cartoons, the Stevpris MK6 anchor, and the latest DEA designs. It can be seen that the load capacity-to-anchor weight is increased by altering the shape of the anchor, increasing the load capacity tenfold compared to the stockless anchor.

Uncertainties are high in determining the capacity of large anchors in diverse soil conditions due to the scarcity of test data. Regarding capacity development, the anchor weight's contribution is negligible, while the more significant element is the fluke area, which is naturally related to the anchor weight.[26]

Drag embedment anchor recovery

Clay properties like consolidation heavily influence the anchor's post-installation capabilities. Recovery loads for anchors in cohesionless soils like sand and gravel typically range from 20% to 30% of the installation load or the peak stress experienced by the anchor. In contrast, recovery loads in soft cohesive soils such as clays and silts are generally higher. The anchor recovery load is determined by multiple factors, including soil properties, anchor size, embedment depth, applied installation load, and recovery load application angle. Recovering an anchor from clay can be time-consuming, so it is essential to exercise patience. Gradually increasing the tension to the expected recovery loads and holding it there for a predetermined time can help overcome suction forces. Recovery loads for clays can range from 80% to 100% of the applied installation load, but in clays with high sensitivity, it may be necessary to exceed these limits up to 110%-140%. Once suction effects have subsided, the anchor should release easily.[26]

Side loading

When one mooring line fails, the FOWT will drift back and forth, guided by environmental conditions. In a three-leg mooring system, the mooring lines are typically spaced at intervals of 120 degrees. The

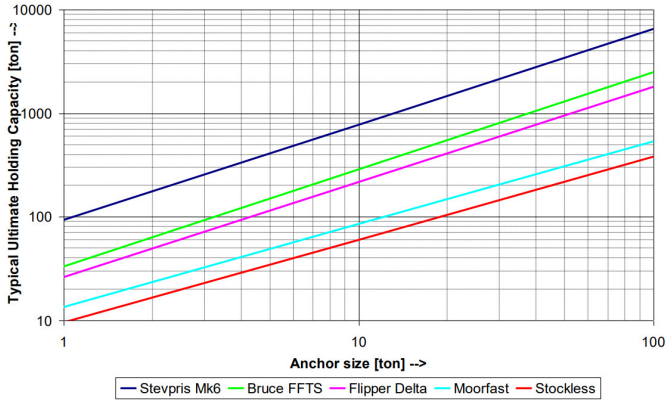

Figure 3.3: Anchor holding capacity in medium dense silica sand[30]

angle of the force on the anchor will therefore be 60 degrees when drifting away from the original position after mooring line failure. DEAs are designed to be retrieved by applying a load in the direction opposite to the installation direction. Therefore, it is noteworthy to examine how an anchor responds when loaded at a significant angle from its installed direction. The anchor manufacturer Vryhof has conducted research on behalf of Shell to investigate this behaviour.

The side load angles are varied to roughly the maximum of 60 degrees. The tests are carried out in an instrumented sand test tank using a Stevshark model anchor and loaded with representative loading. The side load test results demonstrate that the anchor reliably resists increasing side loads as side angles grow. The anchor's performance under side loading is consistently stable. Depending on the tension level and side angle, the anchor either repositions itself in the pull direction or withstands the new tension without moving. Considering a broken line's equilibrium and excursion, these findings indicate no risk to anchor stability post-mooring line failure. The remaining two anchors will likely maintain position after a mooring line failure.

3.2. Environmental

3.2.1. Wind loads

The wind is typically defined by direction, speed, and spectrum. The wind speed varies with time but also with height above the sea surface due to the influence of the roughness of the sea surface and follows a power profile. For this reason, the mean wind speed is defined by a time average at a reference elevation (z_r) above the sea level. The power law denoted in equation 3.1 is often used in wind assessments where wind speeds at the height of a turbine must be estimated from near-surface wind observations or where wind speed data at various heights must be adjusted to a standard height prior to use.[26] Where α is an empirically derived coefficient that varies depending upon the atmosphere's stability. $\frac{1}{7}$ is a typical value for α, but in calm water, $\frac{1}{9}$ is more accurate due to the absence of trees and other obstacles. Depending on wave height, an α somewhere in between $\frac{1}{7}$ and $\frac{1}{9}$ is assumed.[16]

$$U(z) = u_z(\frac{z}{z_r})^{\alpha} \tag{3.1}$$

Fluctuating wind can be modelled by a steady component based on an average velocity calculated using equation 3.1, plus a time-varying component calculated from a suitable empirical wind gust spectrum. Several wind spectra have been developed from various resources, such as the Ochi, Davenport, Harris, American Petroleum Institute (API), and Norwegian petroleum directorate (NPD) spectra.[26] The power spectrum describes power distribution into frequency components comprising the wind. Depending on the chosen spectrum, a shift will happen to a higher or lower frequency, being more or less conservative or resembling the real world better. Depending on the structure's location, different wind spectra could prove a better fit. Figure 3.4 shows a representation of the theoretical NPD spectrum and a measured spectrum. The wind speed will generate a load on the structure which will cause a steady-state mean excursion, rotational movements and dynamic components. The gusts exert a fluctuating level of force

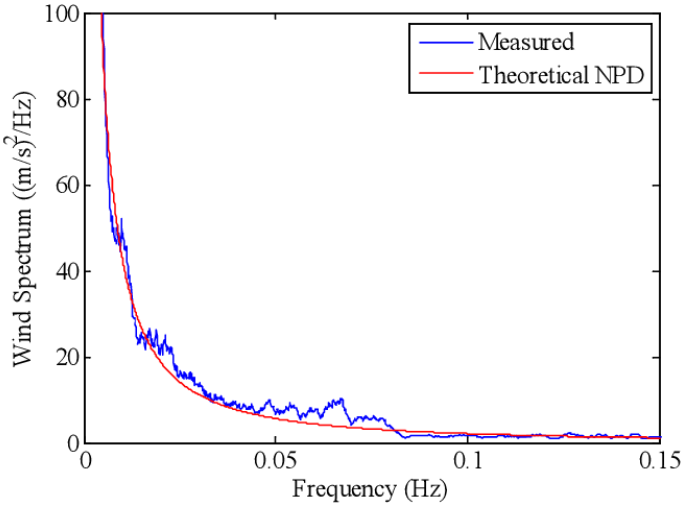

Figure 3.4: Measured and theoretical NPD wind spectra [13]

on the structure. However, it is not expected that this has an enormous influence on the mooring system due to the high inertia of the complete structure and the relatively high frequency of these fluctuations compared to the natural frequency. The resulting force on the FOWT due to wind can therefore be estimated using the mean wind using formula 3.2.

$$F_w = \frac{1}{2}\rho_a C_s A {U_z}^2(z) \tag{3.2}$$

Here F_w is the wind force; ρ_a is the air density; C_s is the shape factor; A is the projected area, and U_z is the wind speed relative to the structure. As the name implies, the shape factor depends on the structure's shape to be analysed. For example, a shape factor of 0.5 for Cylindrical shapes and 1.0 for boxes can be assumed. The TetraSpar is comprised mainly of tubes making the calculation seemingly simple. The entire structure does, however, not experience free flow as parts of the structure disturb the free flow of air for parts on the leeward side of the structure, changing the force exerted by the wind. The sheltered parts will be multiplied by a shielding factor, lowering the total force. However, this is more conveniently calculated using simulation software like OrcaFlex.

3.2.2. Wave loads

Waves are defined by wave height H as the vertical distance between a wave's highest and lowest surface elevation. In a wave record with N waves, the mean wave height H is defined as equation 3.3.[15]

$$\overline{H} = \frac{1}{N}\sum_{i=1}^{N} H_i \tag{3.3}$$

N is the number of waves running from i to N, and H_i is the wave height of wave i. Sometimes the wave height is represented by the root-mean-square wave height H_{rms} equation 3.4 or the significant wave height $H_{\frac{1}{3}}$ equation 3.5. In equation 3.5 j does not resemble the number of the wave but rather a ranking from highest to lowest, where $j = 1$ is the highest wave, $j = 2$ is the second highest and so on.

$$H_{rms} = (\frac{1}{N}\sum_{i=1}^{N} H_i^2)^{\frac{1}{2}} \tag{3.4}$$

$$H_{1/3} = \frac{1}{N/3}\sum_{j=1}^{N/3} H_j \tag{3.5}$$

Like the wave height wave period is represented by a mean wave period $\overline{T}$ equation 3.6 and can be represented by a significant wave period $T_{1/3}$ equation 3.7.

$$\overline{T} = \frac{1}{N} \sum i = 1^{N} T_i \tag{3.6}$$

$$T_{1/3} = \frac{1}{N/3} \sum_{j=1}^{N/3} T_j \tag{3.7}$$

For simple calculations, regular waves are used, which are sinusoidal and are described by linear theory, also known as the airy wave theory. The harmonic wave involved is, therefore, sometimes called the Airy wave. The main requirement for the linear theory to apply is that the amplitudes of the waves are small compared to the wavelength and small compared to the water depth, where h/λ>1/2 is considered deep water, the wave does not 'feel' the bottom to this depth with $\lambda = \frac{gT^2}{2}$.

$$\eta(x,t) = a\cos(kx - \omega t) \tag{3.8}$$

Where λ is the wavelength in meter; $a = \frac{1}{2}H$ the wave amplitude in meters; $k = \frac{2\pi}{\lambda}$ the angular wavenumber in radians per meter; $\omega = \frac{2\pi}{T}$ the angular frequency in radians per second and h is water depth. The DLC used in the introduction (chapter 3), which represents extreme environmental conditions with a 50-year reoccurrence for the TetraSpar location. This DLC has a period of 16 seconds and can be used to calculate if we are in deep water. A wavelength of 399 meters is found, resulting in a h/λ of 0.55 which is larger than 1/2 and thus is deep water.

The real ocean consists of irregular waves, which are a superposition of regular-shaped waves. Waves of different wave heights, lengths, periods, phases and propagation directions are superimposed to create a realistic wave field graphically shown in figure 3.5. With this simplification, the waves can be represented by an energy spectrum which gives the distribution of wave energy among different wave frequencies and heights on the sea surface.[26]

$$\underline{\eta}(x,y,t) = \sum_{i=1}^{N} \sum_{j=1}^{M} \underline{a}_{i,j} \cos\left(\omega_i t - k_i x \cos\theta_j - k_i y \sin\theta_j + \underline{\alpha}_{i,j}\right) \tag{3.9}$$

This wave spectrum is mathematically represented by various idealised wave spectra like Pierson

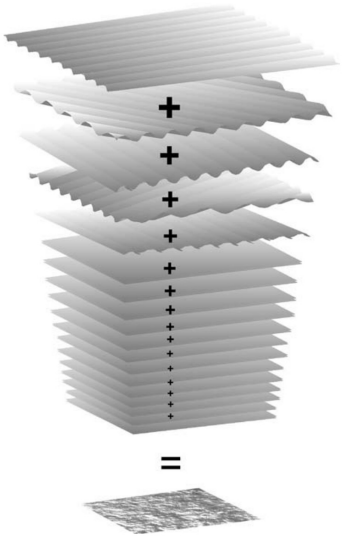

Figure 3.5: Superposition harmonic waves[15]

and Moskowitz, JONSWAP or Torsethaugen with the latter two depicted in figure 3.6. Pierson and Moskowitz is a spectrum recommended for open-ocean wave conditions. JONSWAP is an alteration

on the Pierson and Moskowitz spectrum limiting the fetch due to geographical boundaries in the wave-generating area spectrum. Like wind spectra, every location has a spectrum that represents it best, shifting the spectrum lower or higher and making the peak broader or narrower. Torsethaugen is a double-peaked spectrum best suited to North Sea conditions representing sea states that include both a remotely generated swell and local wind-generated waves and is based on measured spectra for Norwegian waters. Making the Torsethaugen a perfect spectrum for calculations on the TetraSpar.[40] To get a good first impression of the wave loads on the structure, the Morison equation 3.10 can be used,

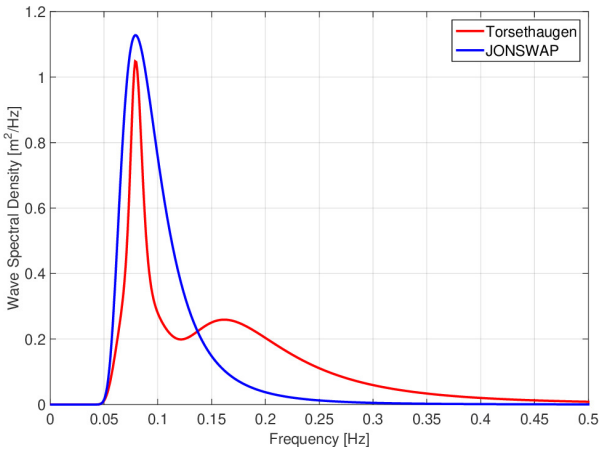

Figure 3.6: Torsethaugen and JONSWAP spectrum[5]

which is built up from inertia and a drag component.

$$F = \underbrace{\rho_w C_m V \dot{u}}_{F_{inertia}} + \underbrace{\frac{1}{2}\rho_w C_d A u|u|}_{F_{drag}} \tag{3.10}$$

Where F is the force on the structure in line with the direction of waves; ρ_w is the water density; $C_m$is the inertia coefficient, which is an altered added mass coefficient; C_d is the drag coefficient; A is the cross-sectional area;V is the volume of the body; u the water particle speed and $\dot{u}$ is the water particle acceleration. As with the wind, the sheltered parts are to be multiplied by a shielding factor.

3.2.3. Current loads

The force due to current is the F_{drag} part of equation 3.10 and will result in equation 3.11. This is because current speed is seen as constant and therefore does not have a time-varying part as $F_{inertia}$ does.

$$F_d = \frac{1}{2}\rho_w C_d A u|u| \tag{3.11}$$

3.2.4. First- and second-order forces

First-order wave forces refer to the linear oscillatory components of wave action on a structure, which have the same frequency as the waves, and their amplitude is directly proportional to the amplitude of the waves. First-order movements primarily affect the degrees of freedom in pitch, roll, and heave.

The second-order wave forces primarily affect the degrees of freedom in surge, sway and yaw. Second-order wave drift forces have higher and lower frequencies than wave frequencies. These forces are proportional to the square of the wave amplitudes. Low-frequency second-order wave forces have frequencies that match the frequencies of wave groups in irregular waves. These are called wave drift forces and contain time-varying and non-zero mean components. When a vessel is floating freely in waves, it tends to drift in the direction of wave propagation under the influence of second-order forces. High-frequency second-order forces have frequencies that are double the frequency of the waves (sum frequencies). The response of moored structures to the sum frequency forces is generally small.[19] Figure 3.7 shows the wave elevation record and the motions of a permanently moored tanker in high, head-on sea conditions. It is seen that the heave and pitch motions contain the same frequencies;

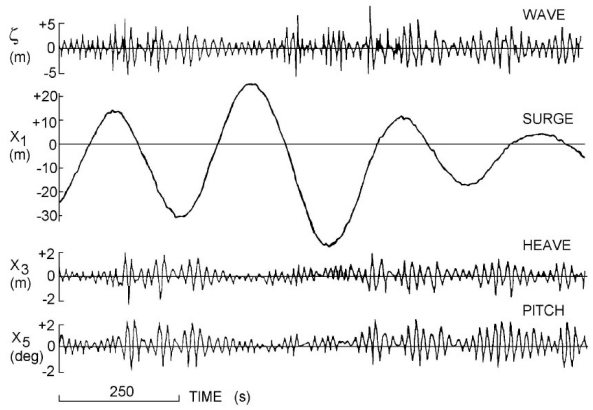

Figure 3.7: Record of the motions of a moored tanker model in head waves[19]

their amplitudes are in the order of the wave amplitudes and wave slopes, respectively. In addition to containing a minor wave frequency motion component, the surge motion is predominantly influenced by a low-frequency component with a substantially larger amplitude. This low-frequency influence also leads to large amplitude horizontal motions in surge, sway, and yaw, which could generate significant peak loads in the mooring system resulting from second-order wave forces.

3.3. Mooring line

3.3.1. Catenary vs taut leg mooring

Floating structures are moored using different mooring methods. For every use case, there are specific advantages and disadvantages.
In a catenary mooring, the mooring lines are allowed to form a natural curve, or catenary, as they run from the vessel to the mooring point. The floater can move freely following the first-order wave forces but restricts the second-order forces. This allows the vessel to move freely in response to environmental forces in pitch, roll and heave, but drift is restricted. Allowing first-order degrees of motion helps reduce the stress on mooring lines but keeps the floater in the desired location, as a mooring system should. The mooring lines, most often chain, will run along the seabed for the last section running up to the anchor. The anchor points in a catenary mooring system are designed to be only subjected to horizontal forces. The mooring stiffness of the catenary system is mainly dependent on the weight, geometry and pretension of the mooring system.[3][18]

In a taut mooring, the mooring lines are kept taut, allowing little or no movement of the floater. This can be used to hold a vessel in a relatively fixed position, but it can also strain the mooring lines and the vessel itself and may not be suitable for use in areas with strong winds or waves. Contrary to catenary mooring systems, first- *and* second-order movements are restricted, increasing strain. The restoring forces are created through axial elastic stretching of the mooring line rather than geometry changes. The mooring system is, therefore, highly dependent on the material properties EA/L. Currently, taut mooring systems possess low technology readiness (TRL) for FOW and are not yet recognised as proven technology.[3][18][10]

One key difference between the two methods is the amount of movement allowed for the floater. Catenary mooring allows for more movement, while taut mooring holds the vessel in a more or less fixed position. The choice of method will be determined by the specific conditions of the mooring location and the needs of the vessel.

In deep waters, taut mooring systems can be more cost-effective than catenary mooring systems due to the widespread and, thus, long line lengths of the catenary mooring lines and high fairlead forces at the floater due to the weight of the catenary mooring line. The financial tipping point varies per project, but catenary systems are generally expected below 500m water depth; between 500 to 1000 meters, both catenary and taut systems are applicable, and beyond 1000 meter water depth, taut leg systems are cost-effective. Due to the financial pressure, it is not expected to see FOWTs in deep water

as cost increase with water depth.[18][26]

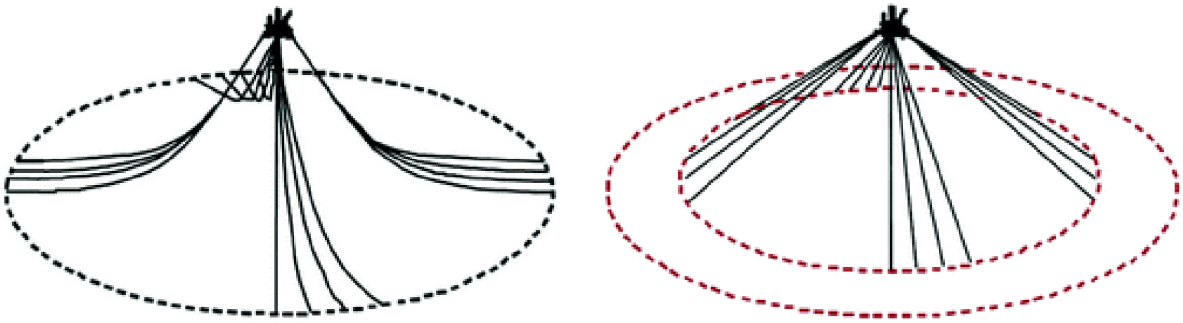

(a) Cateneray mooring **(b)** Taut mooring

Figure 3.8: Mooring types[18]

3.3.2. Line types

Mooring lines of a catenary mooring system often comprise multiple sections of sometimes different line types to use their specific properties at the desired location.

- Chain, typically made of high-tensile steel, is a durable and strong option for mooring lines. It has good abrasion resistance and can withstand large loads. A common variation of chains is studded chains. The studded chain link will better prevent knot formation but will be more sensitive to fatigue failure than the studless chain link and is more expensive. Chain is expensive and heavy and therefore is not always suited for the entire mooring system.
- Wire rope, made of multiple steel wires twisted together, is a flexible and robust option for mooring lines. It is also resistant to abrasion and can withstand large loads with a lower weight than chain and is therefore used to the mooring lines self-weight. Wire rope, however, can suffer from excessive bending and bird caging when put in compression and is best suited to the mid-section of the line.
- Synthetic fibre rope made of materials such as polypropylene, nylon, or Dyneema is a lightweight and flexible option for mooring lines. It has a lower environmental impact than steel and does not lose strength rapidly due to fatigue. It is, however, susceptible to abrasion and marine growth and should, therefore, generally only be used in the midsection of the line. It can be used to lower the self-weight of the mooring system, just like wire rope. Unlike wire rope and chain, synthetic fibres suffer from elongation, which should be accounted for. Dyneema is the newest, with a high tensile force-to-weight ratio but comes with high cost.

The main objective of the mooring system includes two goals. Firstly, to secure the floating structure within established tolerances during both standard and extreme weather conditions, ensuring that the floater's movement remains within boundaries. Secondly, it provide the necessary strength and resistance to fatigue to uphold the offshore system's functionality and dependability. To meet these objectives, a detailed assessment of various factors is needed, including design elements such as water depth, marine growth, loading conditions, and location-specific elements. Furthermore, the system must be capable of withstanding environmental forces, such as wind, waves, and currents, adhering to standard requirements. Additionally, considerations regarding the cost, including materials, installation, maintenance, and potential complexity of material combinations, must be balanced against other factors, such as the environmental impact, where alternative options like synthetic ropes may present a more environmentally friendly solution than steel cables.

3.3.3. Standards

Developing optimised and dependable designs is crucial for minimising costs. This involves adhering to classification society guidelines which account for various environmental conditions, including Fatigue Limit State (FLS), ULS, and ALS. These guidelines encompass all necessary load conditions to ensure reliability and safety in design.

Regulatory bodies such as the DNV provide a regulatory framework for the design of mooring systems and floating wind turbines, including documents like DNV-ST-0119 (Design of Floating Wind Turbine Structures) and DNV-OS-E301 (Position Mooring). These documents are instrumental in guiding the design process for FOWT mooring systems.

For FOWTs, which are typically unmanned during extreme environmental events, the consequences of failure are predominantly economic, which results in a lower safety factor. DNV-ST-0119 states that redundancy is the ability of a component or system to maintain or restore its function after a failure of a member or connection has occurred. Redundancy in a system can be accomplished by reinforcing or introducing alternative load paths. If a mooring system loses one mooring line, but the remaining part still meets the survival criterion for at least a one-year load, the original undamaged mooring system is considered to serve as redundant.

The N+1 redundancy principle could be applied to a three-leg mooring system. In this context, N signifies the minimum number of mooring lines required to ensure safe station-keeping of a vessel or platform under specified environmental conditions. Thus, an N+1 system includes one additional mooring line beyond the essential minimum. Consequently, a three-line system can be considered suitable, provided it maintains safety following the failure of one mooring line still following N+1.

3.3.4. Mooring line failures

Failure of a mooring line is seldom the result of a single event. It is caused by smaller but significant factors applying stress to the system over time, leading to overload as the final failure mode. Multiple Joint Industry Projects (JIP) have been carried out throughout history to grasp mooring line failures. The Noble Denton Phase 1 Mooring Integrity JIP, based on data for the period 1980 to 2001, reported that, on average, an FPU would experience a mooring line failure every nine years. Contrary to the TetraSpar, which utilises three mooring lines, FPUs typically employ between 8 and 12 mooring lines, although this number can be larger. The reported average failure rate of once every nine years for FPUs loosely translates to an annual failure rate of 1.1E-2 per mooring line per year, given an average of 10 mooring lines per FPU.[12] Deepstar has conducted industry surveys reporting the amount, makeup and nature of mooring line failures with data from 1997 to 2013. This research was later expanded with data up to 2020.[11][41] Although the research was done for the oil industry and failures have been registered for FPUs, the mooring systems components are the same as in FOW, and failure modes carry over. Lessons have been learned from these JIPs, but no revolutionary changes have been made to mooring systems components or compositions. Therefore, statistics from these reports are assumed to be valid, knowing they are more conservative used now. So far, FOW is most prevalent in relatively shallow water. This is due to the high-cost part of the mooring system in the total cost of a FOWT and the increasing cost of mooring systems at increasing water depth.[22] Figure 3.9 shows 58% of the survey population of the Deepstar JIP is in shallow or intermediate water depth corresponding to less than 100m and in between 100 and 350m, respectively. These water depths are in line with FOW water depths commonly operated. Therefore, the data set of FPU failures is a good representation of FOW failures in the future.

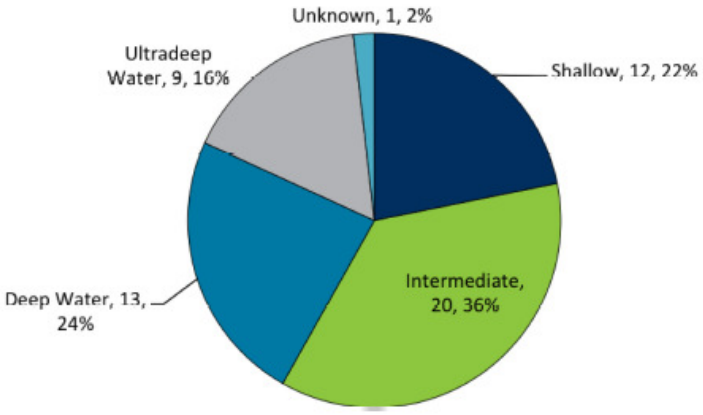

Figure 3.9: Water depth survey population FPUs Deepstar research[11]

Figure 3.11 shows causation for the reported failure events. The most prevalent reported causes of failure were fatigue and corrosion, which together represent 45% of failures. Installation failures represent 16%, with the residual comprising mechanical damage, design issues, manufacturing defects, overload and unknown/unreported. Figure 3.10 shows the phase of the mooring system life cycle most likely associated with failure inception, 19% of the reported failures were due to design causes, with another 22% due to installation causes, 6% due to construction/manufacturing causes, 49% due to damage sustained, or maintenance failures, during operations and the remaining 4% unknown. [11]
The annual rate of single line failure per mooring line per year, depicted in figure 3.12, stays stable but

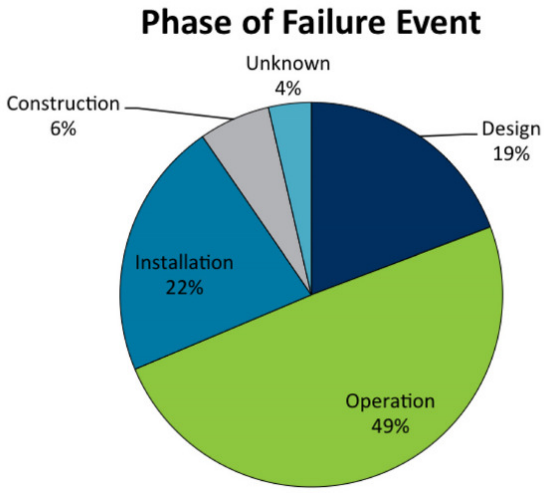

Figure 3.10: Proportion of failure associated with each project phase [11]

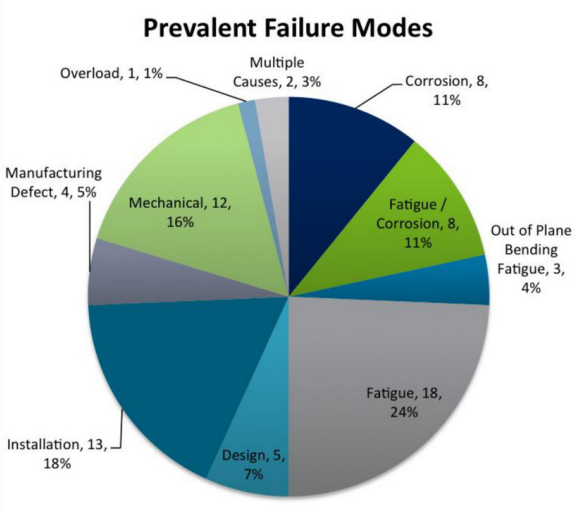

Figure 3.11: Root cause of failure [11]

slightly decreases to 2.2E-3 in 2020.[41] The number of failures has been almost consistent from 1997 to 2020, and it is expected that without significant changes in mooring line technology or rules, this trend will continue. For a field of 150 turbines, a minimum of 450 mooring lines are expected, assuming three mooring lines per FOWT. With a failure rate of 2.2E–3 per mooring line per year, one mooring line failure is expected per wind farm per year. This failure rate appears to be a order of magnitude greater than industry targets. For instance, DNV-OS-E301 has been calibrated to give a target single-line failure rate of once every 10,000 operating years(1E-4) and a target multi-line failure rate of once every 100,000 years(1E-5).[41]

From the data set, the conditional frequency of a single-line failure leading to a multiple-line failure was approximately 1 to 5. Where in the system the additional failure took place is not known. The precise interval between the initial failure and subsequent ones remains undefined in the Deepstar research, beyond the description of 'occurring at or around the same point in time'. In systems with groups of mooring lines, as often seen in offshore oil and gas, the same failure mechanisms might occur due to the same nature of the load and fatigue development, thus, causing additional failures at the same moment in time. This might not be true for a mooring system with three lines and presumably different loads and fatigue development for every line. If 1 to 5 would be the ratio between single-line to multiple-line failures, a field of 150 turbines would roughly have one FOWT with two or more mooring lines failures at the same time once every five years, possibly setting loose a FOWT untethered through a FOW field, which is not a good foresight.

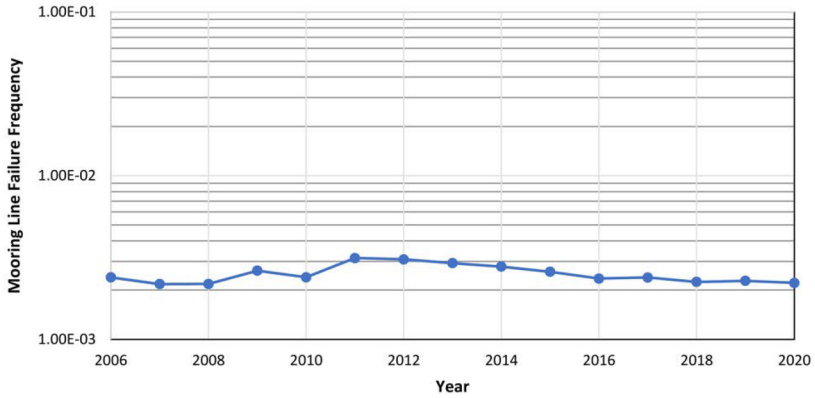

Figure 3.12: Annual single line failure rate per year[41]

3.3.5. Failure point

The mooring line setup of the TetraSpar consists of a combination of Dyneema and chain. Failure probabilities on either chain or fiber can, therefore not be used directly. The use of Dyneema was not common during the sample time of the Deepstar report and was, therefore, not reported. Though Dyneema is becoming increasingly popular, polyester continues to be used in mooring lines, often favoured for its price advantage and distinct characteristics, such as elasticity. Polyester lines are more elastic than Dyneema, which is beneficial for mooring applications as they can absorb energy and reduce peak loads on the mooring system when subjected to loads from environmental forces. While Dyneema has superior strength, it is a low-stretch material, so it does not absorb shock loads as effectively. To get a sense of failures to be expected, polyester is looked at, as this is present in the report and has the closest resemblance to Dyneema from the options. Thus, information from the graph does not directly carry over to the TetraSpar project with a chain-Dyneema mooring system.

The Deepstar report indicates that there is not one failure location. However, failures often occur at interfaces between line and vessel, connectors between different line types or connections between line segments and elements like spring buoys, clump weights, and tri-plates. Chain contributes to 54% of mooring line failures and is thus the main contributor to mooring line failure. Figure 3.13 shows no failures in the chain's mid-line, while there are *only* failures in the mid-line for polyester. This can be explained by noting that the chain is often replaced by polyester lines for the mid-segment of the mooring line to lower self-weight and save on cost. Failure in the middle part of the chain is, therefore, less common. Fibres are not often used in the splash and touchdown zones due to the high amount of marine growth, UV and harsh environment, and the risk for abrasion and particle ingress after touchdown. The mooring line's first section, from the TetraSpar's fairlead, is made of Dyneema. This is, however, not in the splash zone as the fairlead is permanently submerged and will, therefore, not suffer from the complications mentioned above.

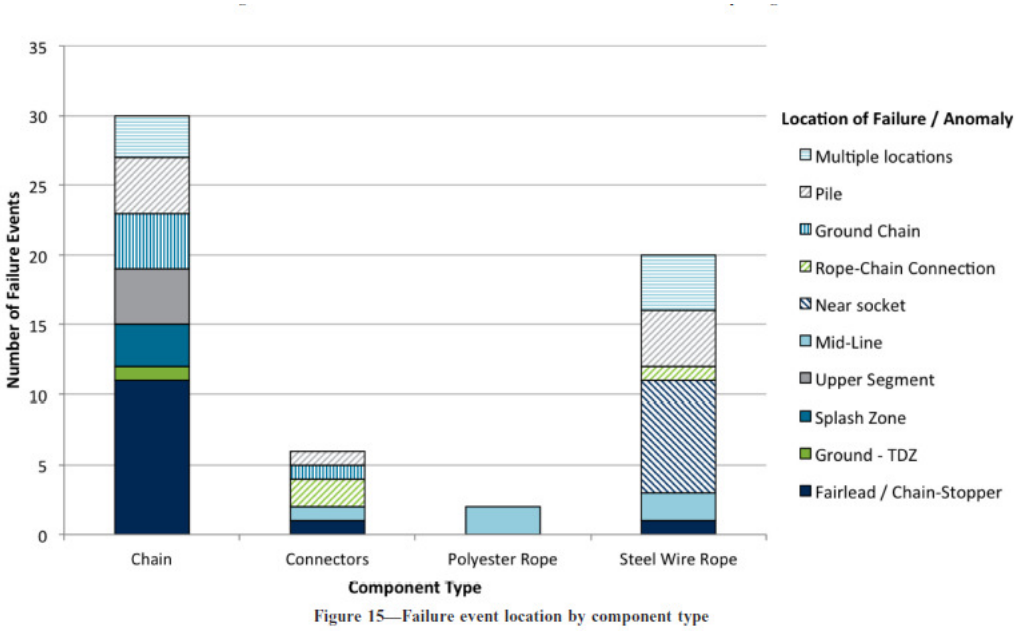

Figure 3.13: Location of failure[11]

3.3.6. Failure modes

It is a popular misconception that mooring lines fail due to overloading from severe weather. In other words, the mooring system was subjected to a severe environmental event, and part of the lines simply snapped under overload, and the design parameters were exceeded. Various other failure causes, rather than just weather overload, were to blame for most failures. These failure mechanisms included Out of plane bending fatigue, pitting corrosion, flawed flash welds, unauthorised chain repair, chain hocking (knotting) due to twist, low fracture toughness, and many others.[26] Failures still happen often during extreme weather events as this are moments which stress the mooring line, but the underlying failure mechanism is not overload.

Chain is overrepresented concerning fibre in the Deepstar study because it is an integral part of almost all permanent mooring systems. There is, therefore, more knowledge on the cause of failure for chains represented in figure 3.14. A total of 64% of failures in chain is attributed to a combination of fatigue and corrosion.[11] As chain is a part of the TetraSpar system and chain is often the culprit in mooring line failure, with fatigue and corrosion the main contributor, this will be further analysed. Another analysis of six incidents from mobile units in Norwegian waters reported that the leading cause of fibre ropes is 50% mechanical damage and 50% installation error. [1] Similarly, Deepstar noted that external damage was the most common cause of failure for synthetic fibre rope. External damage, classified as mechanical damage in the figure on chain 3.14, was most commonly caused by remote operated vehicle (ROV) tether or other work lines rubbing against the wire rope or synthetic fibre rope during routine inspections resulting in damage.[41]

Synthetic fibre abrasion and particle ingress

Wear from dragging the rope over the seabed is rarely damaging in soft silts and muds but can become significant in coarse sand seabeds, which, like sandpaper, will abrade the fibres.[8] It should also be mentioned that synthetic fibres like Dyneema often have a protective layer. Wear from dragging the fibre mooring line across the seabed is typically minimal in soft silts and muds but can become substantial on coarse sand seabeds, which abrade the fibres like sandpaper[8]. It is worth noting that synthetic fibres, such as Dyneema, often include a protective layer to mitigate this wear. Particle ingress is an important factor in using polyester mooring lines and is so for Dyneema as well. It has been observed that small particles allowed to be embedded into the inner load-bearing fibres of synthetic ropes can reduce the MBL and fatigue life over time. If the line's external protective layer is compromised, barnacle larvae or other tiny marine organisms could infiltrate the line, causing internal damage and deterioration of the line's strength. These issues have prompted regulatory agencies in the Gulf of Mexico to require that

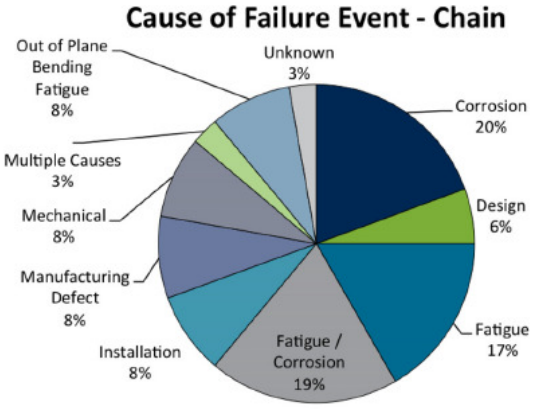

Figure 3.14: Cause of failure event for chain [11]

Table 3.2: Residual strength as result of damage [14]

Category	DM*	Risudual strength (%)
Mild damage	0 <DM <10	84
Modest damage	10 <DM <50	69
Severe damage	50 <DM <100	29

*DM is damage as percentage of crossectional area

polyester mooring lines never contact the sea bed. To prevent such an occurrence, mooring designers and installation contractors take this requirement into account when developing and installing the mooring system.[44]

Mooring touchdown should be minimal for the TetraSpar due to the natural buoyancy of Dyneema. This will cause the line to float and not touch the seafloor in case of mooring line failure. The end of the Dyneema line will also have some splice or connector, making the end heavier and causing a touchdown in case the mooring line hangs slack after the mooring line fails. Lastly, Dyneema is still less common in mooring systems, and it is reasonable to say that designs will be made using polyester also, which is not naturally buoyant.

Fatigue

Fatigue accumulates damage in material over time due to fluctuating stresses, as introduced in the introduction. Failure typically occurs after the component has experienced a certain number of load fluctuations, which cause accumulated damage to reach a critical level.

There are two main approaches to fatigue analysis:

- The S-N approach uses stress-life cumulative damage models to predict fatigue life based on cumulative fatigue damage.
- The fracture mechanics approach uses fatigue crack growth models to examine the fracture behaviour of mechanical elements under dynamic loading.

In straightforward cases, the S-N approach is preferred, owing to its simplicity and status as a well-established method. In the context of mooring lines, fatigue life is affected by cyclic loading, corrosion, wear, and initial defects. Hostile environments such as seawater can accelerate the initiation and growth of fatigue cracks, particularly in the presence of mean tensile stresses, as present in mooring lines. Mooring line failures have occurred due to crack propagation in chain links, which can be accelerated by corrosion.[12][26]

Statistics from the oil and gas industry show that fatigue is one of the main causes of mooring line failure. The same can be expected for FOWTs, which have livelier motions than FPUs due to their smaller size and lower weight. These platform motions create cyclic tensions in the mooring lines, reducing their fatigue lives accordingly. [26]

Chain twist
After ML failure, relatively large excursions are expected, which could result in the remaining mooring lines losing tension and hanging slack. A study done in 2006 did research into the torsion of mooring chains and highlighted that torsion in mooring chains might develop relatively high and potentially destructive stresses in a chain link which is in a high state of twist under relatively modest loads or in a low twist state but with high axial load.[35] This could be when a mooring chain becomes hockled or when the chain is dragged over the seafloor, putting torsion on a chain link.

The research showed the same principle stress was obtained for a tension that is 25 times higher when a larger (13 against 28 degrees) twist is applied. This will lower fatigue life and increase crack growth when chains become hockled. In the case of studded mooring chains, where the links are specifically designed to resist twisting, the likelihood of hockling is generally reduced. The studs act as spacers between the links, helping maintain the proper alignment and preventing the links from twisting into a hockled state.[35]

3.3.7. Behavior after failure
Zhang et al. presented a study in 2022 on the changed behaviour of a FOWT after mooring line failure. The research uses the OC4 DeepCwind FOWT with the NREL 5 MW wind turbine at 200 m water depth with three catenary mooring lines, similar to the TetraSpar FOWT. The research concluded that after upwind line failure, significant peaks occurred in the tensions of the remaining lines. Figure 3.15 shows the load cases used and the fairlead tension in one of the remaining mooring lines in normal- and broken-line cases for a mooring line failure of an upwind mooring line. The mean tensions decreased under the broken-line condition for the steady-state responses, but the standard deviations showed an opposite trend. In addition, line failure generally decreased the maximum line tension, and the effect of line fracture on the standard deviations of the line tensions was more significant compared to the mean and maximum values. The turbine shows a periodic movement in a surge direction with a lower frequency but larger amplitude. The low-frequency periodic movements can be attributed to low-frequency second-order drift forces and a lower mooring stiffness. The research indicates that higher environmental intensity does not automatically increase maximum mooring force when comparing intact and broken states. Rather, environmental conditions that correspond with the surge frequency affecting the FOWT result in greater excursion amplitudes, leading to higher relative peak forces.[45]

No. of load cases	Mean wind speed (m/s)	Significant wave height (m)	Wave peak period (s)	Turbulence intensity of wind (%)	State of the wind turbine
1	8	2.5	9.8	15	Operating
2	12	3.1	10.1	13	Operating
3	16	3.9	10.4	12	Operating
4	25	5.7	11.3	10	Operating

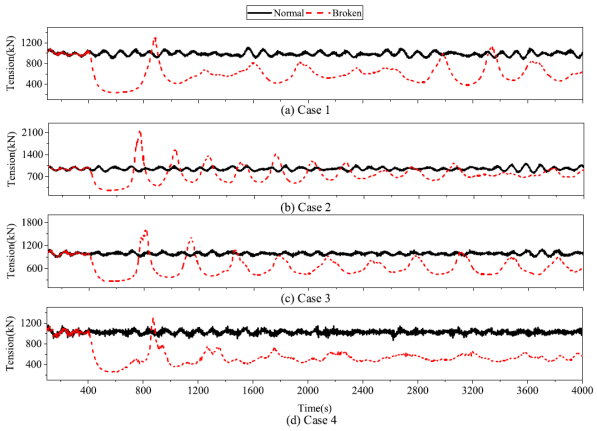

Figure 3.15: Load cases for simulations and time histories of fairlead tension under the normal- and broken-line conditions[45]

3.4. Fault tree analysis
A FTA is a well-known technique used to evaluate the dependability of a system. It involves representing the logical connections between faults and their causes through a directed acyclic graph consisting of two types of nodes: events and gates. The events are the occurrences within the system, which can be basic or intermediate and are represented through logic gates that demonstrate the process of failure

evolution. FTA is a deductive process where the analysis starts from the top event and works backwards towards the leaves of the tree to identify the root causes of the system failure. FTA can be analysed at two levels: qualitative and quantitative. Qualitative analysis reduces the fault tree to minimal cut sets, which are combinations of basic events necessary and sufficient to cause the top event. The cut-set approach in fault tree analysis helps identify the critical components and subsystems for system reliability and maintenance. It allows analysts to focus on the most critical elements of a system and prioritise maintenance and inspection activities accordingly. Quantitative analysis involves calculating the probability of occurrence of the top event and other reliability indices. The most commonly used logic gates in FTA are AND and OR gates. The probability of a gate's output event depends on the type of the gate as well as input event probabilities. An AND gate represents the intersection of the events attached to the gate. Assuming A and B are two independent events, then the probability of their intersection is just the product of their probabilities.[21] Thus,

$$P(A \text{ AND } B) = P(A \cap B) = P(A) \times P(B)$$

On the other hand, an OR gate corresponds to set union and thus the probability of the OR gate output is given by:

$$P(A \text{ OR } B) = P(A \cup B) = P(A) + P(B) - P(A \cap B)$$

Kang et al. made a in-depth FTA of FOWTs in 2018. Failure rates of relevant offshore structures were

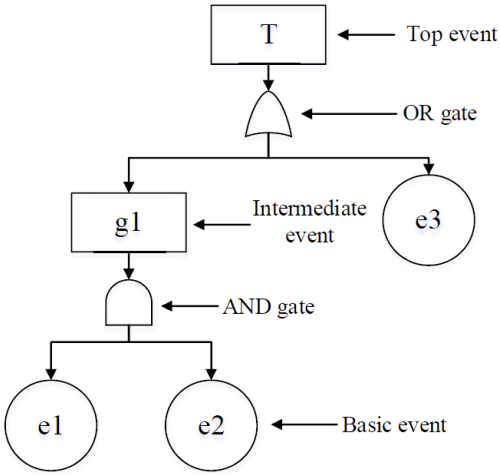

Figure 3.16: Structure of a fault tree[21]

collected from previous studies, reports and reliability databases. Historical failure data of basic events are required to implement the quantitative FTA, which is difficult to achieve due to the insufficient FOWT samples. Data on the FOWT's floating foundation and mooring system are estimated by integrating failure cases of offshore structures.[21]

Kang et al. divided the FOWT into eight subsystems according to the functions: support structures, pitch and hydraulic system, gearbox, generator, speed train, electronic components, blades system and yaw system. The support structure is subdivided into mooring system failure, tower failure and floating foundation failure. Mooring system failure is of importance for this thesis and is further explained. Figure 3.17 and table 3.3 show sub-component, mooring system failure, in greater detail, data and parts of the FTA not showing mooring failure related information is excluded.

Using failure rates and the FTA presented by Kang et al. for mooring system failure, a failure rate of 1.26E-4 per hour, which translates to 1.11 mooring system failures per year per three-line FOWT. This is not for a mooring line but for the complete mooring system. Abnormal stress is the main factor that should be considered to optimise the mooring lines' reliability. According to Kang et al., anchor and fairlead failure are the second and third most prominent contributors to mooring system malfunction.

End of 2022 Mahmood Shafiee published a failure analysis of a spar buoy FOWT system based on the OC3-Hywind spar-type platform moored to the seabed with three anchor piles. The floating platform supports the NREL 5 MW reference wind turbine with a rotor diameter of 126 meters. It is moored with

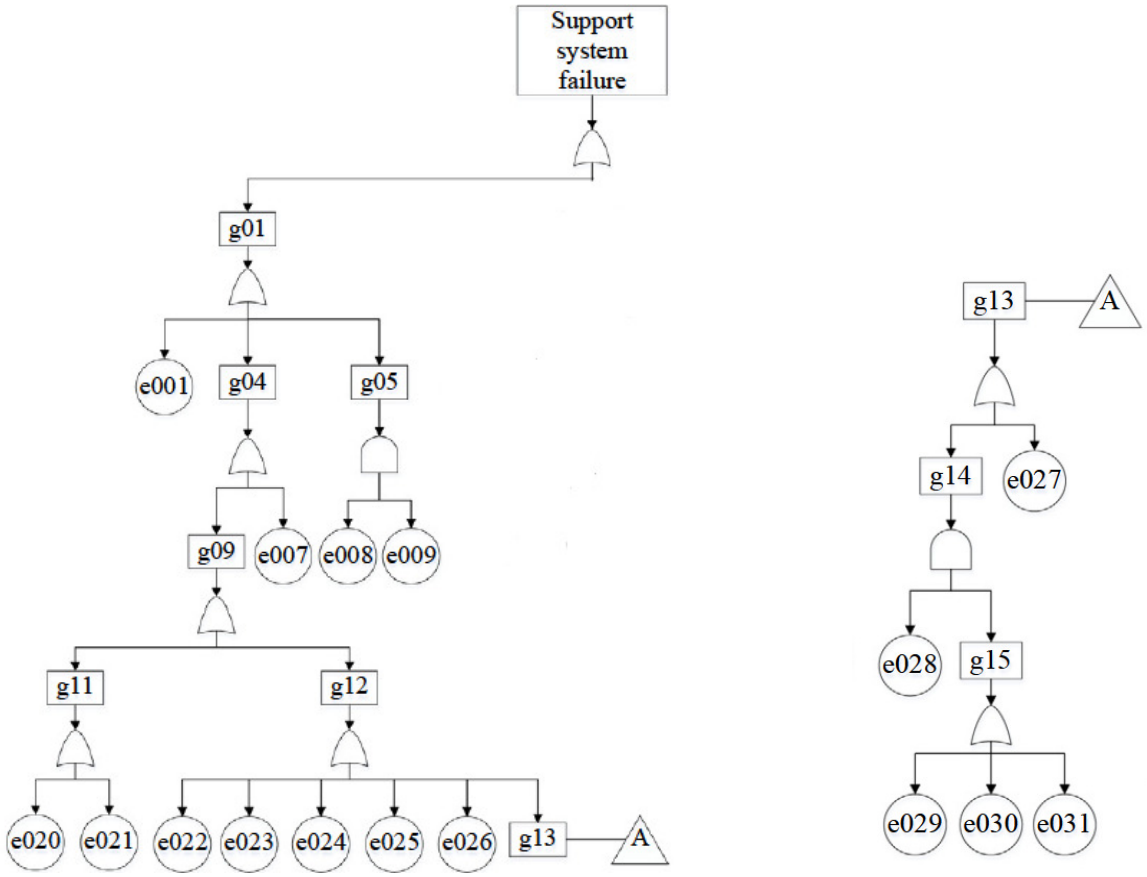

Figure 3.17: Fault tree diagram of a FOWT[21]

Table 3.3: Failure rates and Logic gates[21]

Basic events	Codes	Failure rates (h-1)
Human error	e001	6.00E-06
Anchor failure	e007	1.80E-05
Poor operation environment	e008	7.80E-05
Insufficient emergency measures	e009	1.00E-06
Fairlead corrosion	e020	1.00E-05
Fairlead fatigue	e021	1.70E-05
Transitional chain wear	e022	1.01E-05
Friction chain wear	e023	6.93E-06
Mooring winch failure	e024	8.00E-06
Buoys friction chain wear	e025	4.19E-06
Anchor pickup device damaged	e026	5.56E-06
Abnormal stress	e027	4.07E-05
Invalid maintenance	e028	3.78E-05
Mooring lines wear	e029	1.60E-05
Mooring lines fatigue	e030	1.70E-05
Mooring lines corrosion	e031	5.38E-06

Logic gates	Codes
Mooring system failure	g01
Devices failure	g04
Extreme sea conditions	g05
Other devices failure	g09
Fairlead failure	g11
Mooring lines broken	g12
Mooring lines breakage	g13
Mooring lines wear	g14
Accumulating wear	g15

a three-leg catenary mooring system at a water depth of 320 m. Contrary to the research of Kang et al., which was based on FOW as a whole and thus generalised the FOWT, the research of Mahmood Shafiee is on a spar-type FOWT with many similarities to the TetraSpar project and additionally considers the mooring system as a separate system in the FTA. The most considerable difference is the use of pile anchors instead of DEAs and a water depth that is 1.5 times the water depth of the TetraSpar's at 205 m

against 320 m. The forces and movements of the OC3-Hywind spar will be different to the TetraSpar; however, it serves as a good comparison. Failure information of the FOWT sub-assemblies is collected from previous studies, industry databases such as 4C Offshore, as well as the reports published by floating wind power companies such as Equinor,BW Ideol, Principle Power and the previous studies include work done by Kang et al.[39]

Using failure rates and the FTA presented by Shafiee for mooring system failure, a failure rate of 1.25E-4 h^{-1} (per hour per FOWT) is found, resulting in 1.10 mooring system failures per year per FOWT.

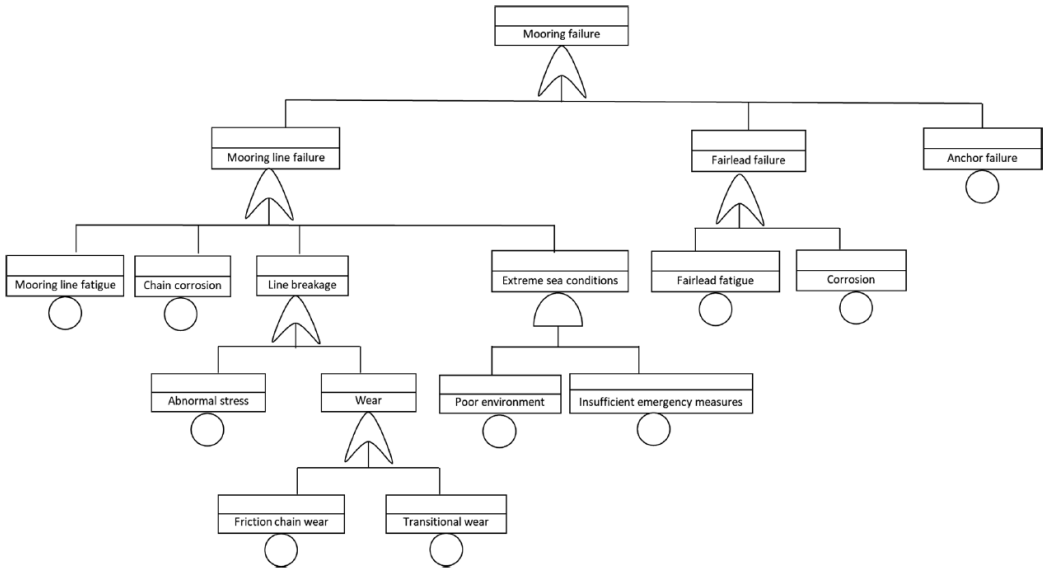

Figure 3.18: Fault tree diagram of a spar-buoy mooring system[39]

Table 3.4: failure rates of the basic events for a mooring system[39]

Basic / intermediate event			**Failure rate (h-1)**
Mooring line failure	Mooring line fatigue		1.70E-05
	Chain corrosion		5.38E-06
	Mooring lines breakage	Abnormal stress	4.07E-05
		Friction chain wear	6.93E-06
		Transitional chain wear	1.01E-05
	Extreme sea conditions	Poor operation environment	7.80E-05
		Insufficient emergency measures	1.00E-06
Fairlead failure	Fairlead fatigue		1.70E-05
	Corrosion		1.00E-05
Anchor failure			1.80E-05

Both Kang et al. and M. Shafiee found a similar failure rate. That they are the same could mean three things, both studies used the same sources and therefore ended up with the same results, M. Shafiee used Kang et al. as a basis for his mooring line failure, or they arrived at the same conclusion independently, proving a correct result. It is unclear from the research papers to which of the three options the similarities can be attributed. It should be noted that 1.1 is very high compared to statistical mooring failure of 2.2E–3 per mooring line per year found by the Deepstar report. For a three-leg mooring system, this would be 6.6E-3 mooring failures per year, a probability 167 times lower than the probability found using the FTA. Shafiee points out that although FPUs and FOWTs mooring systems fundamentally work similarly, there are also several differences, causing them to have a different, shorter lifespans. Statistical mooring failure found for FPUs might be a conservative estimate for FOW mooring line failure due to the limited budget to compete with other renewable energy sources and the lower safety factors. Research into floating wind is relatively new when looking at offshore industry research as a whole. In 2018 only 12 FOWT were operating, compared to around 50 turbines in 2022.

Between 2018 and 2022, when research by Kang et al. and Shafiee was published, respectively, more knowledge was gained about floating wind. Therefore updating failure rates and understanding of FOWT components, this did however, not lead to a change in the mooring system failure rate.[38]

3.5. Conclusion

Drag embedment anchors are often favoured for floating wind applications because of their straightforward installation, compatibility with many soil types and cost-effective pricing. Consequently, they are anticipated to be used in future offshore projects. Nevertheless, the anchor's holding power may be compromised if the force direction reverses post a mooring line failure.

In cohesionless soils like sand and gravel, recovery loads typically range from 20% to 30%. In contrast, in soft cohesive soils such as clays and silts, the recovery loads can reach up to 110%-140% of the installation load or peak stress experienced. However, this becomes a concern only if two out of three mooring lines fail.

The anchor has been tested for performance under side loading up to approximately the maximum angle associated with mooring line failure. The results demonstrate reliable resistance to increased side loads, showcasing stable performance. Depending on the tension level and side angle, the anchor either adjusts itself in the pull direction or withstands the new tension without movement.

There is a risk of large horizontal movements compared to intact after mooring line failure in surge, sway, and yaw due to low-frequency second-order wave drift forces causing peak loads and large force amplitude in the mooring system. The effect increases following a mooring line failure due to reduced mooring stiffness. Despite a lower mean force due to a lower pre tension in the mooring line, the force amplitude and period may increase after failure, potentially escalating fatigue.

Historical data on mooring line failures from the Deepstar report reveal that 54% of failures were due to chains, which is a key component of the TetraSpar. Fatigue, corrosion, or a combination of both contribute to 64% of chain failures. The other TetraSpar mooring system component is Dyneema fibre which, while not extensively covered in historical studies due to its recent development, is expected to fail mainly due to installation errors or mechanical damage as seen in other fibre mooring line parts.

A failure rate of 2.2E-3 per mooring line per year has been noted, which significantly exceeds the DNV standard of 1E-4 per mooring line per year. If extrapolated to a floating wind turbine with three mooring lines, the failure rate would be 6.6E-3. However, this is still lower than the failure rate suggested by a fault tree analysis conducted on a spar-type floating wind turbine, at 1.1 mooring line failures per FOWT with three mooring lines, a failure rate 167 times higher compared with historical data presented by the Deepstar report.

Deepstar's research also uncovers an intriguing ratio of single to multiple line failures, suggesting a 1 to 5 ratio. It should be noted, however, that this research is based on data from oil and gas sectors where multiple mooring lines (8-12 or more) are often used. As these lines are grouped and potentially experience similar loading and failure mode development, they could fail simultaneously. Although no information on grouping was provided in the study, this hypothesis remains plausible.

4

Research plan

4.1. Research question

Three-leg mooring systems may present certain risks compared to mooring systems supporting more mooring lines to be cost-competitive with other renewable energy sources. Decreasing installation, maintenance and procurement costs by lowering the number of mooring lines installed to the minimum is a quick way of lowering costs considering the significant cost part of mooring lines of the total system. However, is the cost reduction worth it, considering the increased risk this brings to the FOWT and the entire field? One broken FOWT mooring line could be a problem, but setting one loose into a field of FOWTs could cause substantial financial and reputation loss. When one mooring line breaks, the repair could take more than six months, depending on spare part philosophy, before a vessel is chartered and weather allows maintenance if cost and safety are prioritised. Knowing if the mooring system integrity is preserved after one mooring line failure and will do so for the months to come without the need for intermediate site visits is essential. Knowing the weak link to mooring system failure after mooring line failure is crucial for creating a system with a ALARP risk. The main objective of ALARP, short for as low as reasonably practicable, is to reduce the risks associated with a particular operation or activity to the lowest possible level while considering the practicality and cost-effectiveness of the risk mitigation measures, which will be further expanded on in the next section. Considering the identified concerns, the following research questions are established:

Main-research question

- *Are the risks of a three-leg mooring system of a floating offshore wind turbine ALARP?*

Sub-research questions

- *What causes mooring line failure?*
- *What consequences does mooring line failure have for the system?*
- *What are additional failure mechanisms after mooring line failure?*
- *How are the additional failure mechanisms affecting the reliability?*
- *What is the probability that one mooring line failure results in complete mooring system failure?*

4.2. ALARP

As mentioned in the previous section, ALARP stands for 'as low as reasonably practicable'. It is a principle used in risk management, particularly in industries like offshore oil and gas where safety is paramount, a principle which carries over to offshore renewable energy. The ALARP principle implies that the risks associated with a particular activity should be reduced to the lowest level that can be achieved without inducing disproportionate costs or effort.

The ALARP process aims to demonstrate that the level of residual risk after all risk control measures have been applied, is tolerable. The residual risk is deemed ALARP when further risk reduction is not practicable or if the cost (money, time or trouble) is grossly disproportionate to the risk reduction achieved.

Compared to offshore oil and gas, where structures are often manned, and damage could lead to environmental harm, risks are lower for FOW. Contrary to oil and gas, a damaged structure is favoured to wait for repair till the repair and maintenance campaign in the summer due to the large number of expected failures for a complete FOW field having hundreds of mooring lines and the lower financial and environmental consequences of FOWT failure in comparison to FPUs. The shift in mentality regarding repair window will cause other factors to introduce risks that must be accounted for.

The process of determining whether a system's risks are ALARP involves several steps:

- Risk Identification: Identify all potential hazards associated with the offshore operation, which is mooring line failure in this case. These hazards may include operational, environmental, and personnel health and safety risks.
- Risk Analysis: Evaluate the risks associated with each identified hazard. This evaluation is typically done using quantitative methods, such as failure mode and effect analysis (FMEA), event tree analysis (ETA) or fault tree analysis (FTA), with the latter used in this research together with simulations to determine failure rates. The analysis considers the likelihood of each hazard occurring and the potential severity of its impact.
- Risk Evaluation: Compare the level of risk found in the analysis phase with risk acceptance criteria, which refers to the level of risk deemed tolerable or acceptable in a specific context or situation. If the risk is above the acceptance criteria, it must be reduced.
- Risk Reduction: Identify measures to reduce the risk. Risk reduction might involve changes to design or operations, new safety system implementation, or increased personnel training.
- Cost-Benefit Analysis: Evaluate the cost of implementing each risk reduction measure against the reduced risk benefit. The objective is to identify measures that reduce the greatest risk for the lowest cost.
- Documentation: Document the whole process, demonstrating that all potential risks have been identified and assessed and that reasonable measures have been taken to reduce the risk to an acceptable level.

Risk acceptance criteria are crucial for risk management and decision-making in the offshore industry. They guide the identification of significant risks and the development and prioritisation of risk mitigation measures. This research aims to evaluate the shift in risk levels between scenarios with intact and broken lines, disregarding the absolute risk level concerning the risk acceptance criteria. A substantial increase in the failure rate may suggest that risks are not ALARP when the TetraSpar is left unattended after mooring line failure till the repair campaign, pressing for immediate intervention after mooring line failure.

While a quantitative cost-benefit analysis will not be conducted in this study, it will be factored into the recommendations provided in the conclusion.

The ALARP process is iterative. If the level of risk remains too high after implementing risk reduction measures, the process must be repeated, identifying further measures to reduce risk. It is important to note that while the ALARP principle helps to manage and reduce risk, it does not eliminate risk entirely. Some residual risk will remain even when all practicable measures have been taken. The ALARP process ensures that this risk is understood and managed to an acceptable level.

4.3. Assumptions

To set out the borders and limits of the research and answer the research questions, assumptions are made:

Repair time is six months:
Emergency solutions would require going out in bad weather, risking lives, scrambling for vessels and having all spare parts ready at all times, costing money. If the same problems are present in FOW as in FPUs and maybe even more severe, it is expected that the top event will happen multiple times in the lifetime of a FOW field. Doing all repairs in a single campaign during calm weather is sensible. A repair time window of six months is therefore assumed to, on average, bridge winter weather in the North Sea.

The complete mooring system fails after the second mooring line failure of a three-line mooring system:
DEAs are tested for side loading within the range of 60 degrees, an angle expected after mooring line failure of a three-line mooring system. DEAs are, however, not designed for forces in opposite direction. Recovery forces of a DEA in cohesionless soils like sand and gravel typically range from 20% to 30% of the installation load or the peak stress experienced by the anchor. A force coming 180 degrees from the installed direction could cause the FOWT to set a drift into the field. Next to problems associated with DEAs, rotation around the anchor causing twist or interaction of the Dyneema mooring line with the keel of the TetraSpar could cause the mooring line to break, keeping in mind the six-month repair time.

The power cable fails within repair time:
Due to the large excursions and the power cable's low breaking strength and bending radius, it is assumed the cable will lose functionality shortly after the mooring line failure and fail, most definitely within the repair window of 6 months. The power cable failure will be expected, therefore, will not be considered in the analysis and will not influence the excursion of the floater after the top event.

The first mooring line is broken:
It will not be further investigated if a mooring line failure will occur beyond known statistics about mooring line failure, but rather if the first failure will lead to the second failure within the repair window.

Mooring line failure occurs at the top of the mooring line:
Should the mooring line break at the anchor, the chain would be dragged back and forth, likely coming into contact with the floater's keel. Due to its low abrasion resistance compared to chain, the Dyneema may be abraded and cut by surface roughness and sharp objects, separating the mooring line at the top. If the break occurs lower in the Dyneema, it is not expected to create significant changes compared to a separation at the fairlead, owing to Dyneema's low density. While a low mooring line failure near the anchor could alter the transient effect, it is assumed to fail at the top and have no impact on the system in this thesis.

The OrcaFlex model used is correct:
A model of the TetraSpar FOWT is provided in the modelling software Orcaflex. This model is assumed to be correctly modelled using the software.

Station keeping is lost when the turbine capsizes:
In the event of a turbine capsizing, the remaining mooring lines are anticipated to fail shortly after that. The collision of the turbine blades with the water could create sharp fragments, causing the fibre sections of the mooring lines to fail due to undesired contact with the floating structure and the potentially sharp edges of the damaged wind turbine blades. A turbine capsizing is undesirable in itself, but the capsized state will also be regarded as a failed state associated with complete mooring system failure.

The turbine tower did not fail due to the first mooring line failure:
The introduction suggests that accelerations of the turbine tower could potentially impact its structural integrity. Absolute certainty is lacking if this will lead to damage. In the context of this study, it is assumed that the turbine does not sustain any damage during the transient phase following a mooring line failure.

RNA heading is assumed to play an insignificant role in stability:
To simplify simulations, this study assumes that the weight of the RNA, situated atop the turbine tower, does not significantly influence stability regarding the heading.

4.4. Method

Previous research on mooring line failure, conducted by Deepstar, and a FTA by M. Shafiee, will be integrated with insights obtained from OrcaFlex simulations and comparable research carried out by C. Zhang et al.citezhang2022effects.

A FTA on a spar-type FOWT failure is used and altered to determine the probability that one mooring line failure results in a second mooring line failure and, thus, consequently, complete mooring system failure.[39] Alterations to the fault tree are made by researching the changes to the system after the first mooring line failure and the effects this has on the mooring system.

The failure modes found by M.Shafiee are split up into two categories: unchanged failure modes and altered failure modes. Unchanged failure modes will be left unchanged as they are not expected to be influenced by mooring line failure, thus retaining their failure rate. Altered failure modes will be assessed for their change in failure rate. Using cases and simulations found in C. Zhang et al., simplified calculations demonstrate the possible effect on fatigue of the mooring lines and fairleads.

Next to failure modes found by M.Shafiee, new failure modes are identified, and an attempt is made to find the failure rate. These new failure modes are simulated in OrcaFlex using a simplified correlated wind-wave heading scatter diagram over different return period storms.

If possible, changes in failure rates and new failure rates are applied to the FTA of M.Shafiee. Results are discussed, and possible solutions reducing risks are presented, following the ALARP method (identify, analyse, evaluate, reduce risk, assess cost-effectiveness and document).

5

Failure modes

Upon mooring line failure, the behaviour of a FOWT is significantly altered, resulting in three main scenarios. First, unexpected loadings can elevate the absolute stress in parts, potentially causing damage and system failure. Second, altered motions can accelerate fatigue accumulation, compromising safety margins and possibly leading to component failures, both during the failure state and afterwards, due to increased fatigue damage sustained in this state. The new state introduces instability risks and may result in positions not initially considered, presenting new challenges.

We can classify failure modes of the Tetraspar's mooring system into three categories based on failure modes presented in the FTA work by M.Shafiee, as presented in the literature study section 3.4. These include:

- Unchanged failure modes: These continue unabated regardless of mooring line failure, such as the effects of corrosion.
- Altered failure modes: The altered dynamics of the FOWT could affect fatigue development in components like fairleads or mooring chains. These failure modes were already present in an intact state but became more problematic after mooring line failure.
- New failure modes: These failure modes, though considered insignificant in the intact state, become problematic in the broken line state or are specific to Tetraspar, such as the potential for turbine capsizing, keel line snap loads, and contact of fibre mooring line parts with the seafloor. These particular failure modes were not included in the FTA work conducted by M. Shafiee.

Subsequent sections will delve deeper into these altered and new failure modes, where failure modes deemed unchanged will not be further discussed. The aim is to estimate the failure rates of new modes and understand how existing failure modes change, thereby enhancing our knowledge of FOWT behaviour during and after mooring line failure.

5.1. New failure modes

The left side of the bow tie is analysed, an analysis method introduced in the introduction, for a second mooring line failure. Without showing the complete bow tie analysis, two new viable failure modes emerge: the instance where Dyneema breaks due to contact with the seabed, referred to as 'fibre touchdown', and turbine capsizing. Turbine capsizing can be subdivided into two causes: instability and failure of the keel suspension line due to snap loads. Although not entirely new, these scenarios become pertinent to floating wind systems, particularly the Tetraspar, when comparing a broken-line mooring system to an intact one. As described in the literature, an intact mooring system is designed such that the fibre mooring line avoids contact with the seabed during regular operation and the floating structure remains stable. Capsizing could occur in an intact state under harsh environmental conditions combined with a 'freak wave'. However, this is not typically accounted for in designs, as accounting for the risks associated with, for example, a million-year wave is considered excessive.

5.1.1. simulation

Contrary to existing failure modes, there is no good estimate of the failure rate of these "new" failure modes. This failure rate is estimated using an OrcaFlex model of the Tetraspar and known local environmental conditions. The known local environmental conditions for the location of the Tetraspar carry one problem, the wind, wave and current environmental metocean data are only known independently of each other. At the same time, the force on the Tetraspar mooring system is a combination of the three variables. To overcome this problem, Principia, an engineering company that initially did simulations for the Tetraspar project, estimated a correlated wind-wave heading scatter diagram, shown in figure 5.1, and further explained in the section 'Scatter diagram' of this chapter. The current is assumed to be colinear to the wind direction as the current is wind driven at this location. This process generates 34 non-zero combinations of wind/current and wave directions, each associated with a unique scatter case value (SCV), with the scatter cases read from top to bottom and left to right, as indicated by the blue arrow. The scatter table depicts the likelihood of these specific environmental combinations arising at the Tetraspar's location. Each combination's probability is denoted by its SCV; a higher SCV corresponds to an increased probability of occurrence. However, the SCV does not reflect the potential for failure or the intensity of the environmental combination. Using the cases presented in figure 5.1 and Orcaflex, a set of simulations is done to test what environmental conditions will trigger the new failure modes for the Tetraspar.

The 34 unique combinations, also called cases, from the scatter diagram of wind/current and wave

		WIND heading												
		0deg	30deg	60deg	90deg	120deg	150deg	180deg	210deg	240deg	270deg	300deg	330deg	OMNI
Wave heading	0deg	0.33												0.33
	30deg		0.06											0.06
	60deg			0.06										0.06
	90deg				0.04									0.04
	120deg					0.14								0.14
	150deg					1.54	2.30							3.84
	180deg						13.49	1.50						14.99
	210deg						1.10	8.76	1.10					10.95
	240deg							3.47	3.47	4.62				11.56
	270deg								2.41	1.61	6.42	3.21	2.41	16.06
	300deg	1.16	0.37	0.31	0.40	1.32						3.30	9.75	16.60
	330deg	9.67	2.55	2.29	3.05	3.82						1.02	3.05	25.45
	OMNI	11.2	3.0	2.7	3.5	6.8	16.9	13.7	7.0	6.2	6.4	7.5	15.2	100

Figure 5.1: Correlated wind-wave heading scatter diagram assumption by Prinicipia

direction are evaluated over varying return periods (RPs) conditions to identify the environmental conditions at which specific events occur. An example of such a new failure mode is Tetraspar capsize, which could happen given that the environmental forces are strong enough and in the right direction. The simulations search for the discrete moment for what environmental intensity and for which directions this specific event stops happening, where environmental intensity is decreased in steps. This method is simplified using the abstract model, equation 5.1. British Standards recommend doing design tests for permanent structures with extreme environmental events with a return period of 500 to 1000 years. Consequently, a maximum RP of 1000 years is set for the simulations. It is economically unreasonable to design beyond this RP; hence, the offshore structure's failure beyond these extremes is commonly accepted from an engineer's view. The RP is reduced in steps from 1000 years until it reaches a point where the environmental combinations do not trigger the specific event. The last RP to trigger the event is recorded, expressed as the average frequency of occurrence E shown in table 5.1, which is the reciprocal of the return period. The Poisson distribution is not applied here instead of the reciprocal, though it might serve as a superior representation compared to the reciprocal. This selection is explained in the conclusion (Section 7.2.7). The return period is decreased in nine fixed steps, created by roughly dividing the previous value by two, presented in table 5.1. This approach is applied to all three mooring lines independently because the environmental intensity and occurrence are not spread uniformly over all directions, as seen in figure 2.3. Therefore, all three independent line breaks will cause a different situation and thus have to be run independently. Scatter cases that did not trigger an event during a storm with a return period of 1000 years will be attributed $E = 0$ because 1000 years is a limit for economical design. Upon summing all combinations of E multiplied by the SCV, the sum is divided by the total sum of all $SCVs$ (T). In this table, the total sum (T) is 100. This conversion is necessary as probability takes a value between 0 and 1, with 0 indicating that a failure is impossible and 1 indicating that a failure is certain.[37]

To summarise, the proposed method involves 34 cases, comprising combinations of wind/current and wave conditions, across ten return periods and for three mooring lines, totalling 1020 simulations. Each simulation is executed in OrcaFlex and analysed for the three new failure modes (instability, snap loads, and fibre touchdown). The maximum value of E (corresponding to the lowest return period) is recorded for each mode. This value E is then multiplied by the SCV of the corresponding case. The overall total is calculated by summing the values for all cases and dividing by the total sum of all cases, T. This process provides an annual probability for each event, computed separately for all three mooring lines.

Table 5.1: Return periods used for calculations

Return Period	E (average frequency of occurrence)
1000	0.001
500	0.002
200	0.005
100	0.01
50	0.02
25	0.04
10	0.1
5	0.2
2	0.5
1	1

$$\frac{1}{\mathrm{T}} \sum_{i=1}^{N} E_i * SCV_i = P \tag{5.1}$$

Where: P = Failure probability[1/Year]
E = Largest 'average frequency of occurrence' to trigger an event
SCV = Scatter Case Value
T = Total sum of all SCVs
N = Number of non-zero cases in the scatter table

The forthcoming sections will delve into the simulation-based research methodology, which uses the scatter diagram and equation 5.1. The nuances of the simulation time, scatter diagram, Weibull distribution, joint probability, and the reasoning behind the specific choices will be explained.

Simulation time
The determination of simulation time hinges on several aspects:

- Transient effects: The simulation duration must ensure transient effects have diminished and a new equilibrium is reached.
- Event duration: The time required for the trigger event to occur, usually during or shortly after the transient phase. For instance, when examining the response of a floating structure to a wave period, the simulation should cover the duration of several such periods once transient effects have subsided.
- Wave height: The wind and wave height are simulated using the NPD and Torsethaugen spectra, respectively, which are inherently random and time-varying. This random behaviour causes a variability between wave heights and wind speed in time. These models capture the statistical properties of these environmental loads but do not specify the exact sequence of loadings at every instant in time. Therefore, short simulations might give misleading results because they could randomly coincide with unusually calm or harsh conditions. By running the simulations

longer, the impact of such random variations can be averaged out, providing a more reliable and representative evaluation of the floating structure's performance under typical environmental conditions. The relationship between $H_{\max}$ and H_s, as illustrated with Equation 5.2, further supports this need. Most wave statistics are based on measurements taken at 3-hour intervals, so the simulation time should generally be at most 10800 seconds (3 hours).

- Computational resources: Simulations in OrcaFlex for floating structures are computationally heavy and thus take long to run due to their inherent complexity, necessitating complex fluid-structure interactions, non-linearities, and time-varying responses. Extended simulations quickly accumulate substantial processing time when performing hundreds or thousands of analyses for a structure.

$$H_{\max} = kH_s \left(\frac{1}{2} \ln N\right)^{1/2} \tag{5.2}$$

The minimal simulation time for 'Transient effects' and 'event duration' are determined by observing the simulations. In low-intensity environmental conditions, the transient period is prolonged as the mooring line slowly creeps over the seafloor. While the mooring line continues to creep towards a new equilibrium position, indicating that transient effects have not entirely subsided. The rate of creep is, however, considered negligible in terms of impact and considering the simulation time. Hence, the simulation is deemed valid for very slow creep. The transient effects are assumed to subside, and the event duration will be met after 800 seconds into the simulation. Balancing computational resource constraints and the need for a comprehensive overview, a total simulation duration, including transient, of 1800 seconds (30 minutes) is chosen. Despite being shorter than the one-hour simulation duration used by Principia, the chosen length adequately captures the representative conditions. If repeated, a more extended simulation is advisable to average random variations.

Scatter diagram
An estimation of the joint probability for the Tetraspar location, shown in figure 5.1, is devised as follows:

- Current is always collinear with the wind.
- All collinear cases are maintained.
- From a 120° wind heading, the wave heading is incremented by +30°, and sometimes more, reflecting the trend observed in figure 5.3a.
- Probabilities for wave headings at 300° and 330° are distributed among other wind headings to ensure a balanced fit between wind and wave probabilities.

This arrangement is an assumption; nonetheless, it can be logically justified considering the configuration of the coast.

Weibull distribution
Environmental conditions matching the return period storms from table 5.1 are derived using a three-parameter Weibull distribution (equation 5.3), using the 'location', 'shape' and 'scale' parameters. For each of the 12 sectors (30 degrees each), a set of wind speeds, current speeds, and wave heights are calculated for all return periods. Every environmental variable has its own three-parameter Weibull parameters for all 12 sectors. Using the wave height from the Weibull distribution, the wave period is computed as per equation 5.4. Due to non-disclosure agreements, this data is not shared.

$$u_R = \propto + \beta \left[-\ln\left(\frac{\tau}{pR}\right)\right]^{1/\gamma} \tag{5.3}$$

$$T_p = 6.6H_s^{1/3} \tag{5.4}$$

Where: u_R = Extreme value
$\propto$ = Location
γ = Shape
β = Scale
p = Sector probability
τ = Sample time (current 3 hours, wind 10 mins, wave 1 hour)
R = Return period
H_s = Significant wave height
T_p = Peak period

Joint probability
When conducting storm modelling for offshore structures, the simultaneous occurrence and interdependence of environmental factors are crucial to consider. These extreme conditions may not always coincide, even during severe storms. For example, a 10-year wave might occur concurrently with a 7-year wind, reflecting the complexities of the large-scale weather systems involved. Applying both 10-year wind and wave conditions in a simulation may inadvertently represent a storm more severe than an actual 10-year event.

A joint probability approach can be utilised to obtain a more accurate representation of a 10-year storm. This method considers the correlations between environmental variables and assesses various combinations of conditions. However, implementing this approach necessitates comprehensive datasets of simultaneous wind, wave and current measurements, which are lacking at the Tetraspar location and are costly to acquire. In the absence of such data, an alternative is the N-year rule, with N representing the return period of an extreme value, formerly referred to as R. This rule of thumb pairs the N-year wind, wave and current conditions to simulate an N-year storm, assuming a perfect correlation between these three variables. Although simple and practical, this approach can potentially lead to overdesign due to its conservative nature.[33]

While the N-year rule can be an advantageous starting point for preliminary design or feasibility studies, its basis in a perfect correlation between wind, wave and current events is not universally applicable. In summary, while the N-year rule can provide a valid approximation, its usage requires careful consideration of the limitations and validation against data. More rigorous analysis of the joint distribution of wind and waves is recommended for detailed design, necessitating site-specific variability in metocean conditions and long-term joint probability distribution of extreme wind and waves.

5.1.2. Most probable line failure
The primary focus of this research is on the probability of a second mooring line failure, yet the initial line failure influences this outcome. To accurately include this interdependence, it is essential to determine the failure probability of each of the three lines for an intact system, subsequently factoring this data into the final simulation-based results. Thus, in contrast to the rest of the research that examines the second mooring line failure, this section uniquely addresses the first mooring line failure. Although all three mooring lines are identical, the failure probability per line is not. Figure 2.1 shows the mainland nearby, on the right of the Tetraspar. The mainland strongly influences the prevailing environmental directions, lowering the probability of the occurrence of environmental force from the North-West. As waves are made by wind and travel far to gain energy (fetch), it is impossible to have large waves with long periods coming from land.

For the same reason, the wind is less powerful from land than from the open ocean. Therefore, not all mooring lines see the same failure rate, as some mooring lines see more extreme environmental conditions more often and thus build up more damage. Designers have tried to reduce this problem by applying an asymmetric mooring design regarding the lay-azimuth, therefore making sure the mooring line that takes on the most occurring environmental direction sees relief by shifting the other mooring lines closer. This mitigation will help but will not solve the problem. Considering the difference in mooring load and degradation, a distribution is sought to determine the mooring line with the highest

likelihood of failure. The outcome is presented as a failure probability of a line as a percentage of all lines. These probabilities subsequently contribute to the weighting of results from simulation-based research in this chapter to produce a more accurate representation of reality by assuming not all mooring lines have the same failure probability.

Using equation 5.1, the yearly probability of failure is found per mooring line with the condition that one mooring line has failed for all three new events. If it is certain that a mooring line will fail, then the probability of each individual line failing can be expressed relative to the sum of the failure probabilities for all three lines. The failure probabilities for the three lines shall be denoted as $P1$, $P2$, and $P3$, respectively. The probability that line 1 fails, given that *a* line will fail, assuming it is not known which line failed, can be calculated as:

$$P(Line1Fails|ALineFails) = P1/(P1 + P2 + P3) \tag{5.5}$$

Similarly, the probabilities that line 2 or line 3 fails, given that a line will fail, can be calculated as:

$$P(Line2Fails|ALineFails) = P2/(P1 + P2 + P3)$$

$$P(Line3Fails|ALineFails) = P3/(P1 + P2 + P3)$$

So if, for example, $P1 = 0.2$, $P2 = 0.3$, and $P3 = 0.5$, the probabilities of line 1, line 2, or line 3 failing given that a line will fail would be 0.2, 0.3, and 0.5, respectively. Similarly, if all three lines have the same failure probability, the distribution would be $P1 = P2 = P3 = \frac{1}{3}$. Section 4 on the research plan stating the assumptions states: The first mooring line is broken. It is important to note that these are conditional probabilities, which describe the likelihood of each line failing, given that one line has failed. In reality, the failure probability of a mooring line is in the range 1.1, 2.2E–3, 1E-4 per mooring line per year as found by the fault tree analysis of M. Shafiee, the OTC report by Deepstar and DNV, respectively. Hence, the actual annual probability of failure for the total mooring system is either P_{2nd}*1.1, P_{2nd}*2.2E–3 or P_{2nd}*1E–4, depending on the chosen source. Here P_{2nd} is the probability of failure of the second mooring line, given that the first mooring line has failed, which is the aim of this thesis. Following probability rules presented in the literature:

$$P(A \text{ AND } B) = P(A \cap B) = P(A) \times P(B)$$

The literature study shows a range of failure modes, which are divided in three categories:

- Failure modes environmentally accelerated by environmental forces and thus also sensitive to environmental direction like fatigue(red)
- Failure modes where environmental forces are not the root cause of the failure mode (green)
- Failure modes which are not accelerated by environmental factors but display an overall diminished strength are likely to fail under the direction of environmental loading with the highest occurrence probability(blue)

In the literature review, figure 3.11 depicts the leading causes of mooring line failure. They are categorised using the three categories presented in figure 5.2: red signifies environmentally accelerated failure modes; green indicates failures independent of environmental forces, and blue represents failures that, while uniform across all lines, occur due to environmental force. Even though environmental forces do not instigate green-marked causes, they will ultimately fail because of them. With "mechanical" referring to external factors such as damage from a fish trawler or the umbilical of an ROV. Damage accumulation of red and blue varies with direction, increasing the likelihood of failure from high occurrence directions. In contrast, green is damaged irrespective of occurrence or strength, but its failure is still environmentally induced.

Mooring line wear accelerates when environmental forces align with its direction, increasing mean tension and force amplitude, thereby accelerating fatigue. The occurrence probability of each environmental variable is depicted in figure 5.3a. The three variables are combined to find the resultant environmental force on the Tetraspar of these three variables. The result is then normalised around one, illustrating the occurrence of environmental influence due to the resultant environmental force.

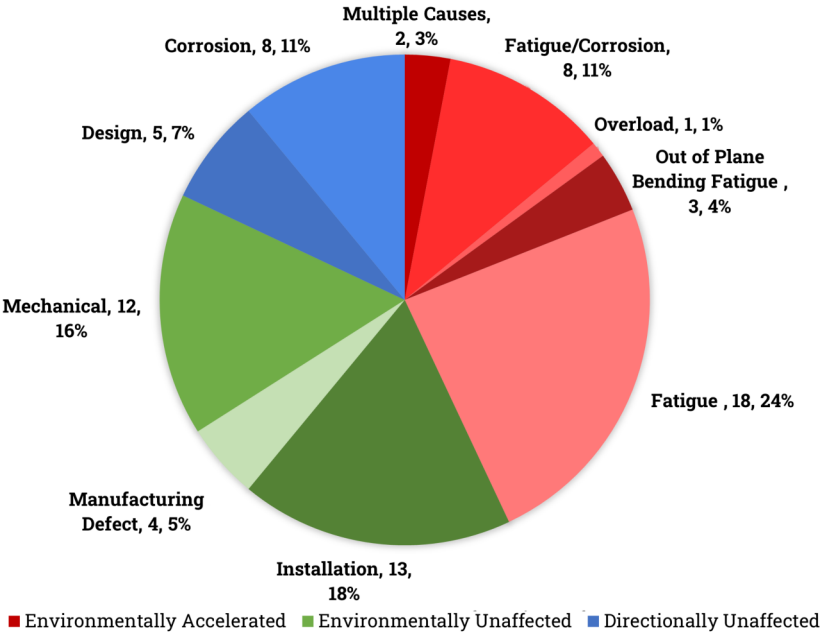

Figure 5.2: Root cause of failure, sorted to effect from environmental direction [Cause, recorded failures, percentage of total] [11]

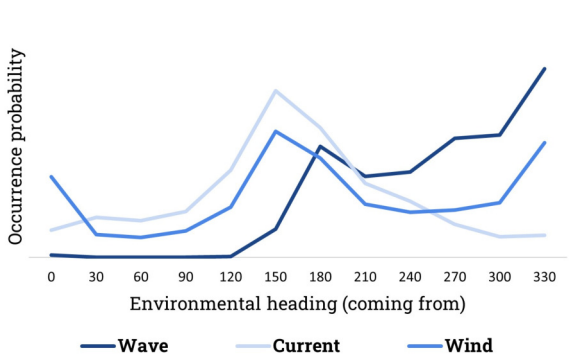

(a) Figure 2.2 repeated, Environment probability vs heading

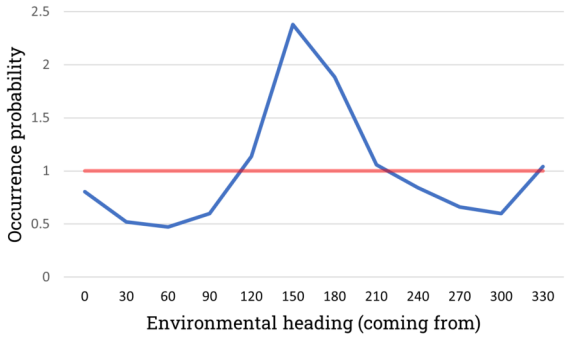

(b) Normalised combined occurrence, normalised around one highlighted in red

Figure 5.3: Occurrence probability

The resultant force is measured by applying the variables separately and contrasting the mooring line force at the fairlead against the static case, thus the pretension, using OrcaFlex simulations. Environmental cases are determined using averages over all directions for both 1-year and 100-year return periods. The return periods are arbitrarily selected and compared, ensuring fair representation (table 5.2). Normalisation allows weighting adjustments for specific mooring line results in future sections. Notably from table 5.2 is the small influence on total environmental force from waves and the slight difference between the influence of all environmental variables between 1-year and 100-year storm conditions, making this a good approach. Henceforth, 1-year conditions will be used for further calculations as this is closer to regular operation, and the difference between the two return periods was deemed small enough.

A straightforward approach is to divide the normalised combined occurrence, depicted in Figure 5.3b, into three sections, each ranging from +60 to -60 degrees from the mooring line azimuth. The area under the graph within these sections is then computed. However, it's worth noting that the load is often shared between two mooring lines, while the third maintains tension due to self-weight and pretension, as illustrated in Figure 5.4. Additionally, the mooring design's asymmetry regarding the lay-azimuth results in an uneven distribution for the same constant force. Consequently, a more accurate

Table 5.2: Environmental influence per variable

	Influence percentage [%]	
	1 Year	**100 Year**
Wind	42.5	37.5
Wave	1.7	0.9
Current	55.8	61.6

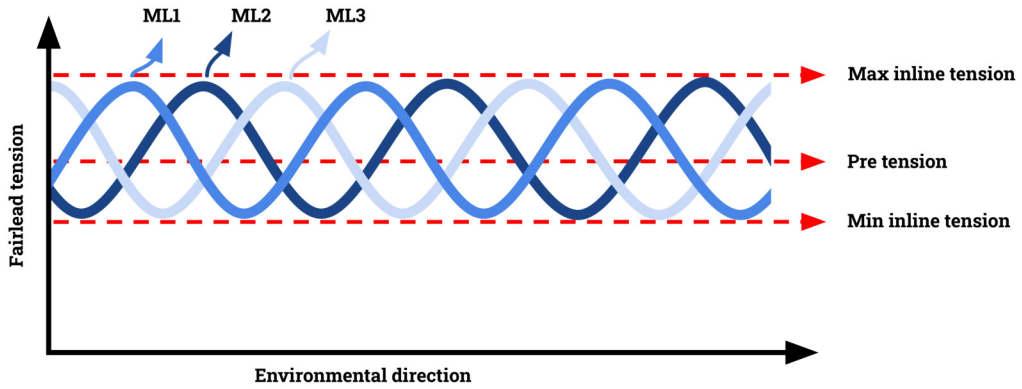

Figure 5.4: Visual representation of mooring line force over environmental direction

approach is needed than the division by +60 and -60 degrees.

An OrcaFlex simulation was performed to capture this effect, wherein a single current speed was rotated across all 12 environmental directions, and the fairlead tension of each mooring line was recorded. Due to the asymmetric design, the same current speed does not deliver the same force profile for every mooring line as depicted in figure 5.5a. Mooring line one is identified as the assisted line, supported by mooring lines two and three, evident by the lower peak as it is directed towards the open ocean and is expected to endure the strongest environmental forces. Among the lines, mooring line three exhibits the highest peak, indicating that it is the most sheltered. Multiplying the results from figures 5.3b and 5.5a yields figure 5.5b, which represents the relative failure probability for each line over all directions. The relative area under each line of figure 5.5b indicates the line-specific relative probability of failure. Results of this area are found in table 5.3.

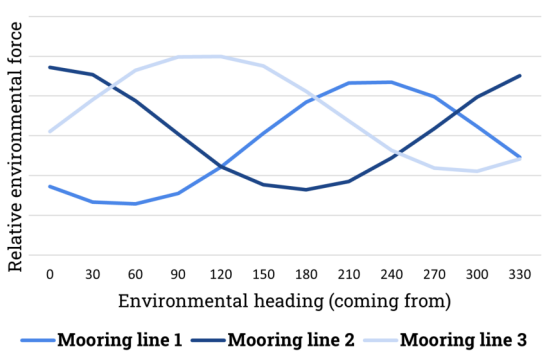

(a) Fairlead tension with fixed current from 360 degrees

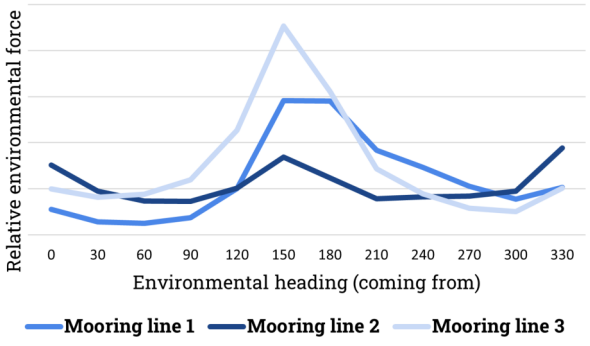

(b) Normalised combined occurrence, combined with mooring line force over environmental direction

Figure 5.5: Weighted relative mooring line

In the event of manufacturing defects, mechanical damage or installation problems, the probability is uniformly distributed across all lines ($P1 = P2 = P3 = \frac{1}{3}$). For other failure causes, the distribution varies $P1 = 0.315$, $P2 = 0.287$, and $P3 = 0.398$. This distribution will be adjusted based on findings from

Table 5.3: Weighted relative mooring line failure probability

	Mooring line 1	Mooring line 2	Mooring line 3	Unit
Relative probability	31.5	28.7	39.8	%
Weighted relative probability	32.2	30.5	37.3	%

figure 5.2, leading to a 39% evenly distributed and a 61% environmentally influenced. The final result is displayed in the second row of table 5.3.

The weighted relative probability found in table 5.3 will be used in section 5.1.6 to weight the results derived in the coming sections.

5.1.3. Turbine instability

The Tetraspar has been tested for 1000-year RP storms, and simulations show that the Tetraspar does not lose stability with all lines intact. When one mooring line fails, this event becomes more likely. Figure 5.6 shows how the force balance changes due to a mooring line failure when the Tetraspar floats between the remaining lines. As pointed out in the introduction, mooring lines cause the stability to decrease after mooring line failure, contrary to their usual role of improving it. In an intact situation, the mooring lines help counter the wind-induced tilt of the turbine. However, with a broken line, this stabilising effect is diminished or could even exacerbate the tilt. When the combination of environmental forces becomes too large, the turbine could become unstable and capsize.

The newly established equilibrium could induce tilt, altering the load distribution across the suspension

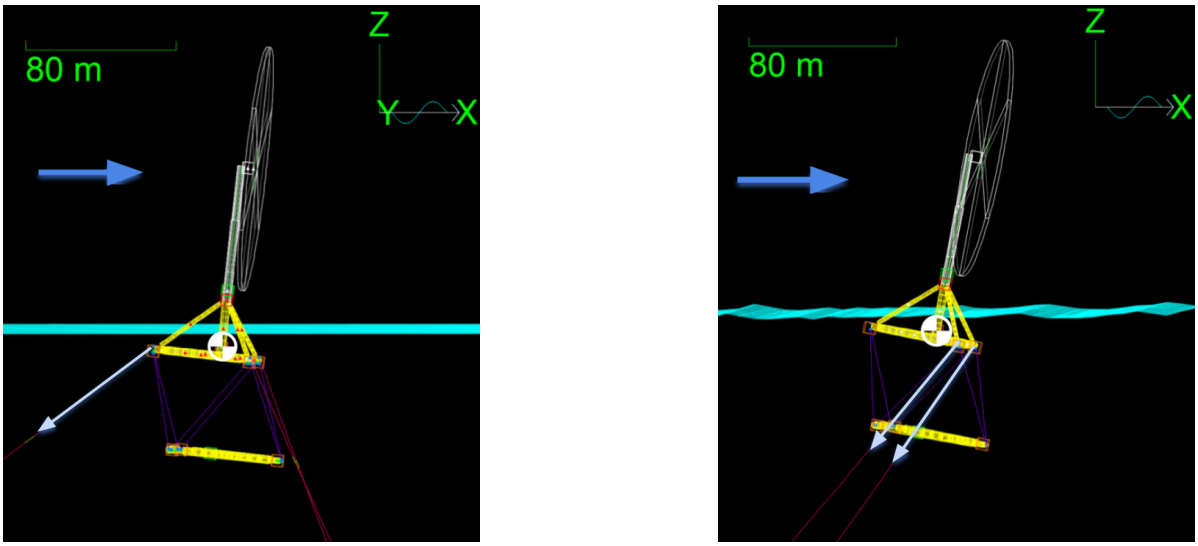

(a) Intact line **(b)** Broken line

Figure 5.6: Difference in line of engagement between intact and broken line

lines and potentially instigating slack line events leading to snap loads and suspension line failure. OrcaFlex simulations have demonstrated that the Tetraspar will capsize irrespective of which suspension line fails. Thus, the Tetraspar's potential for capsizing is not solely due to instability but could also be instigated by the failure of a keel suspension line or the fairlead of this suspension line. The probability of these slack line events causing snap loads is further investigated in the next section 5.1.4.

External factors may lead to the capsizing of the turbine, including the failure of the floater's members to remain buoyant. Such an occurrence could arise from events like a boat impact, accelerated corrosion, or fatigue cracks from altered loads on the floating structure. Unforeseen loads might put undue stress on the fairleads, resulting in cracks and leaks within the floating structure. Capsizing would probably precede sinking as water gathers in one of the Tetraspar's tubular sections. However, this research does not explore the likelihood of a member becoming flooded or whether a single flooded member would cause the Tetraspar to sink.

The capsizing of a turbine marks an unfortunate event, with any chances of operational recovery through mere mooring line replacement effectively eliminated. A capsized Tetraspar could cause the fibre mooring lines to fail due to undesired contact with the floating structure and the potentially sharp edges of the damaged wind turbine blades. However, this research will not explore these elements in further detail. Instead, the capsized state will be regarded as a failed state, associated with complete mooring system failure, consistent with the assumptions in the research plan (Chapter 4).

The probability of instability is tested using methods explained in section 5.1.1 with equation 5.1. The trigger event used to check for instability in the OrcaFlex simulation is the inclination of the turbine, specifically if it has capsized due to instability. An inclination of more than 30 degrees would signify a turbine tip. It can be argued that an inclination of more than 15 degrees might be problematic. However, the specific level of this limit has not been determined. A choice was made to look for a complete failure, not a problematic level.

Table 5.4 shows a clear group for every mooring line at a different group of combinations. A failure of mooring line 2 has the highest product after application of equation 5.1 with a probability of 0.129 per year. Interestingly, when all the average frequency of occurrences (E) of a failure of mooring line 2 are summed without multiplication, the total is the lowest. This result shows how a combination with a high SCV influences the results. Figure 5.7 shows which locations turbine instability is measured and how this relates to the remaining mooring lines where a dotted mooring line indicates a the broken line. The figures confirm the suspicion of instability explained with figure 5.6. In figure 5.7, the darker blue directions correspond to all directions which posses the annual probability of one year ($E = 1$), while the lighter blue includes all directions that represent any non-zero E up to a 1000 year return period, as per table 5.4. In the middle of the figure, the intensity of the leading environmental variable is overlaid, which is wind in this failure mode. It is worrying that turbine capsizing is possible even in a one-year return period storm, indicated in table 5.4 with $E = 1$.

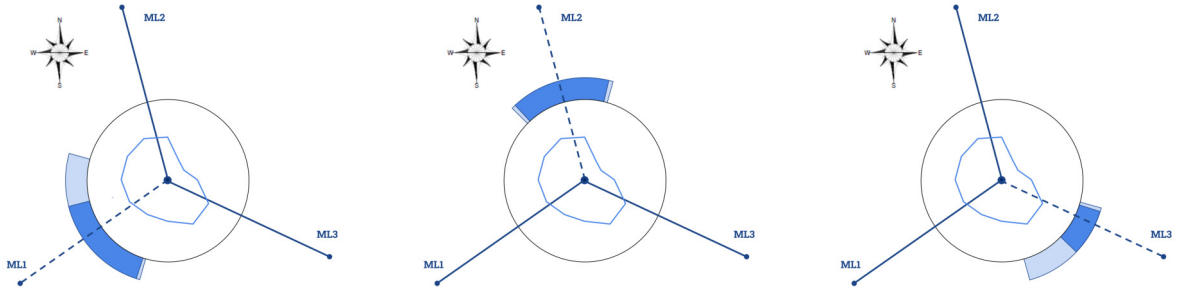

(a) Mooring line 1 failure **(b)** Mooring line 2 failure **(c)** Mooring line 3 failure

Figure 5.7: Wind direction (coming from wrt North) of failures from table 5.4 on instability with wind intensity overlaid from figure 2.3c

5.1.4. Snap load keel-line

In the event of mooring line failure of a FOWT, an increased tilt of the turbine occurs, altering the load distribution across the suspension lines. This imbalance, combined with pitch and roll movements, causes the tension in some of the keel lines to drop in storm events, resulting in slack line events. During the re-engagement, these slack line events generate snap loads which can induce shock on the line material and fairleads, reducing fatigue life. The reduction of fatigue life is most likely only limited to the fairleads and not the suspension lines themselves, as Dyneema has favourable behaviour in fatigue. Besides great fatigue life, Dyneema also has a high tension stiffness, transferring high peak loads to the fairleads in case of snap loads. All assuming the peak loads do not surpass the MBL of the Dyneema lines.[17]

The probability of slack line events is tested using the method explained in section 5.1.1 with equation 5.1, of which the results are presented in table 5.5. End force in all suspension lines is measured to check for slack line events. The static force of a suspension line is between 2500 and 3000 kN; at roughly

Table 5.4: Annual probability of turbine instability using method 5.1

Combination	SCV	ML1 [E]	ML2 [E]	ML3 [E]
1	0.33		0.001	
2	1.16		0.005	
3	9.67		0.005	
4	0.06			
5	0.37			
6	2.55			
7	0.06			
8	0.31			
9	2.29			
10	0.04			
11	0.4			
12	3.05			
13	0.14			1
14	1.54			1
15	1.32			1
16	3.82			1
17	2.3			0.001
18	13.49			
19	1.1			
20	1.5			
21	8.76			
22	3.47			
23	1.1	1		
24	3.47	1		
25	2.41	0.01		
26	4.62	1		
27	1.61	1		
28	6.42	0.005		
29	3.21			
30	3.3			
31	1.02			
32	2.41		0.01	
33	9.75		1	
34	3.05		1	
Product (eq:5.1) [$^1/_{Year}$]		0.109	0.129	0.0682

10% of static force, 300 kN is chosen as a trigger to look for slack lines. When the trigger would have been 50% of static load, snap loads are possible, and when the trigger is 1% of static, snap loads could be more extreme. The trigger 10% of static suspension line force, or more precisely 300 kN, has been chosen arbitrarily.

Table 5.5 shows a high density of keel line slack for combinations 15 to 34 and combinations 2, 5, 8 and 11, making little distinction between different mooring lines. Combination 15 to 34 represents cases with a general direction from 150 degrees to 330 degrees with respect to the North, wind and wave in multiple cases being offset in heading, as explained in previous paragraphs. It feels natural as this excludes degrees coming from land and thus has less environmental strength, as seen with the wave intensity overlaid in figure 5.8. A first gut feeling would be that combinations 2, 5, 8 and 11 would represent the colinear cases as these are combinations with the highest environmental force; however, this is not true. These cases have wind coming from different directions but have in common that wave is incoming from 300 degrees with respect to the North, which is the direction with the strongest intensity for waves. We can therefore conclude that snap loads in the suspension lines are

Table 5.5: Annual probability of snap loads in suspension line of the keel using method 5.1

Combination	SCV	ML1 [E]	ML2 [E]	ML3 [E]
1	0.33		1	
2	1.16	1	1	1
3	9.67		1	
4	0.06			
5	0.37	1	1	0.1
6	2.55		0.001	0.001
7	0.06			
8	0.31	1	1	0.005
9	2.29			
10	0.04			
11	0.4	1	1	1
12	3.05			0.001
13	0.14			1
14	1.54		0.002	1
15	1.32	1	1	1
16	3.82	0.01	0.001	1
17	2.3	1	0.005	1
18	13.49	1	0.005	1
19	1.1	1	0.01	1
20	1.5	1		0.005
21	8.76	1	0.002	0.005
22	3.47	1	0.005	1
23	1.1	1	0.001	
24	3.47	1	0.005	
25	2.41	1	0.01	1
26	4.62	1	0.005	0.005
27	1.61	1	1	1
28	6.42	1	1	1
29	3.21	1	1	1
30	3.3	1	1	1
31	1.02	0.001	1	0.001
32	2.41	1	1	1
33	9.75	0.1	1	1
34	3.05	0.001	1	0.001
Product (eq:5.1) [$^{1}/_{Year}$]		0.637	0.445	0.580

mainly driven by waves. Cases which experienced instability, as seen in table 5.4, also experienced slack lines. However, this is not limited to only cases with instability problems. Cases with a strong wave intensity will generally experience slack lines causing snap loads.

Snap loads are a transient phenomenon that occurs suddenly and is relatively short. Therefore, small simulation time steps are required to accurately capture the effect, significantly increasing the computational effort. Snap loads are typically categorised by a highly nonlinear behaviour. These complexities can make the problem difficult to model accurately. Therefore the level of snap loads is unknown; rather, if snap loads will happen using the simulation.

5.1.5. Fiber touchdown

Wear from dragging the fibre mooring line over the seabed is rarely damaging in soft silts and muds but can become significant in coarse sand seabeds, which, like sandpaper, will abrade the fibres, as explained in the literature study. To prevent this, synthetic fibres like Dyneema often have a protective layer. These layers protect the strength fibres lowering the risk of light damage and particles entering

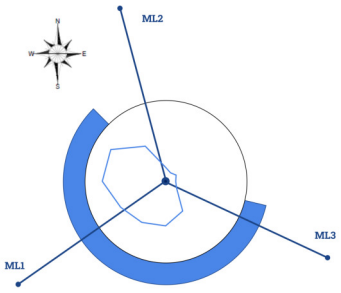

Figure 5.8: Wave direction (coming from wrt North) of failures from table 5.5 on snap loads with wave intensity overlaid from figure 2.3a

the strength fibres influencing the MBL.[8]

Particle ingress in polyester and Dyneema mooring lines, which allows small particles to embed into the load-bearing fibres, reducing their maximum breaking load (MBL) and fatigue life, which has led regulatory agencies in the Gulf of Mexico to mandate that polyester lines must not contact the seabed.

Mooring touchdown should be minimal for the Tetraspar due to the natural buoyancy of Dyneema. This buoyancy will cause the line to float and not touch the seafloor in case of mooring line failure. However, the end of the Dyneema line will have some splice or connector, making the end heavier and causing a touchdown, causing the mooring line to possibly touch the seafloor in case of a slack line. Dyneema is still less common in mooring systems, and it is reasonable to say that designs will also be made using polyester, which is not naturally buoyant.

At the moment of interaction with the seafloor, the mooring line is not in tension but hanging slack, as shown in figure 5.9. The Dyneema protective layer should be sufficient to protect the mooring line from light abrasion without tension. The danger here is snagging the mooring line on subsea structures like the power cable infrastructure, (tension-) devices on its own mooring line or large rocks. When the mooring line regains tension, the line could suffer damage. The probability of Dyneema

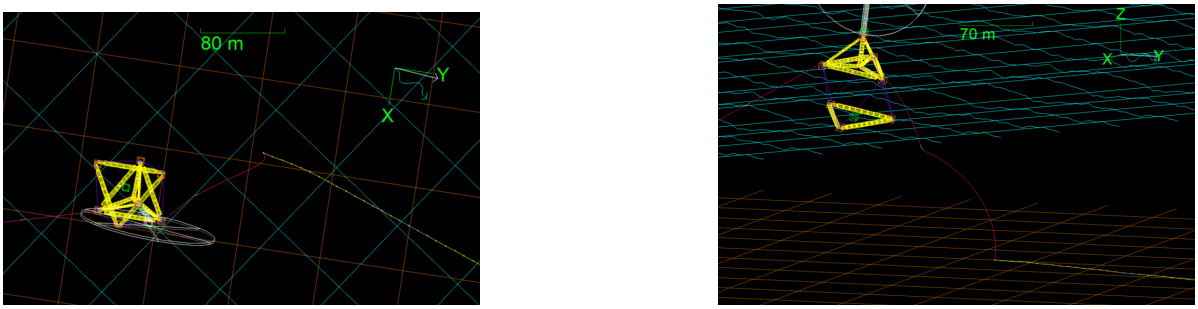

(a) Top view

(b) Side view

Figure 5.9: Orcaflex simulation showing a fibre touchdown with pink lines being Dyneema and yellow lines being chain

contacting the sea floor (Fiber touchdown) is tested using the method explained in section 5.1.1 with equation 5.1. The distance between the last node of the Dyneema part with respect to the anchor and the seafloor is measured. The event was triggered when the distance between this node and the seafloor was zero or less than zero in the OrcaFlex simulation. A node other than the last node would unlikely contact the seafloor before the last node, if at all, as the Dyneema part of the mooring line is buoyant in the simulation. It was unclear from the literature if worldwide rules about a mandatory distance between mooring line fibres and the seafloor other than "never contact the sea bed" exist. Therefore the choice has been made to choose the distance, zero or less than zero. Like results from table 5.4 on turbine instability, there are clear groups of blocks per mooring line. However, mooring line one has two blocks. These blocks are attributed to the fact that a fibre touchdown needs strong environmental force in the direction of the mooring line to cause strong drift, resulting in large excursions. There are no 'gaps' in the individual blocks because the effect is wind and current-driven, not wave-driven. As

Table 5.6: Annual probability of Dyneema contact with the sea floor using method 5.1

Combination	SCV	ML1 [E]	ML2 [E]	ML3 [E]
1	0.33			
2	1.16			
3	9.67			
4	0.06			
5	0.37			
6	2.55			
7	0.06			
8	0.31			
9	2.29			
10	0.04			
11	0.4			
12	3.05			
13	0.14	0.01		1
14	1.54	1		1
15	1.32	1		1
16	3.82	1		1
17	2.3	1		1
18	13.49	1		1
19	1.1	1		1
20	1.5	1		1
21	8.76	1		1
22	3.47	1		1
23	1.1			1
24	3.47			1
25	2.41			1
26	4.62		1	
27	1.61		1	
28	6.42	1	1	
29	3.21	1	1	
30	3.3	1	1	
31	1.02	1	1	
32	2.41	1	1	
33	9.75	1	1	
34	3.05	1	1	
Product (eq:5.1) [$^{1}/_{Year}$]		0.665	0.354	0.444

waves attribute less of the total drift force of the FOWT, as can be seen in table 5.2. The environmental combinations are counted per wind block (figure 5.1) and therefore show great grouping when the wind is dominant and less grouping when waves are dominant (table 5.5). Mooring line one has two blocks instead of one compared to mooring lines two and three as both mooring lines two and three see large excursions due to their azimuth directed towards the mainland, with a strong environmental force directed over them. However, when forces are directed between the mooring lines, it is impossible to see forces directed over them and get the excursions needed to get a mooring line touchdown. Figure 5.10 clearly shows how fibre touchdown problems are centred over the mooring lines but never from shore.

The results from table 5.6 only present the probability of a fibre touchdown event happening, not how long this fibre touchdown occurs, what snagging would look like or for which mooring line this occurred, while the last can be concluded from the environmental direction. The results from 5.6 conclude it is worthwhile investigating further.

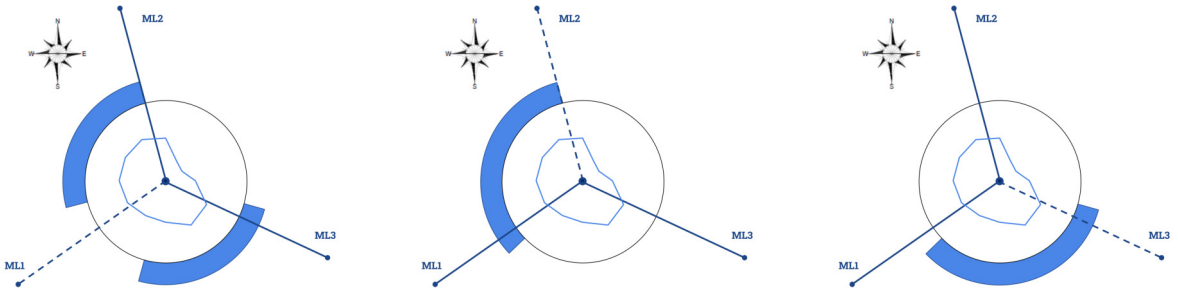

(a) Mooring line 1 failure **(b)** Mooring line 2 failure **(c)** Mooring line 3 failure

Figure 5.10: Wind direction (coming from wrt North) of failures from table 5.6 on fibre touchdown with wind intensity overlaid from figure 2.3c

5.1.6. Intact and Conclusion

Results for intact conditions are calculated using the same methodology outlined in preceding sections, using equation 5.1. A simulation is conducted for an intact condition without losing mooring lines. The results, collected in table 5.7, combine all failure methods. The events depicted here represent up to a one-year storm or none at all, a pattern observed in previous results, although to a lesser extent. Table 5.8 presents the aggregated probability of all three lines, calculated using the methodology explained in section 5.1.2 and using the weighted relative probabilities from table 5.3. It highlights a significant concern of turbine instability following the loss of a mooring line, whilst snap loads and fibre touchdown, previously observed, persist and grow. Turbine instability, though absent in the intact scenario, even during 1000-year storms, becomes a real threat in a broken line condition, potentially causing a capsize in a one-year storm or less, with the exact limit of storm intensity undetermined. The increase of 27.8% for snap loads and 61.0% for fiber touchdown, which can be found in table 5.8, is small, considering this is the yearly probability and will be compared to a longer lifetime in the intact situation. The turbine should survive for six months with an increased probability, while a FOWT in the intact situation should survive 20 years. Because the turbine has to survive for shorter in broken line, a higher probability of failure is often accepted as there is a reduced likelihood of extreme events impacting them.

The severity of events, differing between intact and broken line conditions, is not reflected in these results. Greater pitch angles in a broken line condition could induce larger snap loads than in an intact situation. Thus, while snap load probabilities are comparable in some cases, the impact of these is unaccounted for. In a broken line scenario, fibre touchdown occurs over uncleared seafloor, potentially encountering power cable infrastructure, tensioning devices, or large rocks, thereby possibly damaging the mooring line in case of this line snagging. Thus, comprehensive seafloor clearance or risk mitigation strategies should be considered during layout design. These may include distancing tensioning devices from chain-Dyneema transition points, routing power cables between anchors (an existing common practice), and ensuring power cable anchors do not intersect with possible paths of chain-Dyneema transition points, which is an issue for the Tetraspar. However, a more straightforward solution could be to design the mooring system with a fibre rope length slightly less than the water depth if fibre rope is preferred. The Tetraspar has a Dyneema length of 226 meters from the fairlead. With a water depth of 205 meters, a reduction in Dyneema length of 41 meters considering fairlead depth plus an additional safety margin for wave height, tides and surge changes would suffice to prevent fibre touchdown issues. This would however change the mooring system fundamentally.

Limitations of simulation

Most results fall within the one-year return period category, which was unexpected at the simulation's start. One year is the lowest environmental condition tested and was not intended as a stopping point for all cases. Ideally, testing would continue until no events occurred within a specific return period. Hence, the true instability of some events remains undefined. If events occur during a one-year storm, they might also occur during a one-month storm, though this remains speculative. From the simulations conducted, it is evident that certain combinations pose higher event probabilities. These combinations warrant testing under environmental conditions below a one-year storm return period.

Table 5.7: Annual probability of intact mooring line using method 5.1

Combination	SCV	Instability [E]	Touchdown [E]	Slack [E]
1	0.33			
2	1.16			1
3	9.67			
4	0.06			
5	0.37			1
6	2.55			
7	0.06			
8	0.31			1
9	2.29			
10	0.04			
11	0.4			1
12	3.05			
13	0.14			
14	1.54			
15	1.32			1
16	3.82			
17	2.3		1	
18	13.49		1	
19	1.1		1	
20	1.5		1	
21	8.76		1	
22	3.47		1	
23	1.1			
24	3.47			
25	2.41			
26	4.62			
27	1.61			1
28	6.42		1	1
29	3.21		1	1
30	3.3		1	1
31	1.02			
32	2.41			1
33	9.75			1
34	3.05			
Product (eq:5.1) [$^1/_{Year}$]		0	0.436	0.303

Table 5.8: Weighted total probability of tested events in yearly probability and the increase expressed in per cent

	Broken[$^1/_Y$]	**Intact**[$^1/_Y$]	**Increase [%]**
Instability	0.0999	0	-
Snap load	0.557	0.436	27.8
Fiber touchdown	0.488	0.303	61.0

The low return period of the results could be due to the application of the N-year rule, which typically yields conservative outcomes by assuming the simultaneous occurrence of all N-year storm return variables. This simultaneous occurrence may generate unrealistic results. To rectify this, generating site-specific joint probability data would enhance simulation accuracy, though this is costly. Nevertheless, results indicate the independence of tested event-specific variables. An example is the instability findings, with results suggesting potential capsizing for cases 13 and 16 should mooring line 3 break. Despite experiencing the same wind speed, these cases present a 6.3-fold larger wave height and a period 1.85 times longer yet remain unstable, from which it can be concluded that this event is

wind driven. Additionally, the simulation duration was shorter than desired; hence longer simulation times would yield more averaged random variations improving results.

5.2. Altered failure modes

The altered failure modes are defined by the variations in fatigue within the mooring line and fairlead, stemming from changed motions following a mooring line failure. Rather than displaying absolute results, the findings will be expressed as an increase compared to the FTA research conducted by M. Shafiee.[39]

5.2.1. Natural frequency

Changing the floating structure can be dangerous as natural frequencies of floating structures are tuned to steer clear of frequencies of environmental forces with a high spectral density. When the weight of the Tetraspar is decreased, there could be a risk of approaching these spectral peaks, thus risking more excitement. Two things influence the floater's natural frequency when a mooring line breaks. The weight changes due to the release of the mooring line, and the mooring stiffness is lowered. A floating offshore structure's six degrees of freedom- heave, sway, surge, pitch, roll, and yaw- are split over both events. Where the changes in weight primarily impact the natural frequencies of the heave, pitch, and roll, the decrease in mooring stiffness primarily impacts the natural frequencies of the sway, surge and yaw.

The weight of a mooring line is dropped from one side of the FOWT when a mooring line is lost. This weight shift will cause the Tetraspar to tilt and change the natural frequency. However, The weight is small compared to the total weight of the floater. Using information from section 2, the weight of the mooring line parts is calculated up till and not including the clump weights, which is 4.4×10^4 kg of submerged weight. Comparing this to the weight of the Tetraspar at 5.5×10^6 kg, the mooring line part, which has separated, only makes up 0.8% of the total weight. Therefore, a large alteration in natural frequency is not anticipated for movements most susceptible to a change in weight, being heave, pitch, and roll.

A floating structure's sway, surge and yaw natural frequencies are influenced by the stiffness of the mooring system holding the structure in place. The mooring lines provide a restoring force when environmental conditions displace the structure, and their overall stiffness dictates the speed at which the structure can return to equilibrium.

When a mooring line is lost, the mooring system's total stiffness decreases, leading to a longer period or, in other words, a lower natural frequency. This lower longer period is because less restoring force is available to counteract displacement, making it take longer for the structure to return to its equilibrium position after a displacement.

Conceptually, mooring lines might be thought of as springs. If a spring is stiffer, it will pull back harder when stretched, and the system to which it is attached will oscillate at a higher frequency. If the spring is less stiff (like when a mooring line is lost), it will not pull back as hard, leading to a lower oscillation frequency.

This decrease in natural frequency can influence the structure's dynamic response, particularly if it nears the frequency of wave action or other environmental forces. This proximity could induce resonance, causing significant, potentially hazardous oscillations. Such a phenomenon is vital in considering structural integrity, as the amplitude of force fluctuations largely affects fatigue development. Although the annual number of fluctuations should reduce owing to the extended period, the force amplitude will correspondingly increase.

This thesis will further examine the impact of alterations in period and amplitude for the mooring lines and fairlead, focusing on surge motions. While changes in sway and yaw are anticipated for similar reasons to surge, these modifications are expected to exert less influence on the fatigue development of the mooring lines and fairlead, even though they may introduce additional fluctuations and create a larger angle of incidence with the fairlead. To achieve an understanding of the issue, the analysis is simplified to focus exclusively on surge rather than incorporating sway and yaw. Changes in heave, pitch, and roll are expected to play an insignificant role in the change in development of fatigue

in mooring lines and fairleads. They will, therefore, also be excluded from further research, leaving surge as the focus.

5.2.2. Second-order wave drift force

Mooring systems primarily affect the response of floating structures to low-frequency second-order wave drift force and other environmental variables like wind and current. The mooring system is designed to resist the excursions of the structure.

First-order wave forces, which correspond to the wave frequency, cause high-frequency, small-amplitude oscillations of the floating structure in heave, pitch, and roll. These movements are primarily determined by the structure's shape, buoyancy, mass distribution, and wave characteristics. The mooring system's impact on these first-order wave-induced motions is usually small because the stiffness of the mooring lines is relatively low compared to the hydrostatic stiffness of the floating structure.

However, the mooring system is crucial for limiting the low-frequency, large-amplitude sway, surge, and yaw motions caused by second-order effects. Figure 3.7 clearly shows how heave and pitch strongly correlate to the wave spectrum, while the surge motion has a sizeable low-frequency motion.

When considering the dynamic response of a floating structure, it is essential to account for the combined effects of first-order wave forces, low-frequency second-order wave drift forces, wind and current loads, and the mooring system's restoring and damping forces. Accounting for all these effects typically requires complex numerical modelling or experimental testing.

The literature presented a study by Zhang et al. from 2022 on the changed behaviour of a FOWT after mooring line failure. The research uses the OC4 DeepCwind FOWT with the NREL 5 MW wind turbine at 200 m water depth with three catenary mooring lines, similar to the Tetraspar FOWT. The direction of wind and waves relative to the platform used in the simulations by Zhang et al. are shown in figure 5.12b, where mooring line 1 is broken for all cases.[36]

The cases presented in this research are adopted for further research into the development of fatigue in the mooring line and fatigue development in the fairlead. The same load cases presented in the literature study are presented in figure 5.11 for convenience.[45]

No. of load cases	Mean wind speed (m/s)	Significant wave height (m)	Wave peak period (s)	Turbulence intensity of wind (%)	State of the wind turbine
1	8	2.5	9.8	15	Operating
2	12	3.1	10.1	13	Operating
3	16	3.9	10.4	12	Operating
4	25	5.7	11.3	10	Operating

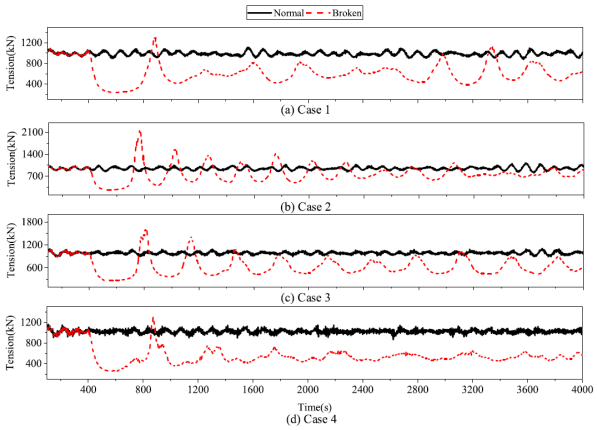

Figure 5.11: Figure 2.2 Repeated, Load cases for simulations and time histories of fairlead tension under the normal- and broken-line conditions[45]

5.2.3. Simulation and differences

Figure 5.11 perfectly represents how surge and sway movements change due to mooring line failure due to low-frequency second-order wave loads. However, because the Tetraspar FOWT and the OC4 FOWT are both FOWTs with three catenary mooring lines at 200 meters of water depth of roughly the same size, they do not see the same second-order forces and move the same. The OC4 project is a semisubmersible in contrast to the spar-type construction of the Tetraspar. This floater's construction is built up of large tubular sections of respectively 12 and 24 meters in diameter on the three corners of the floater as seen in figure 5.12a. This configuration creates a sizeable water-plane area, greatly enhancing

the structure's stability in response to wave action and wind loads. In contrast, a spar-type FOWT has a small water-plane area with a more significant draft, relying on a ballasted keel for stability. The stability of the OC4 FOWT arises from the hydrostatic restoring force, while the stability of Tetraspar designs arises from the low centre of gravity. However, this larger water plane area will also mean a larger vertical wetted surface area around the waterline than Tetraspar FOWT, which causes more effect from second-order drift. The OC4 turbine also weighs more than the Tetraspar, at 1.3×10^7 kg versus 5.5×10^6 kg, almost two and a half times the weight of the Tetraspar. The increased weight could cause higher peaks during the periodic surge motions due to more inertia build-up. However, inertia plays a smaller role in sway and surge directions for floating structures due to the water's damping effect. Unlike in air, damping moderates a structure's motion in water.

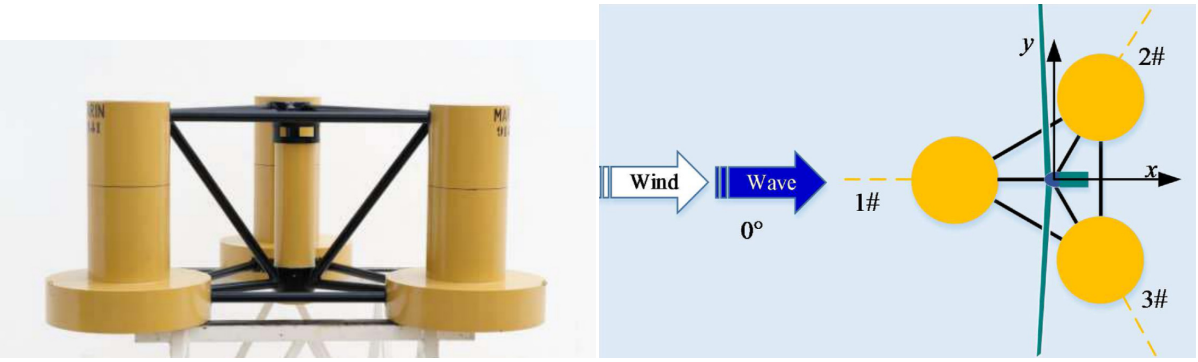

(a) Foundation of the OC4 FOWT[36] **(b)** direction of wind and waves relative to the platform[45]

Figure 5.12: OC4 FOWT

In OrcaFlex, Newman's approximation is used to solve for second-order wave forces in the model used, which might not be a good estimation in this situation. It is observed that Newman's approximation compares well with experiments in deep water and underestimates the experiments in shallow water ($h/\lambda < 0.2$). The location of the Tetraspar considering waves with a period of 10 seconds as per figure 5.11 is well into "deep water" considering the criteria given 205/156.6 = 1.3 with λ as per 5.6. This is consistent with the requirement for Newman's approximation.[32]

$$\lambda = \frac{gT^2}{2\pi} \tag{5.6}$$

However, Newman's approximation tends to lose accuracy when the wavelength becomes significantly

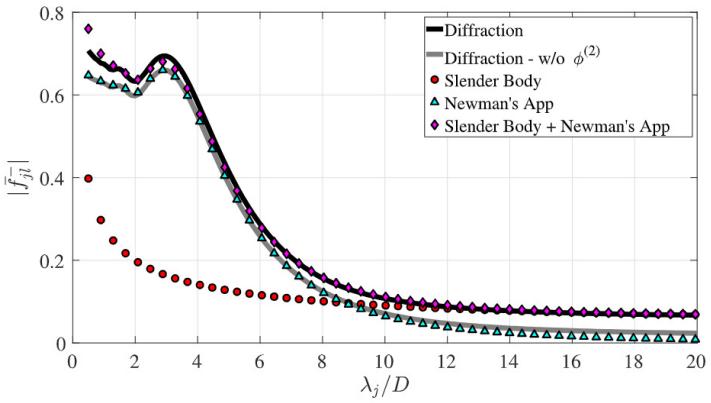

Figure 5.13: Nondimensional horizontal force acting on the bottom mounted cylinder calculated with diffraction theory, slender-body and Newman's approximations[7]

larger than the diameter of the floating structure, which is the case for the TetraSpar, build-up of relatively small tubular brace elements. As the wavelength increases, the real part of the force becomes

increasingly less relevant, which Newman's approximation is primarily based on. On the contrary, the slender-body approximation, which aligns more closely with the imaginary part of the force, performs better in such situations, as seen in figure 5.13 where the black line labeled 'diffraction' is assumed to be the best representation. Thus, the limitations of Newman's approximation become apparent in situations with large wavelengths relative to the structure's diameter, as it fails to account adequately for the dynamics captured by the imaginary part of the force. Tubular brace elements on the TetraSpar have a diameter between 2.2 and 4.3 meters, making the wavelengths relatively large in open ocean conditions compared to TetraSpar brace elements. The wavelength λ is 156.6 for a period T of 10 seconds, giving a ratio of 71 and 36 depending on the brace diameter. Which is far beyond the accepted area presented in figure 5.13.

However, not all members are perpendicular to the incident wave. Therefore, not all members will be 'felt' by the wave drift force as a member of 2.2 to 4.3 meters; thus, the effect of Newmans's approximation will not be lost completely. [7]

The TetraSpar is simulated using the same input presented in figure 5.11 using Orcaflex. Results from the paper are compared to the results from the simulation, where only results from case 3 are presented. Figure 5.14a shows the amplitude is much smaller than is observed in figure 5.11. Fairlead tension is mainly made of noise, making it hard to see the second-order motions. In figure 5.14b, the movement in the x direction (surge) is displayed, showing a better resemblance to the periodic movement seen in figure 5.11. When overlaying a selection presented in figure 5.15a and filtering noise, a similar periodic pattern can be seen in the simulations presented by Zhang et al., presented in figure 5.15b. Results derived in OrcaFlex from the TetraSpar are, however, zoomed in, thus, do not represent the same scale of amplitude. The results from the Orcaflex simulation are thus not the same as those presented in figure 5.11. As discussed, the difference can be attributed to physical differences, like the lower weight or smaller vertical wetted surface area around the waterline. However, it can also be attributed to an unrepresentative simulation. Implementing the full QTF of the TetraSpar could provide more representative results.

The TetraSpar, however, has a minimal waterplane area compared to other semisubmersible type FOWT demos. Therefore, the problem presented in the results is relevant to floating wind. The simulations found by Zhang et al. will therefore be used for further calculations of chain fatigue and fairlead fatigue, knowing the effect will be smaller for the TetraSpar, giving a conservative estimate for the TetraSpar but a realistic estimate for the floating wind industry.

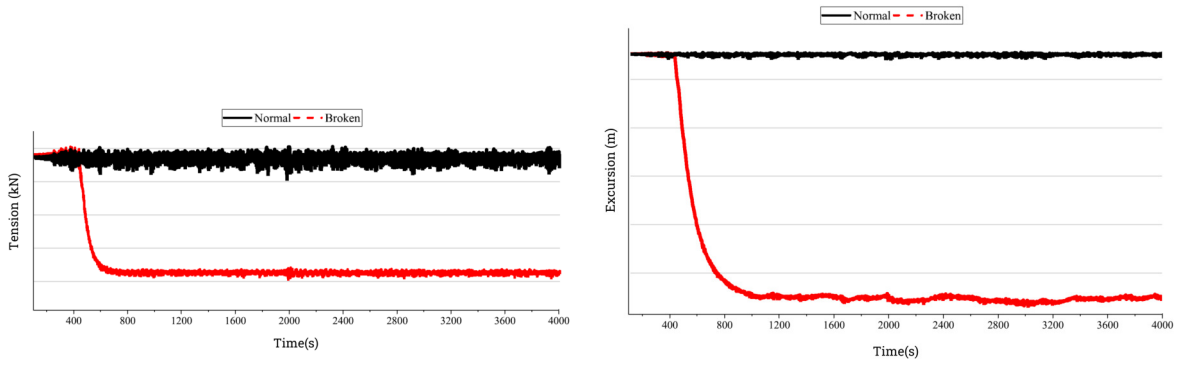

(a) Fairlead tension mooring line two

(b) Surge excursion

Figure 5.14: Results from Case 3

5.2.4. Chain fatigue

After mooring line failure, the mean mooring forces decrease due to lower pretension, but the amplitude and, in some instances, the peak of the force increases. After the transient effects subside, the force amplitude and period of the fairlead tension in the mooring line from 5.18 is simplified and traced to a sinusoidal signal to make a simple fatigue calculation. Fatigue is assumed to be dominant in the chain part of the mooring line, as Dyneema has significantly better fatigue characteristics. The TetraSpar does, however, not have a chain running up to the top of the fairlead. This fatigue development is therefore

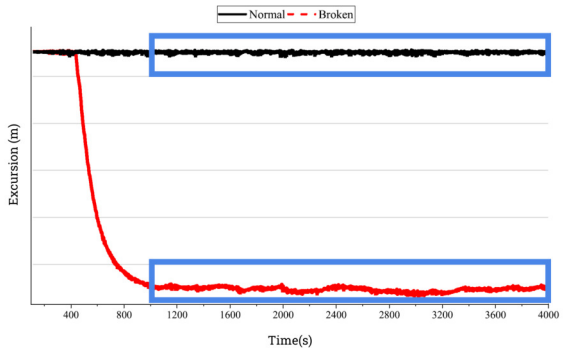

(a) Selection of surge excursion

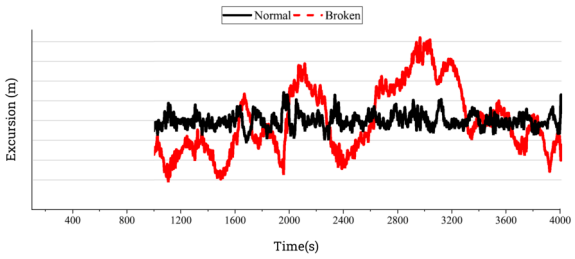

(b) Surge excursion of intact and broken line overlaid, cleaned using moving average

Figure 5.15: Case 3 surge analyzed

assumed to develop in section two of figure 2.5. No significant changes are expected between the fairlead force and the force in the chain of section two as self-weight is nonexistent due to the buoyancy of Dyneema. Figure 5.11 shows how amplitude from the second-order effects becomes less pronounced roughly 1000 seconds after failure. This change could be because the FOWT is transitioning to a new equilibrium. When the mooring lines start to align to the new equilibrium position, the mooring lines are dragged in between the anchors, causing the floater to be in between the two anchors giving more slack to the mooring lines, lowering pre tension even more and increasing the effect. This could, however, also be the build-up of inertia due to drift following mooring line failure.

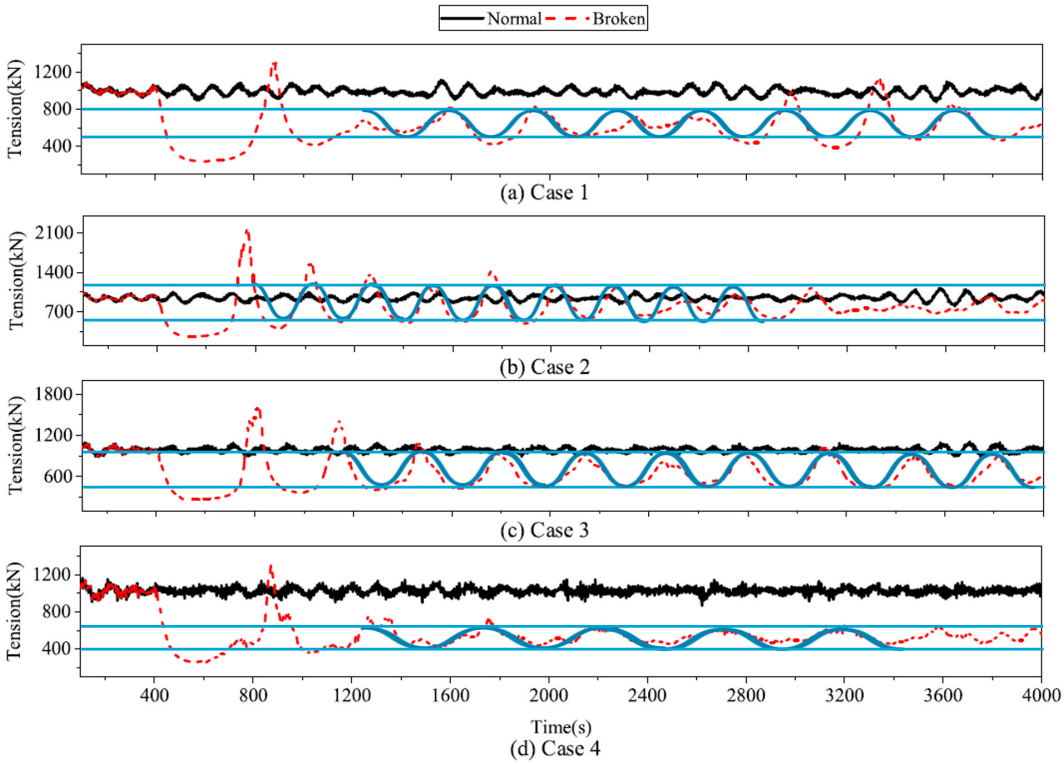

Figure 5.16: Sinusoid fitted to results by Zhang et al.[45]

Using the Palmgren-Miner linear damage rule, damage accumulation is calculated for the intact and broken line situation. This rule involves summing the damage contributions from each stress cycle

Table 5.9: Amplitude and period approximated to fit data from Zhang et al. in figure 5.16[45]

	Intact			Broken		
	Amplitude [kN]			Amplitude [kN]		
	Max	Min	Period [s]	Max	Min	Period [s]
Case 1	1050	950	105	800	500	340
Case 2	1050	850	105	1150	525	245
Case 3	1100	900	115	900	450	333
Case 4	1100	900	60	650	400	475

Table 5.10: 107mm - R4 studlink T-N curve parameters

Nominal Diameter		107	[mm]
Mid-life corroded diameter		105	[mm]
Corroded RBS		621	[MPa]
Cross section		17318	[mm^2]
T-N Curve parameter	K	453.6	-
	m	3	-

using equation 5.7

$$\text{Damage} = \Sigma(\text{N}/\text{N}_\text{k}) \tag{5.7}$$

N is the number of cycles at a particular stress level, and N_K is the number of cycles to failure at that stress level. Mooring line fatigue calculations are based on Tension-Tension fatigue, with damage calculated from a T-N curve, described using the unitless numbers K and m. These unitless numbers are used to calculate the number of cycles to failure N_k using equation 5.9. When a material is repeatedly cycled through a given effective tension range ΔT with a reference breaking strength (RBS) and surpasses the number of cycles to failure N_K, the material has failed. The cross-sectional area of the components is taken as two times the nominal diameter for chains, taking into account the corrosion at mid-life and, thus, the corroded diameter.

To account for the non-zero mean of mooring lines due to self-weight and pre tension in mooring lines, the effective tension range T needs to be shifted. Gerber's model (equation 5.8) is applied to modify the stress range (ΔT_{gerber}) to accommodate the non-zero mean (S_m) as shown in figure 5.17. The amplitude will be increased to accommodate for the non-zero mean. Compared to other methods like Goodman and Soderberg, Gerber's method is generally suitable for ductile materials and is therefore chosen. Table 5.11 shows results from these calculations, and it can be seen that tension is only marginally larger due to the application of Gerber's method (ΔT versus T_{Gerber}). The largest contribution to the fatigue development can be attributed to the magnitude of stress amplitude, not the mean stress.[28]

$$T_{gerber} = \frac{\Delta T}{1 - \frac{S_m}{RBS}} if - RBS < S_m < RBS \tag{5.8}$$

$$N_k = K \left(\frac{T_{gerber}}{RBS} \right)^{-m} \tag{5.9}$$

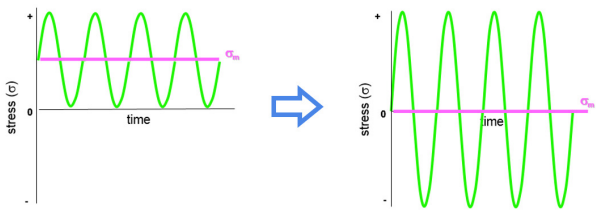

Figure 5.17: Mean stress correction

Table 5.11: Fatigue accumulation comparison Case 3

	Broken-line	**Intact-line**	**Unit**
F_m	675	1000	kN
S_m	39.0	57.7	MPa
ΔF	450	200	kN
ΔT	26.0	11.6	MPa
ΔT_{gerber}	26.1	11.7	MPa
N	94702.7	274226.1	Cycles/year
N_k	6118723.2	68712728.7	Cycles to failure
Damage	0.0155	0.00400	Damage fraction

The damage accumulation is calculated and shown in table 5.11 for Case 3 only. Case 1, 2 and 4 are calculated using the same methodology and presented in Appendix A. For this example, the calculation period is one year, searching for the percentage difference in fatigue development between intact and broken line conditions. The actual period the system would stay in this exact environmental condition could be less than 10 minutes. The same pattern of a longer period with a lower mean stress, but a larger stress amplitude for broken line conditions compared to a higher mean, smaller stress range with a shorter period for intact line mooring system remains. This example shows how mooring fatigue damage accumulation could change due to a mooring line failure. Comparing the broken line and intact line fatigue damage shows there is a 288% increase in mooring line fatigue for Case 3. If mooring lines are designed with enough safety margins, decreasing the fatigue life by a few years is not a problem.

Table 5.12: Percentage increase in fatigue from intact to broken line in the same environmental conditions

	Increase in %
Case 1	144
Case 2	1201
Case 3	288
Case 4	-76

This calculation does not account for the increase in overall fatigue due to the absence of one mooring line. Due to the shifting environmental conditions, the stress and, in turn, fatigue accumulation is spread over all mooring lines during the year. One or two mooring lines, depending on the direction of the environmental forces, are usually dominant in bearing the environmental loads. Due to the absence of the third mooring line, the fatigue accumulation is now spread over two, not three, mooring lines, increasing the fatigue damage on the remaining lines, something not accounted for in this thesis.

Surprisingly and concerning, large amplitudes which cause a strong increase in fatigue are not limited to extreme weather conditions with low probability; instead, Figure 5.11 shows an opposite trend. Moderate weather conditions show more consistent relative large amplitude movements and relative higher peak tensions than high-intensity weather conditions, which show a strong increase in fatigue as seen in table 5.12.

5.2.5. Fairlead fatigue

Due to mooring line failure the excursion of the FOWT will be large compared to normal operation, causing the mooring lines to have an increased angle with the fairlead with respect to regular operation. The largest angle is reached when the FOWT drifts in between the two remaining mooring lines with a theoretical maximum value of 60 degrees. Figure 5.18 shows this situation and the angle between the intact direction of the fairlead and the mooring line.

The fairlead risks not being designed to accommodate the forces the mooring line applies. The two cheeks of the fairlead bracket are designed to carry the force in line with the fairlead and not designed to take on the side loading, which is apparent by the absence of proper side support. The

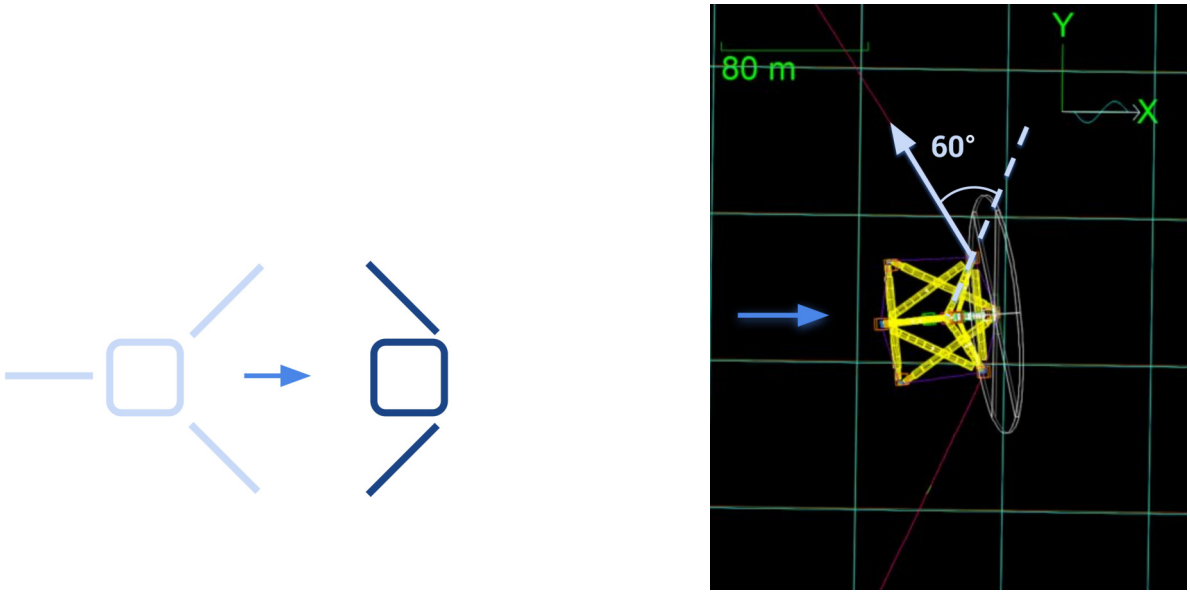

(a) Drift through representation

(b) Maximum fairlead angle

Figure 5.18: Maximum fairlead angle with mooring line simulated with OrcaFlex

change in direction risk higher stresses in the fairlead. It leads to an increase in fatigue and, thus, a decrease in fatigue life.

Figure 5.19: Mooring line fairlead of the TetraSpar FOWT

As outlined in the previous section on chain fatigue (section 5.2.4), the loss of a mooring line not only reduces the mean tension but also extends the period (as depicted in figure 5.11). This sequential effect leads to both an increased period and stress amplitude. A simple representation of the fairlead is given in figure 5.20a, made using Solidworks, which is a modelling software with which a basic finite element analysis (FEA) is done. The dimensions are not an accurate model but are estimated proportional to what can be seen in figure 5.19. Solidworks automatically generates the meshing, and sharp corners in finite element models can cause stiffness irregularities. Therefore, FEA programs might estimate higher stress concentration than actual, even with advanced elements and refined meshes. The FEA made in Solidworks is thus by no means a perfect representation of what is happening in the fairlead but rather a first feeler of what might happen to a fairlead when the intended direction of the force concerning the fairlead is changed due to mooring line failure. FEA simulations are thus complex and small changes can significantly affect the outcome of a FEA and are, therefore, a research topic on its own. This thesis will not focus on perfecting the FEA simulation, nor will it assume the results are accurate. The FEA simu-

lations are used to show that stress concentrations will develop and illustrate the need for extra measures.

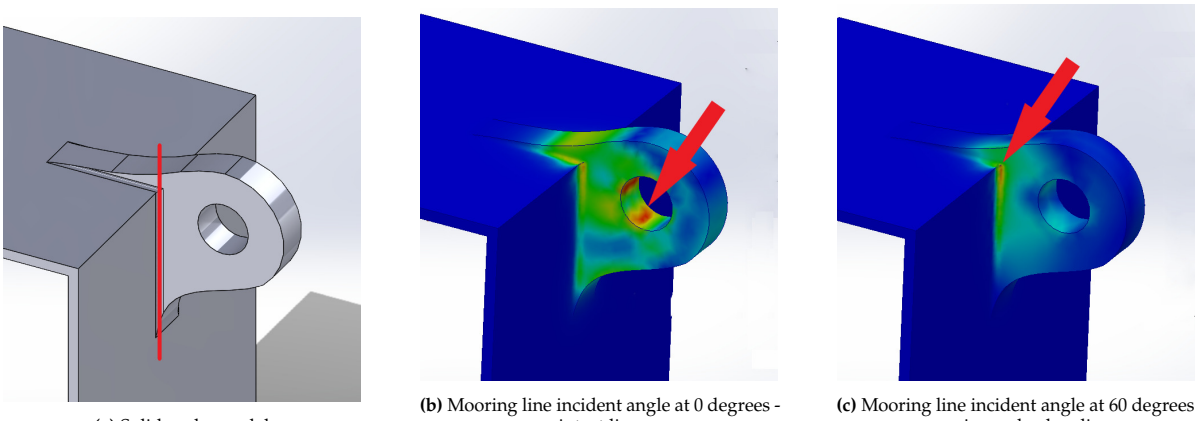

(a) Solidworks model

(b) Mooring line incident angle at 0 degrees - intact line

(c) Mooring line incident angle at 60 degrees - maximum broken line

Figure 5.20: Representation of fairlead forces

The previous section (section 5.2.4) explained and has shown how a lower pretension and thus lower mean tension but a larger stress amplitude increases fatigue development significantly. The same holds in the basis for fairlead fatigue development. The stress amplitude and fatigue development will increase in the fairlead for the same reasons as for mooring line fatigue. Fairlead fatigue is accelerated more after mooring line failure than chain fatigue because fairleads are loaded from the side, introducing stress concentrations. The fairlead is optimally designed to carry loads in line with regular operation. When forces are applied from the side, this will cause stress concentrations in the right-angled joint shown in red in figure 5.20a. Figure 5.20b and 5.20c show how an intact line and broken line at an angle create a different situation regarding stress development, where the red arrow indicates where the peak stress is found. The geometry amplifies fatigue development due to the stress concentration at the right angle. Increased local stresses can initiate and propagate cracks more readily than in areas with uniform stress distribution.

$$N_k = a_D S^{-m} \tag{5.10}$$

Similar to calculations made in the previous section, using Palmgren-Miners rule 5.7, Gerbers equation 5.8, but introducing the new (looking similar to equation 5.9) equation 5.10, with a_D and m material constants sourced from a $S-N$ diagram provided by Principia. Let a_D be the fatigue limit, N_k the cycles to failure, S the stress range, and m the slope on the $S-N$ curve. The value of m for tubular connections is 4 or 5, depending on the particular slope of the $S-N$ curve and the stress range. In high-cycle fatigue, the slope of an $S-N$ curve is typically steeper (with $m = 5$), reflecting reduced tolerance for cyclic stress as the number of cycles increases. Conversely, in low-cycle fatigue, the slope is less steep (with $m = 4$), indicating that the material can endure higher stresses for a more limited number of cycles.

Equation 5.10 shows fatigue life decreases by the power of m and thus by the power of 4 or 5 depending on the stress amplitude. If the stress amplitude increases by 10%, fatigue life will decrease by 46% or 61%, but when stress increases by 100%, fatigue life will decrease by 1500% or 3100%, respectively. The exemplary simulations with 60-degree incident loading, however, insinuated that the increase in stress would be significantly higher than 10%, causing extreme fatigue development. Fairlead fatigue development could exponentially increase when a mooring line is lost. The fairlead should be designed to withstand and efficiently distribute the additional loads to counteract this fatigue acceleration. By introducing adequate gusset's geometric stress concentration, fatigue could be decreased by improving the joint's load-bearing capacity and reducing the stress concentration, thus enhancing the fatigue performance of the structure.

5.2.6. Clump weights

Clump weights have a significant contribution to the motion of floating structures. If used, they are typically added to a short segment of the ground chain near the touch-down zone to increase the

restoring force of a mooring line.

However, clump weights can have integrity issues if not carefully designed. Especially clump weights of half-cast designs tend to fall apart after years of beating up and down in the touch-down zone. Clump weights usually only see vertical motion when excursions are large, and line forces lift the clump weights of the seafloor as intended. Movement of the FOWT to new equilibrium positions will cause the mooring chain to drag over the seafloor, accelerating damage. The problems leading to integrity issues may be accelerated because of the constant movement of mooring chains over the seafloor, where a mooring line failure might instigate the premature failure of clump weights in remaining mooring lines.[26]

The interdependent roles of clump weights are outlined below:

- Mooring stiffness: Clump weights can increase the overall stiffness of the mooring system. A stiffer system can better resist environmental loads and limit the movement of the floating structure, thus providing better stability.
- Limiting excursion: Clump weights can help limit the structure's horizontal movement or excursion. This is crucial in preventing the structure from drifting too far off its intended position.
- Pre tension: Clump weights can create a downward force on the mooring line, creating pre tension. This pre tension can improve the stability of the structure and reduce the likelihood of slack mooring lines, which can lead to snap loads.
- Vertical anchor forces: By increasing the effective weight of the mooring line, clump weights can increase the vertical forces needed to lift the line. By keeping anchor forces horizontal, the anchor's holding power is retained.

The failure of a mooring line substantially alters the mooring system. The role of clump weights is less distinct following mooring line failure. Elements such as damping, mooring stiffness, limiting excursion, and adding pre tension have already undergone significant changes due to the failure; hence clump weights do not provide a significant advantage after mooring line failure. As a result, it is not anticipated that the detachment of clump weights in a broken line situation would compromise system stability to the four factors mentioned above. Nonetheless, vertical anchor forces could pose an issue for FOWT when using DEAs as these are generally not designed for vertical forces, as is the case for the TetraSpar. Depending on the soil type, DEAs lose holding power when vertical forces are applied.

The failure of mooring lines, a scenario anticipated multiple times during the lifespan of a floating wind field, could pose challenging and costly repair issues, particularly if clump weights are damaged and scattered across the seabed. Internal documentation has shown instances of new clump weight detachments occurring at locations where there had been impacts with previously detached clump weights on the seabed. As evident from the imagery of the mooring lines, the chain's friction with the clump weight results in noticeable wear, manifesting as large areas of exposed metal. Thus losing clump weights increases repair and clean-up expenses, thus prompting consideration of opting for safer clump weight designs. Clump weights of a mono-cast design may be more durable than the conventional design, with two half-shells bolted together. In some alternative designs, a segment of a much larger chain is intentionally used to serve the purpose of clump weights. Also, parallel chains ended with large tri-places can be another alternative way to avoid the need for clump weights. However, mooring chains are an expensive component of the mooring system, with mono-cast and half-cast designs providing a more economical alternative to chain parts.[26]

5.2.7. Conclusion

The loss of a mooring line, resulting in minor weight change, negligibly impacts the first-order natural frequency. However, the reduction in mooring stiffness triggers increased movements driven by second-order low-frequency drift forces. Consequently, mooring lines experience greater stress amplitude, though at a lower frequency and reduced mean stress due to decreased pretension.

The elevated stress amplitude significantly increases fatigue development, for one particular case, by 1201%. Second-order motions do not increase with the severity of environmental forces; surprisingly,

Figure 5.21: Clump weights of a mono-cast design fitted on chain [26]

they diminish with respect to the other forces. Regular operating conditions, which have a high probability of occurring, would proportionally cause relative increased fatigue development when comparing intact and broken cases, indicating a strong increase in fatigue during regular operating conditions.

The larger stress amplitude from second-order motions, translating to the fairleads via mooring line tension, accelerates fatigue for the same reason as the mooring line, which is intensified by the right-angled joint geometry of the fairleads. Proper gusset application can distribute stress and reduce stress concentrations, underscoring the importance of considering mooring line failure in fairlead design.

Similar simple design optimisation for designing mooring lines for broken line scenarios is challenging, as they are extensive, interconnected, could fail at any link, and constitute a significant cost portion, making widespread improvements costly.

Providing an exact projection of increased fatigue in mooring lines or fairleads due to line failure and second-order movements is unfeasible with the results obtained. While the results suggest a significant increase in mooring line fatigue, the selected cases do not completely represent the complexity of mooring line or fairlead fatigue.

The four cases of fairlead tension fluctuations used for this research are derived from another turbine which, due to its different geometry, has a very different interaction with waves and resulting second-order wave forces. The fairlead forces derived from the TetraSpar using Orcaflex did not show the same resemblance. This difference can be attributed to the different geometry but also to Newman's approximation which is not valid for this use case. Although beyond this thesis's scope, a comprehensive fatigue analysis using the full QTF would be insightful.

Clump weights significantly contribute to damping motion and improving the efficacy of the FOWTs mooring systems. However, integrity issues can arise, particularly in half-cast designs, exacerbated by ongoing mooring chain movement after mooring line failure. While the detachment of clump weights does not critically destabilise the system, it introduces challenges. Parallel mooring chains, though potentially more expensive, may offer superior durability and should be contemplated for future designs.

When the system remains in a broken state, fatigue accelerates in both the mooring line and the fairlead. This accelerated fatigue does not necessarily become apparent during the period of the damaged line but could manifest later in the structure's lifespan. While the fatigue rate is at an increased level during the six-month repair period, it returns to normal levels once the damaged mooring line is repaired. However, the accelerated fatigue accumulation during this broken period reduces the overall fatigue life, increasing the probability of fatigue failure in the fairlead and mooring line over the remaining lifespan. The design life of the FOWT is 20 years, which means that for six months out of this 20-year design life, the mooring line and fairlead will experience accelerated fatigue accumulation.

The chain mooring line components are classified under Consequence Class 1, using a safety factor 5. Per Palmgren-Miner's rule (damage as cycles to cycles to failure), the accumulated damage for a safe system should be less than 0.2, or 1 over 5, throughout its lifetime. Using Case 3 from table 5.11 as an example, the annual damage fraction for an intact line is 0.00399. Over a planned lifespan of 20

years, this equates to a total damage fraction of 0.0798 (20×0.00399), which is within the safe limit of 0.2. If the floater is expected to be in a broken-line condition for six months of the 20-year life, with a yearly damage fraction of 0.0155, the resultant damage fraction will be 0.08556, which is also within the safe limit. A similar calculation is done for Case 2, which shows a 1201% increase in fatigue in the mooring line, resulting in a total damage fraction of 0.113, which is also deemed safe. Therefore, despite a significant increase in fatigue, the relatively brief duration of the broken-line condition over the entire 20-year design lifetime mitigates the impact of this additional fatigue accumulation. Nevertheless, when designing these systems, this increase in fatigue must be accounted for, ensuring adequate allowances for further fatigue accumulation.

6

Failure probability

Chapter 5 identified multiple failure modes, both new and existing, that contribute to an early failure of the mooring system following a mooring line failure. Regarding new failure modes, simulation-based estimations provided insight into how turbine capsize might become problematic, while the increase in other failure modes may not be as severe.

Relative increases in fatigue for existing failure modes were assessed, showing fatigue increase in both mooring lines and fairleads for selected cases. Mooring line failure is considered in the design of any offshore structure to avoid complete mooring system failure. The oil and gas industry has traditionally adhered to the redundancy of N+1 or even N+2, N signifying the minimal amount of mooring lines, where the system should withstand extreme conditions following a mooring line failure without loss of station keeping.

Though the results are not absolute, particularly regarding fatigue, where a thorough analysis is recommended for definitive conclusions, the influence of all failure modes can be comparatively assessed against the intact case using a fault tree analysis. This approach allows assessment of the cumulative impact of all failure modes compared to the intact case. It shows the sensitivity of these failure modes to the total failure rate, offering a holistic view rather than focusing on the increased failure rate for each individual mode.[27]

6.1. Fault tree analysis

A FTA represents the logical connections between faults and their causes through a directed acyclic graph consisting of two types of nodes: events and gates, presented by figure 3.16. The events are the occurrences within the system, which can be basic or intermediate and are represented through logic gates that demonstrate the process of failure evolution. The logic gates used in the FTA are AND and OR gates. A quantitative analysis will be used by adding new events and altering events using results from chapter 5 to compare the reliability of an intact and broken line mooring system. A qualitative analysis using a cut-set will not yield surprising results, as the system mainly comprises OR gates. Implying that every basic event will result in a failure independently. The probability of a gate's output event depends on the type of the gate as well as input event probabilities. An AND gate represents the intersection of the events attached to the gate. Assuming A, B, and C are three independent events, then the probability of their intersection is just the product of their probabilities.[21] Thus,

$$P(A \text{ AND } B) = P(A \cap B) = P(A) \times P(B)$$

On the other hand, an OR gate corresponds to a set union, and thus the probability of the OR gate output for two and three variables, respectively, is given by:

$$P(A \text{ OR } B) = P(A \cup B) = P(A) + P(B) - P(A \cap B)$$

$$P(A \text{ OR } B \text{ OR } C) = P(A \cup B \cup C) = P(A) + P(B) + P(C) - P(A \cap B) - P(A \cap C) - P(B \cap C) + P(A \cap B \cap C)$$

This thesis's FTA of mooring line failure in FOWTs is based on Mahmood Shafiee's paper on spar buoy FOWT systems failure analysis. The rationale for its relevance to the Tetraspar FOWT is further

elaborated in section 3.4. The failure rates put forth in M. Shafiee's paper, with a translation from hourly to yearly failure rates added, are exhibited in table 6.1.[39]

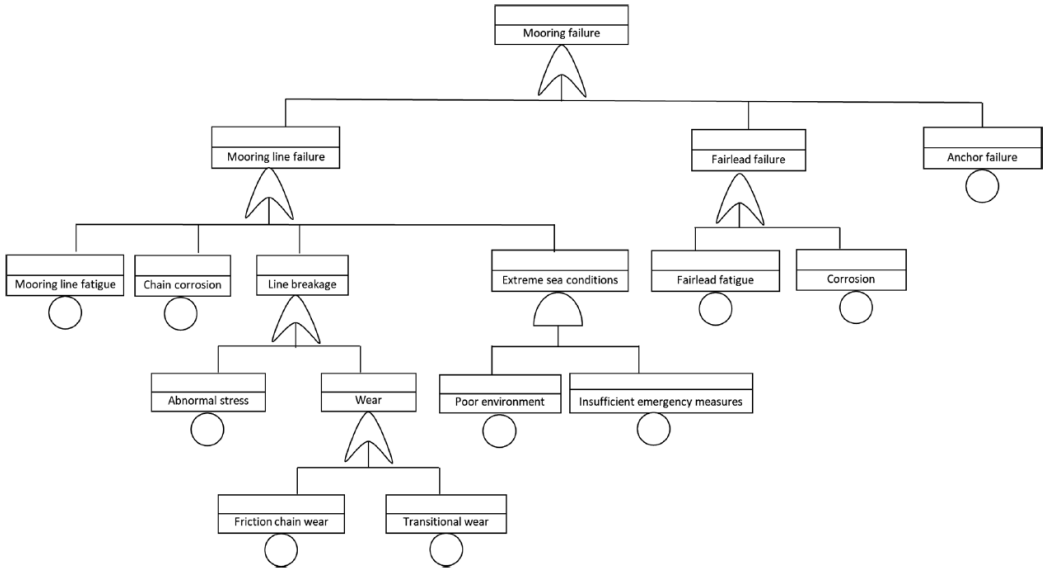

Figure 6.1: Figure 3.17 repeated, fault tree diagram of a spar-buoy mooring system by M. Shafiee[39]

Table 6.1: Table 3.4 repeated, failure rates of the basic events for a mooring system with yearly failure rates added[39]

Basic / intermediate event			**Failure rate** [$^1/_{Hour}$]	**Failure rate** [$^1/_{Year}$]
Mooring line failure	Mooring line fatigue		1.70E-05	0.149
	Chain corrosion		5.38E-06	0.0471
	Mooring lines breakage	Abnormal stress	4.07E-05	0.357
		Friction chain wear	6.93E-06	0.0607
		Transitional chain wear	1.01E-05	0.0885
	Extreme sea conditions	Poor operation environment	7.80E-05	0.683
		Insufficient emergency measures	1.00E-06	0.00876
Fairlead failure	Fairlead fatigue		1.70E-05	0.149
	Corrosion		1.00E-05	0.0876
Anchor failure			1.80E-05	0.158

M. Shafiee's research uses anchor piles for the example FOWT, which differ from the anchors used for the Tetraspar, being DEAs. Due to data limitations, the anchor failure was generalised, not specific to anchor piles. A DEA-specific failure rate would be ideal. However, M. Shafiee's anchor failure rate where adopted as these were general, thus, should not significantly affect the research.

As outlined in section 3.4, M. Shafiee's failure results seem high compared to the statistical mooring line failure rate presented in the Deepstar OTC report. Shafiee's findings suggest 1.1 mooring line failures per year for a three-line system, significantly more than Deepstar's rate of 2.2E–3 per line per year, equating to 6.6E-3 failures annually for a three-line system, a probability 167 times lower than Shafiee's. Despite similar fundamentals between FPUs and FOWTs, the differences can result in varied lifespans, M. Shafiee points out. Such failure rates have yet to be observed. Approximately 50 FOWTs are presently in operation, and there have been no records of mooring line failure, which may suggest a likely overestimation. Given the heavy influence of this input on the final failure rate, the apparent overestimation should be remembered, as a significant difference between the new results and Shafiee's result could influence the sensitivity.

6.2. Fault tree adaptations

Work by M. Shafiee is on mooring line failure for a complete three-leg mooring system. However, as chapter 5 describes, changes to the system due to mooring line failure are expected to impact the system

and alter the mooring system's lifespan. Where 6.1 presents a general three-line system 6.2 presents a Tetraspar mooring system. Not only are there new failure modes due to mooring failure, but also due to the construction of the Tetraspar. One of the assumptions made in section 4 is: that the complete mooring system fails after the second mooring line failure of three line mooring system. Thus, the probability of a second mooring line failure is considered a full system failure resulting in an untethered FOWT without station keeping. However, second mooring line failure may be triggered by failure mechanisms responsible for the first mooring line failure causing consequent failure of other lines, which is further explained in section 6.2.2. As this is represented as a ratio, not a failure probability, this effect is not included in the FTA and will be included after calculating the failure rate.

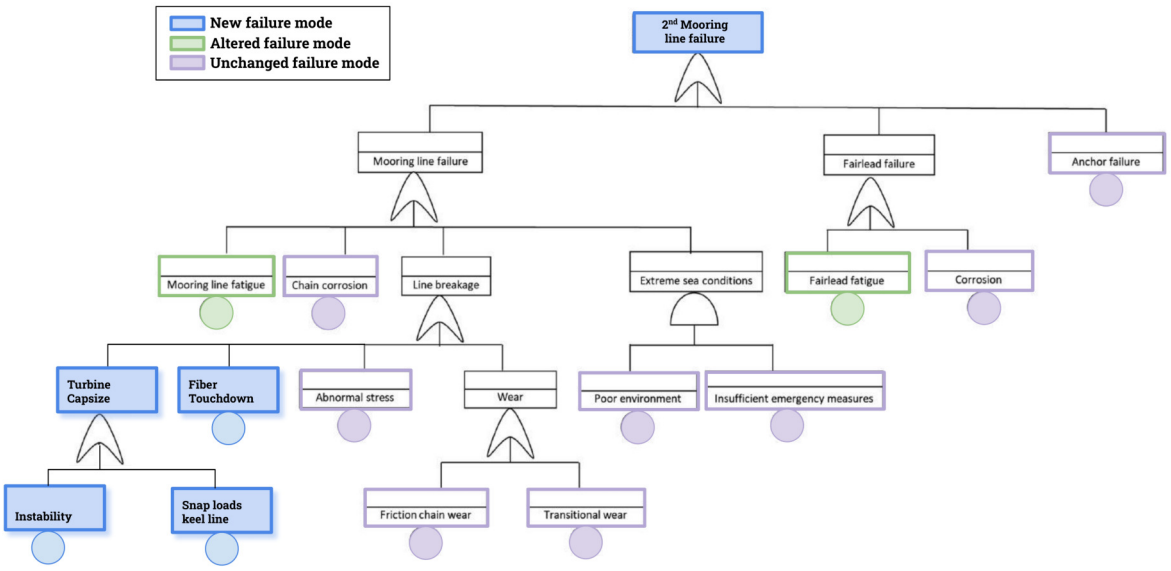

Figure 6.2: Fault tree diagram adjusted to the Tetraspar

Table 6.2: Table 3.4 altered, failure rates of the basic events for a mooring system with bold text indicating changes figure 6.1[39]

Basic / intermediate event			Original Failure rate [$^1/_{Year}$]	Failure rate [$^1/_{Year}$]
Mooring line failure	**Mooring line fatigue**		0.149	**+50%∼+400%**
	Chain corrosion		0.0471	
	Mooring lines breakage	Abnormal stress	0.357	
		Friction chain wear	0.0607	
		Transitional chain wear	0.0885	
		Fiber Touchdown	**0.303**	**0.488**
	Capsize	**Instability**	**0.000**	**0.0999**
		Snap loads	**0.436**	**0.557**
	Extreme sea conditions	Poor operation environment	0.683	
		Insufficient emergency measures	0.00876	
Fairlead failure	**Fairlead fatigue**		0.149	**+50%∼+400%**
	Corrosion		0.0876	
Anchor failure			0.158	

6.2.1. Unchanged failure modes

The altered state due to the first mooring line failure anticipates certain factors to stay unchanged, which have been coloured purple in figure 6.2. The rationale for their consistency is presented below:

- Corrosion: The circumstances remain similar. It is not projected that corrosion on the mooring chain or the fairlead will alter due to mooring line failure.
- Wear: Wear in chain links and transition pieces arises from the friction caused by relative movement, with part load and the movement of relative surfaces being the determining factors. Although the average mooring line load decreases, there may be sporadic peaks that exceed levels seen in intact operation. Periodic motions from second-order movements lead to increased slack and re-tensioning in the chain and transition pieces, thereby increasing relative motions. The wear

resulting from these components is unclear but is likely to be either inconsequential or detectable during a visual inspection and, thus, is not included in this study.

- Extreme Sea Conditions and Abnormal Stress: The forces in the mooring lines are typically borne by one or two lines, so the failure of a mooring line does not trigger an abnormal stress increase compared to an intact line scenario. Even though higher peak forces, caused by second-order movements, are observed in the mooring lines immediately following a mooring line failure, these forces are unlikely to exceed the minimum breaking strength. These peaks typically only occur in moderate weather conditions, not severe ones. Hence, situations involving abnormal stress are not anticipated because of mooring line failure. Given that a mooring line failure does not change the environmental conditions and that existing emergency measures remain effective, along with a lower average force, it is not expected that there will be any changes in extreme sea conditions or that there will be any abnormal stress.
- Anchor failure: Vryhoff's analysis on anchor stability, as discussed in the literature, reveals the anchor's reliable resistance to side loads at diverse angles. The anchor either realigns under tension or resists new tension immovably. These results suggest that the remaining anchors can maintain position post-mooring line failure without threat to platform control. Fatigue is less likely for the anchor, which does not experience periodic force fluctuations due to wave-induced movements, unlike mooring lines or fairleads. Ideally, the anchor only encounters forces during extreme weather, suggesting a different fatigue accumulation pattern than the fairleads or mooring lines. Therefore the failure rate is adopted.

In conclusion, these factors are not expected to significantly change the likelihood of mooring line failure in case of mooring line failure and are left unchanged.

6.2.2. First failure mechanism

Mooring line failure happens most often due to underlying problems which have gone unnoticed during inspection, which would otherwise have been addressed during the yearly repair campaign with a preemptive replacement. The underwater location and challenging marine environment make mooring lines difficult to inspect and maintain. As a result, emerging issues may go undetected until a failure occurs. These underlying and undetected problems may also exist in other mooring lines, potentially triggering a domino effect where the initial failure mechanism induces subsequent mooring line failures, leading to a complete mooring system failure.

Chain mooring systems may fail due to various causes, with fatigue and corrosion being the most prevalent, as shown in section 5.1.2 with figure 5.2.[11] At the same time, synthetic fibres are prone to fail from installation errors or mechanical damage.[41] The Deepstar report revealed that a fifth of single-line mooring failures lead to multiple-line failures shown in figure 6.3a and 6.3b

Multiple-line failure was dominated by steel wire rope (60%) which is rarely seen in FOW and is not present in the Tetraspar. The makeup is instead dominated by chain (13%), polyester rope (synthetic) (7%) and other components 20%. Wire rope is excluded to account for this difference in the mooring line makeup of the research. Beginning an example with an illustrative batch of 500 single-line failures, a 1 to 5 ratio would result in 100 multiple-line failures. Following figure 6.3, 12% is subtracted from the single line failures and 60% from the multiple line failures. This adjustment results in 440 single-line and 40 multiple-line failures, modifying the ratio to 1 to 11. Thus, excluding wire rope alters the multiple-to-single line failure ratio from 1 to 5 to 1 to 11.

However, such a conclusion overlooks the interplay between mooring line components. For instance, incorporating Dyneema could inadvertently weaken other line parts due to its high tension stiffness, generating elevated peak loads elsewhere. While Dyneema may not be the failing part, it could cause failure. Simply eliminating a part is, therefore, a crass conclusion. Hence, the exact ratio of single-line failure to multiple-line failure is estimated to fall between 1 to 5 and 1 to 11, according to research by Deepstar. While our understanding of failure mechanisms has improved, and materials such as Dyneema differ from those discussed in the survey, a range of 1 to 5 and 1 to 11 estimates the ratio between single-line to multiple-line failures, leaving room for refinement.

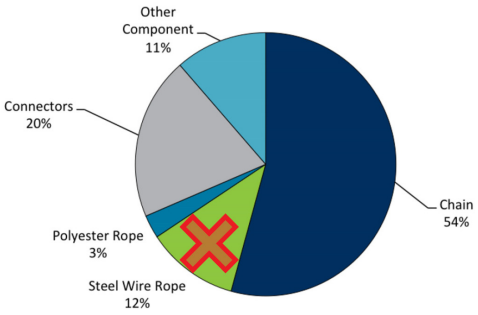

(a) Component types associated with single-line failure events

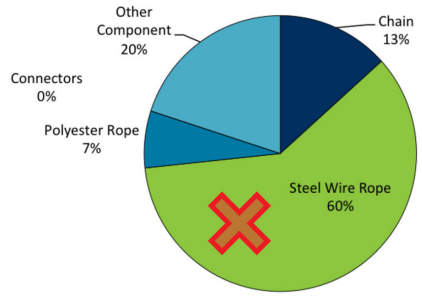

(b) Component types associated with multiple-line failure events

Figure 6.3: Pie charts illustrating the relationship between single and multiple mooring line failures[11]

Three-leg mooring systems have been unusual in the oil and gas industry as redundancy is often necessitated, implying that a backup supports each mooring line (N+1). In such cases, mooring lines are commonly grouped into one point per set, therefore undergoing similar damage accumulation. However, the Tetraspar utilises three lines, each subject to different environmental loads, a factor not considered in the earlier cited research focused on traditional oil and gas setups. While these ratios have been adopted, they may not be directly translatable to FOW scenarios, which could have larger ratios between single-to-multiple line failures. This circumstance would be advantageous and should be remembered.

6.2.3. New failure modes

In comparison to the failure modes shown in figure 6.1 and table 6.1, the newly introduced failure modes-turbine instability, snap loads on the keel suspension lines, and fibre touchdown—have been researched in the prior chapter 5. These can be categorised into two types: those associated with the actual failure event (turbine instability) and those indicative of incident frequency (snap loads on the keel suspension line and fibre touchdown of the mooring line).

The failure rate derived from 'turbine instability' represents the actual failure rate, subject to the credibility of the research. However, 'snap loads keel line' and 'fibre touchdown' merely indicate the frequency of incidents, not whether these incidents will result in a keel suspension line breakage or cause the fairlead of the suspension line to fail, leading to a turbine capsize. Similarly, 'fibre touchdown' does not guarantee a mooring line break but indicates potential for damage due to contact with the seafloor.

Although an increase in these incidents will likely increase the keel suspension line and mooring line failure rates, the exact extent of this correlation is currently unknown. To incorporate the ratio between events and failure, a preliminary estimate of what proportion of snap loads or fibre touchdowns would result in a failure is required, necessitating further investigation to substantiate these assumptions.

Critical questions to be answered include: 'How do the snap loads experienced by the keel lines compare with those in an intact condition?' 'How does this affect the fatigue of the keel suspension line fairleads relative to the intact condition?' 'Could the absolute size of the snap load cause a suspension line break?' 'What would happen if a line snags on a rock or other seafloor object?' These queries underline the necessity for future research.

The probability of snap loads or fibre touchdowns causing a line break has been arbitrarily set at 0.01, or 1%. However, the validity of this figure warrants further investigation. It is also anticipated that snap loads in intact situations will be of lower intensity than those in broken line scenarios, given that tilt, a key factor impacting the severity of snap loads, is increased in the latter. Therefore, a third set has been created where the intact situation carries a lower probability of 0.001 or 0.1%.

Though fibre touchdown has proven possible in intact situations, it is unlikely to result in snagging on rocks or power cable infrastructure causing large issues. This difference between intact and broken situation is because the mooring line's path would initially be cleared of large objects, and a slack mooring line is not typically prone to extensive damage. However, the issue becomes more prominent

in a mooring line failure, as the line will traverse the seafloor. Thus, the bathymetry and seafloor infrastructure can significantly increase the risk, with a snag and subsequent re-tensioning of the mooring line potentially causing damage. Consequently, a third set has also been created for fibre touchdown, where the intact situation carries a lower probability of 0.001 or 0.1%.

Three sets of results have been generated, referred to as S1, S2, and S3, as shown in Table 6.3. These sets are valuable when conducting a sensitivity analysis. When a dash is present in the table, the number immediately to the left of the dash is utilised. By applying the revised FTA from Figure 6.2 and the values from Table 6.2, the cumulative rates of second-line failures and the percentage increase between intact and broken lines is calculated and presented in Table 6.4. These results solely reflect the effects of the previously mentioned three failure modes. The likelihood of the second mooring line failing due to the initial failure mode or the increase in fatigue is not incorporated and will be evaluated in subsequent sections.

Table 6.3: New failure modes sensitivity analysis showing failure rates

	Intact			**Broken**		
	S1 (Sim results)	**S2 (1%)**	**S3 (0.1%)**	**S1 (Sim results)**	**S2 (1%)**	**S3 (0.1%)**
Instability	0	-	-	0.0999	-	-
Snap loads	0.436	4.36E-3	4.36E-4	0.557	5.57E-3	-
Fiber touch	0.303	3.03E-3	3.03E-4	0.488	4.88E-3	-

Table 6.4: Results of new failure modes with the increase in failure rate between intact and broken

	Intact	**Broken**	**Increase**
S1 (Sim results)	1.835	2.241	22.1%
S2 (1%)	1.103	1.206	9.34%
S3 (0.1%)	1.097	1.206	10.0%

Using the FTA and M. Shafiee's data, the base failure rate is calculated as 1.0959 per year. The discrepancy between this rate and that of S3 intact, the most realistic scenario, is a marginal 0.001. This difference is negligible given the magnitude of the outcomes, while two novel failure modes were introduced. Additionally, the increase in failure rate between the intact and broken scenarios is not excessive. Here, the relative scale of M. Shafiee's inputs must be considered, as previously discussed in section 6.1. The outcomes concerning turbine instability, snap loads, and fibre touchdown were independently determined, not representing a proportional increase to M. Shafiee's work. If the scales differ, the total failure rate's sensitivity to the results diminishes. However, this does not necessarily invalidate the findings, although it suggests potential inaccuracies that should be considered when interpreting the results.

6.2.4. Altered failure modes

The fatigue failure modes presented by M. Shafiee will undergo modifications due to mooring line failure. The proportionality concerns identified in the prior section related to M. Shafiee's results will not pose a problem, given that the adjustments will be expressed as a percentage of Shafiee's results, the sensitivity issues relating to the proportion of these results will not pose a problem.

The four cases analysed in section 5.2, derived not from the TetraSpar but the OC4 FOWT, offer a limited perspective on fatigue over the entire lifecycle and across all environmental directions. A comprehensive fatigue analysis, utilising a full QTF or suitable approximation, is strongly recommended for a detailed account of fatigue development in the mooring chain and fairleads. Despite these considerations, the results do indicate an increase in fatigue.

Two scenarios for sensitivity analysis are introduced for the fatigue, a minimal and average case, each representing distinct fatigue levels. By averaging and rounding up the results from the four cases presented in table 5.12, we obtain 400%, serving as our representative average case. A comprehensive

fatigue analysis could yield results that surpass or fall short of the 400%. Nevertheless, the four examined cases provide a preliminary estimate.

Nonetheless, evidence suggests that the TetraSpar may be less prone to second-order low-frequency drift than the structure used in section 5.2. As a result, a 'minimal' case has been developed to reflect a more favourable and realistic scenario for the TetraSpar. Simulations assessing second-order movements for the TetraSpar were inconclusive, owing to the combination of Newman's approximation and the small tubular size of the TetraSpar foundation (as detailed in section 5.2.3). Consequently, an arbitrary lower case representing a potentially more accurate depiction of the TetraSpar situation has been created using a fatigue increase of 50%, as opposed to 400%.

The fairlead and upper portion of the mooring line endure equivalent tension, this tension is translated into stress in the fairlead, yet the stress concentration is amplified at the fairlead in certain excursion cases in broken line condition due to the right-angled geometry of the fairlead as seen in figure 5.20 and outlined in section 5.2.5 on fairlead fatigue. Unless the design considers side loading, stress may concentrate in the joint. In contrast, the stress would be dispersed across the entire fairlead in intact scenarios with mooring forces directed axially into the fairlead. The value of 'm' in equations 5.9 and 5.10 is central in the significant fatigue development. For mooring line fatigue, 'm' equals 3, while for fairlead fatigue, it is either 4 or 5, depending on the stress amplitude. This 'm' decreases the number of cycles to the power of 'm'. A minor stress increment leads to considerable fatigue development, as detailed in section 5.2. The impact will be underestimated if the amplification due to the stress concentration factor is overlooked. Thus, the two scenarios of 50% and 400% will have a tenfold amplification to gauge its influence on the fault tree, emphasising the necessity of efficient stress distribution in the fairlead during broken scenarios.

Table 6.5: Fatigue failure rates adjusted to fatigue increase with values taken from 6.1

	Chain		**Fairlead**		**Fairlead Geometry**	
	Increase	**Failure rate**	**Increase**	**Failure rate**	**Increase**	**Failure rate**
Minimal	50%	0.224	50%	0.224	500%	0.894
Average	400%	0.745	400%	0.745	4000%	6.109

Table 6.6: Results of annual failure rate alterations, as per the modifications outlined in table 6.5, expressed as a percentage increase from the base failure rate

	Chain	**Increase**	**Chain + Fairlead**	**Increase**	**Chain + Fairlead Geometry**	**Increase**
Minimal	1.171	6.85%	1.246	13.7%	1.916	74.8%
Average	1.692	54.4%	2.288	109%	7.651	598%

The effect of fatigue is represented under three categories: 'Chain Fatigue', 'Chain and Fairlead Fatigue', and 'Chain and Fairlead Fatigue', with assumed geometric influence. The percentage increase is evaluated concerning the base failure rate, as found by M. Shafiee's research, which is 1.0959 per year.

6.3. Conclusion

The assumed failure rates for the fairlead and mooring line in M. Shafiee's FTA are identical at 0.149 failures per year. Thus, when accounting for fairlead failure, the failure rate doubles as reflected in Table 6.6. However, factoring in the effect of fairlead geometry heightens the failure rate of the entire structure in the event of a mooring line failure. It is crucial to note that an assumed amplification factor of 10 might not accurately represent the actual value as it largely depends on the fairlead design. However, this is taken to be a plausible estimate in extreme cases. No efforts have been made to accurately determine the fairlead's amplification factor, as FEA simulations can be complex to configure. Due to the nature of these calculations, a minor increase in stress amplitude could precipitate a significant surge in fatigue development, as an increase in stress amplitude is amplified to the power of 3 up to the power of 5, as per equations 5.9 and 5.10. It can be deduced that designing the fairlead to accommodate side loading can lower stress concentrations, thereby significantly enhancing the overall safety of the design. Therefore, a robust design anticipating mooring line failure and the ensuing surge in fatigue development due to drift forces could contribute to a more durable and safer structure.

Notably, a minor increase in failure rate does not necessarily constitute an unsafe design. A temporary increase in failure rate is permissible, provided the rate returns to the initial, acceptable level as outlined in the conclusion of the previous chapter (section 5.2.7). Considering the anticipated future failure accumulation, the design remains safe if the sustained damage does not exceed the safety factor designated for the particular component. In the same section, a basic calculation example is provided for fatigue development in the mooring line, a principle equally applicable to the fairlead.

As highlighted in Section 6.2.2, mooring line failures frequently occur due to undiagnosed underlying issues, potentially triggering a domino effect where subsequent mooring line failures occur for the same reasons. The single-to-multiple line failure ratio varies from 1 to 5 to 1 to 11, reflecting variables such as the component type and the impact of materials on other system parts. This aspect, however, is not incorporated into the FTA as it operates independently from the FTA, possessing a probability rather than a failure rate, which comes into play immediately after the first failure.

In this context, it is again critical to consider the relative scale of M. Shafiee's inputs, as previously discussed in section 6.1, similar to what was done for section 6.2.3 on the FTA for new failure modes. The impact of the probability of 0.200 (1 to 5) or 0.0909 (1 to 11) will significantly differ based on the chosen failure rate. If the annual failure rate for a three-leg floating structure is as low as 6.6E-3, as suggested by Deepstar's research, a probability of 0.200 has a considerably larger relative impact in failure probability.

The fault tree is recalculated to include the new failure modes and altered failure modes. The most plausible combination for new failure modes, S3, is adopted as it considers that not every line touch or snap load leads to failure and recognises the variation between intact and broken conditions. Given that snap loads could be more severe, and fibre parts of the mooring line may be more exposed, S3 is deemed the most appropriate choice for final consideration.

S3 is then merged with both the Minimal and Average case, as the susceptibility of the TetraSpar to second-order mooring force remains uncertain due to simulation uncertainties. Consequently, the annual failure rate during the failed state is anticipated to increase between 31.9% and 137%, as illustrated in table 6.7. Figure 6.4 graphically shows how results for the intact and broken line are combined into the results presented in table 6.7. The steps coloured darker are the end results used, with changed failure modes as a percentage increase from FTA results and new failure modes as a percentage from simulation results.

Table 6.7: combination of likely factors with increase concerning the intact failure rate

	Intact (S3)	**Broken**	**Broken+$^1/_5$**	**Increase**	**Broken+$^1/_{11}$**	**Increase**
Minimal + S3	1.097	1.356	1.556	41.8%	1.447	31.9%
Average + S3	1.097	2.398	2.598	137%	2.488	127%

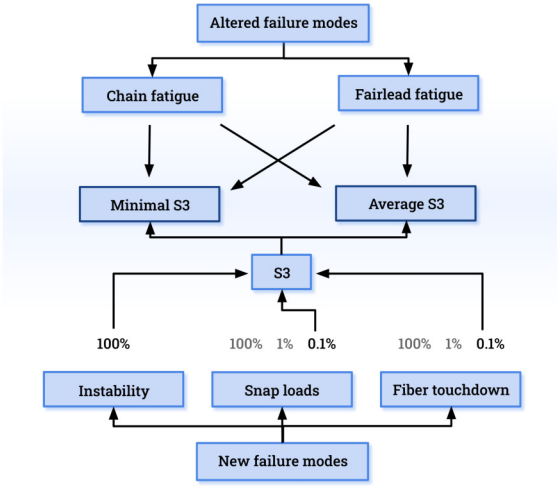

(a) Intact

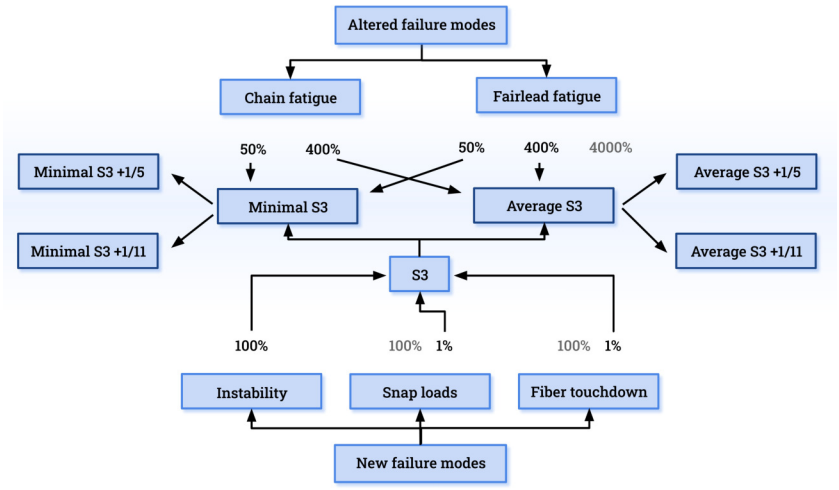

(b) Broken

Figure 6.4: Flow chart of results combination presented in table 6.7, working towards the middle

7

Conclusion

The growing need for renewable energy has inspired innovations such as FOWTs. To control costs and expedite procurement and installation, floating wind developers commonly use fewer mooring lines than is historically seen in the offshore industry. Statistically, mooring line failures can occur annually in large turbine fields, potentially leading to untethered turbines and substantial financial and reputational damages. This research explored whether a single mooring line failure could put the entire mooring system and, therefore, the FOW field at risk and whether the Tetraspar's risks of the mooring system are considered ALARP.

The literature study *identified* that fatigue and corrosion are the primary factors leading to 64% of chain mooring line failures. With chain a key component of most mooring systems, it is also an integral part of the Tetraspar FOWT. Mooring systems significantly influence floating structures' responses to second-order wave loads and other environmental factors like wind and current. The mooring system mitigates large-scale, low-frequency movements from second-order wave drift forces and other environmental influences. Research reveals that a mooring line failure can notably decrease the system's stiffness, facilitating more considerable movements due to low-frequency second-order drift forces. Previously unanticipated issues are introduced for the Tetraspar compared to an intact line.

Simulation-based research has *analysed* failure rates of new failure modes for the Tetraspar, being turbine instability, snap loads in the keel suspension lines, and touchdown of fibre mooring line sections. Compared to the intact mooring line condition, increases of 27.8 % and 61.0% have been observed for snap loads and fibre touchdowns, respectively. This increase is considered small because it represents a yearly probability and will be compared to a longer lifetime in an intact situation. The Tetraspar in a broken line condition is favoured to stay out for six months with an increased probability of failure. At the same time, the Tetraspar, in an intact situation, should endure more than 20 years. A higher failure probability is accepted in a broken-line scenario due to the reduced likelihood of extreme events in the reduced time. However, these results do not reflect the severity of such events, which differs between intact and broken line conditions. For instance, larger pitch angles in a broken line situation could lead to increased snap loads compared to an intact condition. Although snap load probabilities may appear similar, the potential impact of these is not accounted for. Similarly, a fibre touchdown could cause more harm as the mooring line crosses the uncleared seafloor, potentially interacting with power cable infrastructure, tensioning devices, or large rocks, which could damage the mooring line if it becomes snagged. A matter further discussed in the discussion.

Turbine instability, not present in an intact scenario even during 1000-year storms, becomes a significant concern in a broken line condition. Instability in broken line condition can potentially cause a capsize in a one-year storm or less. However, the limit of storm intensity for a capsize remains undetermined and requires more testing with lower environmental intensity. The event's probability, from simulation results, is 0.0999 failures per year, averaged across all mooring lines. The loaded mooring line offsets the turbine's wind-induced tilt in an intact situation. However, a broken line condition compromises this stabilising effect and could exacerbate the tilt (figure 5.6). If the combined environmental forces become too great, the turbine may become unstable and capsize. Contrary to fibre

touchdown and snap loads, the probability of capsizing due to instability is binary: an event implies a complete failure, not a potential one.

There is a strong correlation between the environmental direction in which specific events happen and the failure of a certain mooring line. This relationship is associated either with the wave or a blend of wind and current, as wind and current are taken as collinear. Instability leading to capsizing and fibre touchdown are induced by drift which is mainly driven by a combination of wind and current, while snap loads in the suspension lines are primarily wave-driven. It is, however, anticipated that the severity of snap loads may intensify with an increase in tilt, which is influenced by wind and current conditions.

The increase in movements due to second-order wave drift forces and the lower mooring stiffness leads to a surge in tension amplitude in the mooring lines, resulting in significant fatigue development. This significant increase was evidenced in one particular test case, where a 1200 % increase in fatigue was observed. Surprisingly, second-order motions do not escalate with the intensity of environmental forces but decrease in more intense environmental cases. A 76 % reduction in fatigue was documented for the harshest environmental conditions tested. However, standard operating conditions, characterised by low environmental intensity and high occurrence probability, showed a disproportionately high increase in fatigue development when comparing intact and broken scenarios. This fatigue increase in intensities with high occurrence probability indicates a significant rise in fatigue overall.

The larger tension amplitude in the mooring lines due to second-order motions causes accelerated fatigue at the fairleads, similar to the mooring line. The right-angled joint geometry of the fairleads exacerbates this effect. Implementing a suitable design using gussets can distribute stress and reduce stress concentrations, thus emphasising the need to consider mooring line failure during fairlead design.

Using a FTA, the Tetrapsar's mooring system failure probability of intact and broken lines is *evaluated* comparatively. This approach is based on research by M. Shafiee. The newly introduced and altered failure modes presented are used to determine failure rates. The annual failure rate in the broken line condition is expected to rise compared to the intact state, considering the most plausible combination of new and altered failure modes and other factors. This increase results in between 31.9% and 137% increase in failure rate during broken line condition, as illustrated in table 6.7. It remains challenging to state whether this failure rate is excessive definitively. However, temporary mobile offshore drilling units that stay for 12 months in the same location are designed for a much lower return period, typically 5 to 10 versus 100 years for permanent moorings and have weaker mooring components. This methodology can be applied here, suggesting that an increase in failure rate might be acceptable given the temporary nature of the situation, as long as it does not compromise the safety factor for the rest of the lifespan concerning fatigue accumulation.

Results indicate that even with a 1200% increase in the failure rate, the system might remain within the safety factor. Nevertheless, a comprehensive fatigue analysis should ascertain the actual increase in fatigue in all directions and with all environmental conditions. Even though a system may appear safe, past designs considered to be safe have failed due to fatigue or a combination of other factors. Hence, any increase in fatigue is significant and warrants close and continual monitoring.

Regulatory bodies and governments have yet to crystallise rules regarding mooring line redundancy. Three-leg mooring systems are possible thanks to the lower consequence class of FOW. However, by using the minimum amount of mooring lines and planning repairs during repair campaigns, the design methodology needs to shift to 'design for failure', which does not mean expecting the system to fail but being prepared for when it does. DNV oil and gas standards mandate a minimum single-line failure rate of once every 10,000 years. Despite best efforts, current designs have persistently failed to meet this standard, showing a slow improvement in mooring safety over the years. Given the historical frequency of mooring system failures, designs ought to be equipped to handle such eventualities. The unpredictable nature of mooring line failure and the challenge of monitoring and surveying mean that the initial failure often surprises operators. However, readiness for a potential second mooring line failure is a controllable factor, representing the most considerable step towards a new standard of safety in the industry.

For the Tetraspar in particular, the risk of turbine capsizing is a possibility which was not expected when setting out the research. No simple changes can be made to prepare the system for mooring line failure regarding turbine instability without changing the complete design of the foundation, something

discussed in greater detail in the recommendations. This thesis evaluates if the Tetraspar's mooring system has ALARP risks and will thus be discussed on this topic. However, when considering the structure as a whole, capsize is a serious event which should be avoided at all costs. A capsize of the Tetraspar could entail, next to mooring system failure, damage and consequent foundation flooding due to contact between the keel and the foundation and environmental damage due to glass fibre particles from a collision between the turbine blades and the water. Although not discussed in great detail, environmental damage and a sunken FOWT are of concern. Regulations concerning mooring line redundancy remain undefined by regulatory bodies and governments regarding floating wind. With the lower consequence class for FOW installations compared to oil and gas, it is possible to utilise three-leg mooring systems. Nevertheless, using the minimum number of mooring lines necessitates a shift in design methodology towards 'design for failure'. This approach does not anticipate failure but rather prepares for its eventuality, given the historical precedents of mooring system failures.

The recommendations in the following section suggest adaptations to the mooring system that could improve risk levels to an ALARP level. This research indicates that, through essential modifications, a system may be 'designed for failure,' enabling successful reinstatement without substantial damage or total mooring system loss. This thesis identifies considerations in the design of the TetraSpar, particularly concerning stability, but also offers opportunities for further optimisation and innovation, presenting a promising outlook for three-line mooring systems within the broader FOW landscape.

7.1. Recommendations

The 'ALARP' principle is an iterative process; new findings will expose new risks that must be evaluated and mitigated. This thesis has *identified*, *analysed* and *evaluated* comparatively. The recommendations will introduce *risk reduction* methods and debate if it is *cost-effective*, ultimately completing all the required steps for an 'ALARP' optimisation, considering this conclusion finalizes *documenting*. Five recommendations are suggested for the design phase to ensure the Tetraspar and FOWTs achieve ALARP risk levels considering potential mooring line failure. These recommendations offer solutions that do not necessitate on-site visits, ideally resulting in a system that can endure for six months without intervention. This approach allows for repairs to be conducted during the summer campaign, enabling more cost-effective and safer operations.

7.1.1. Fatigue analysis

A comprehensive fatigue analysis is recommended, incorporating both the mooring line and the fairlead under broken line scenarios. This practice aligns with the offshore structure industry standards for intact line situations but is expanded for broken line scenarios. This change is needed as, contrary to oil and gas, a damaged structure is favoured to wait for repair till the repair campaign in the summer due to the large number of expected failures for a complete FOW field having hundreds of mooring lines and the lower financial and environmental consequences of FOW mooring line failure in comparison to FPUs. Hence, the system must endure increased fatigue due to mooring line loss. Second-order wave drift forces become fundamental in fatigue development and must be accounted for correctly when doing the fatigue analysis.

Fatigue damage accumulation needs to be seen in the light of the total life of the floater, not momentary fatigue, as the failed state would only constitute a marginal part of the total lifetime of the floater. When doing a comprehensive fatigue analysis in intact and failed states, possible fatigue development can be factored into the design, and the mooring system can be designed to stay in the safe zone of the safety factor.

Fairlead fatigue development could exponentially increase when a mooring line is lost, even in comparison to the increased mooring line fatigue. The fairlead should be designed to withstand and efficiently distribute the additional side loads to counteract this fatigue acceleration. By introducing adequate gussets dissipating geometric stress concentration, fatigue could be decreased by improving the joint's load-bearing capacity and reducing the stress concentration, thus enhancing the fatigue performance of the structure.

7.1.2. Fiber section length

In a broken line situation, fibre touchdown could occur on an uncleared seafloor, potentially encountering power cable infrastructure, tensioning devices, or large rocks, which could damage the mooring line if it caught. Mitigation methods include comprehensive seafloor clearance, distancing tensioning devices from chain-Dyneema transition points, routing power cables between anchors, and ensuring power cable anchors do not intersect with potential paths of chain-Dyneema transition points, thereby reducing the risk of Dyneema section snagging and damage. However, a more straightforward and economical solution would be recommended to design the mooring system with a fibre rope length slightly less than the water depth if fibre rope. The TetraSpar has a Dyneema length of 226 meters from the fairlead. With a water depth of 205 meters, a reduction in Dyneema length of 41 meters considering fairlead depth plus an additional safety margin for wave height, tides and surge changes would suffice to prevent fibre touchdown issues. This will improve design safety in broken and intact lines, as shown in table 5.7, but would change the mooring system fundamentally.

7.1.3. Power cable

Although not explored in depth within this thesis, it is recommended to design power cable infrastructure with breakaway points. It is anticipated that the power cable will break due to large excursions, and this process should be managed to prevent widespread damage to the subsea power cable infrastructure. Some floating wind concepts propose interconnected power cables between floaters for cost reduction. However, an independent system is advisable, given the failure statistics of mooring lines. In the event of mooring line failure, a total wind farm string could be lost due to interconnected power cable infrastructure. The consequent power losses could significantly decrease the profits of the wind farm, potentially outweighing the cost benefits of shorter power cables. Using a cost-benefit analysis, the cost of power cable failure can be analysed; damage to subsea infrastructure and possible power loss of a string should be offset by the cost of mitigation measures considering the likelihood of mooring line failure.

7.1.4. Clump weights

The constant movement of clump weights across the seafloor may lead to their breakage as the floater seeks a new equilibrium due to environmental changes. Although it is currently unclear to what extent movement accelerates damage accumulation, an increase can be reasonably assumed. Existing literature suggests the unreliability of half-shell clump weights could lead to the separation of the two halves and subsequent detachment of the clump weight. Increased movement over an uncleared seafloor, with potential obstacles such as rocks and other infrastructure, could accelerate damage and instigate detachment. However, further research is needed to confirm these suspicions. A cost-benefit analysis could serve as helpful to determine if a robust and potentially more expensive design is recommended to mitigate these potential risks.

7.1.5. Instability

The TetraSpar structure, characterised by its relatively broad base, seems to encounter inherent stability issues that could result in capsizing if a mooring line fails. However, these challenges may be addressed by adjusting the mooring line fairleads closer to the centre of flotation, elevating them, or modifying the stability of the TetraSpar itself. Extra care needs to be taken in these aspects to ensure stability after mooring line failure.

Considering the severity and possibility of capsize problems, as demonstrated in this study, extra care needs to be taken in evaluating the situation. Mooring line failures typically occur not because of forces exceeding design limits but due to corrosion, fatigue, or other failure modes. However, these failures often occur during relatively high mooring forces, when environmental forces align with one mooring line under storm conditions. As outlined in this study, if a turbine fails in these circumstances, it may drift through the anchors, leading to instability and potential capsize. The likelihood of capsizing becomes particularly significant during storm conditions, which are anticipated during the first failure. Thus, the study's simulations may underrepresent the risk, as they assume the failure of a single mooring line, irrespective of the simulation of the second line. The possibility of a storm occurring in a direction posing a risk of turbine capsizing is high after the first failure. Also, the likelihood of a storm coinciding with a mooring line failure is higher when assessing the second mooring line failure,

significantly elevating the overall risk of turbine capsizing.

The probability of a storm is also higher for the other new failure modes. However, snap loads only see a small increase in probability, of 27% and were deemed safe in the original design, and fibre touchdown can be easily mitigated by reducing fibre length.

When mooring line failure leads to instability after drifting through the FOWTs anchors, a drastic increase in failure can be expected. It is recommended this is always checked, and minimal safety requirements regarding instability after mooring line failure will be adopted.

7.2. Discussion and Further research

This section presents the necessity for further research in several areas. The intention is to stimulate further studies and improve the understanding of these complex systems promoting more effective design and management of FOWTs in the future.

7.2.1. Acceptance criteria and cost benefit

According to the 'ALARP' method, the final decision hinges on comparing risks against the acceptance criteria and the cost-effectiveness of the recommendations. If the risks are deemed unacceptable, there might be justification for increased expenditure on specific safety measures. Conversely, if a risk mitigation strategy incurs significant costs without yielding a substantial reduction in risk, it may not be deemed beneficial. This thesis, however, did not delve into the specifics of these criteria and the associated costs of the recommendations, which warrants further investigation in future research.

7.2.2. Simulation based results

Most simulation results fall within the one-year return period category, which was unexpected at the simulation's start. One year is the lowest environmental condition tested and was not intended as a stopping point for all cases. Ideally, testing would continue until no events occurred within a specific return period. Hence, the true instability of some events remains undefined. If events occur during a one-year storm, they might also occur during a one-month storm, though this remains speculative. From the simulations conducted, it is evident that certain combinations pose higher event probabilities. These combinations warrant testing under environmental conditions below a one-year storm return period. Therefore, the yearly probability of capsizing could be higher than 0.00999.

7.2.3. Power cable breakaway

As emphasised in the Recommendations, developing strategies for successful disconnection of the power cable in case of excessive drift or high tension from mooring line failure may protect the subsea power cable infrastructure and the Floating Offshore Wind Turbine (FOWT) foundation. Such a method simplifies reconnection following a mooring line failure and guards against damage to entire strings of subsea power cables.

7.2.4. Ratio event and failure

The severity of slack line events differs between intact and broken line conditions, a distinction not captured in these results. Larger pitch angles in a broken line condition could generate higher snap loads than in an intact situation. Therefore, while the probabilities of snap loads are similar in some instances, their impacts have not been considered. Like the mooring line fairleads, the fairleads of the suspension lines must also be designed to withstand failure. Additional research is necessary to assess the magnitude of snap loads on the suspension lines and their fairleads, determine whether these increased loads could cause unacceptable fatigue development, and research the effect of grouping on the ratio between sing-line to multiple-line failures.

7.2.5. FTA failure rate

Research into the validation of failure rates is advised to ensure correct failure rates are used. The relative scale of M. Shafiee FTA results, which serves as the basis for this research, seems high. When a high failure rate is used, other answers will weigh less in the total answer; therefore, results are distorted. Shafiee's findings suggest 1.1 mooring line failures per year for a three-leg system, significantly more than Deepstar's rate of 6.6E-3 failures annually for a three-leg system, a probability 167 times lower than

Shafiee's. Despite similar fundamentals between FPUs and FOWTs, the differences can result in varied lifespans, M. Shafiee points out. Further research is advised to validate this.

7.2.6. RNA heading

The Rotor Nacelle Assembly (RNA) has an off-centre placement relative to the turbine tower centre line. This offset creates variances in capsizing stability, initially considered minor but subsequently tested.

The turbine was tested for stability in Orcaflex in the situation described in figure 5.12b, where the wind was the only environmental factor applied. The wind was not applied as a Torsethaugen spectrum but as a constant and slowly increased till capsize was observed. This has been repeated for the nacelle heading into and from the wind. The wind required to cause a capsize due to wind described in figure 5.12 b required a 4.79 % increase in wind and resulted in an increase of 9.27 % in tilt with respect to vertical. This is a contribution which would be interesting to incorporate in further studies.

The power cable is expected to break early in the failed state, leaving the turbine with a small power reserve to find a desired position for the remaining six months. For stability, it is, therefore, advisable to choose a heading pointing into the direction of the failed mooring line to help stabilise in the direction of the most vulnerable directions, as described in figure 5.7.

7.2.7. Poisson

In the initial stages of the research, the probability of an extreme value's occurrence was represented by using the reciprocal of the return period. However, the Poisson distribution would have been a more suitable representation, as depicted in Equation 7.1. Here, E denotes the reciprocal of the return period, as detailed in Table 7.1. Equation 7.1 calculates the complementary probability that a storm with a return period of R years, or more, occurs within one year. The discrepancy between the two methods is most pronounced for shorter return periods, as illustrated in Figure 7.1. As most findings in this thesis are based on a return period of 1, the actual return period when using the Poisson distribution amounts to 63% of the values mentioned in the conclusion, a factor that favours the risk of the TetraSpar.

$$P = 1 - e^{-E} \tag{7.1}$$

Table 7.1: Comparison reciprocal and poisson of the return period

R (Return Period)	E (Reciprocal)	P (Poisson)
1	1	0.632
2	0.5	0.393
5	0.2	0.181
10	0.1	0.0952
20	0.05	0.0488
50	0.02	0.0198
100	0.01	0.00995
200	0.005	0.00499
500	0.002	0.002
1000	0.001	0.001

7.2.8. Dependence failure modes

Although this FTA model does not address it, if a system fails due to, for example, corrosion, the likelihood of subsequent failures within the following six months tends to increase. This is based on the premise that issues contributing to the first mooring line failure may persist in the remaining lines, as emphasised in the section on the first failure mechanism (Section 6.2.2). This principle applies immediately after the first mooring line failure and for the probability of failures within the ensuing six-month period. The principle is relevant for corrosion and extends to other unchanged and altered failure modes, including fibre touchdown.

However, not all factors will experience an increased failure probability following the initial failure. This variation is mainly dependent on the nature of the original failure. For example, a failure in the first

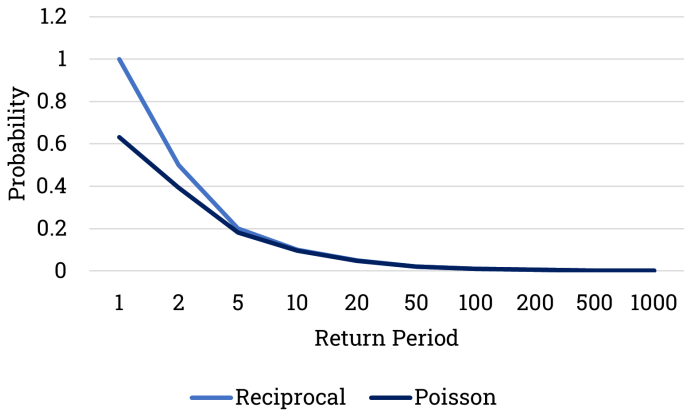

Figure 7.1: Comparison reciprocal and poisson with values from 7.1

mooring line due to fatigue might signal greater-than-anticipated motions, resulting in increased forces on both the mooring and the fairlead. These amplified motions may accelerate wear in transitional pieces and chain links while the risk of corrosion remains unaffected. Similarly, an increase in fairlead corrosion likely signals an increased risk of chain corrosion while leaving other failure modes unaffected.

Quantifying the exact increase in risk due to these dependencies remains challenging. To maintain the model's simplicity, these dependencies have not been integrated. However, their consideration seems worthwhile for future research.

References

[1] Alex Argyros. "Developments in Mooring Integrity Management ". In.

[2] Charles Aubeny. *Geomechanics of marine anchors*. CRC Press, 2017.

[3] Magnus Thorsen Bach-Gansmo et al. "Parametric study of a taut compliant mooring system for a FOWT compared to a catenary mooring". In: *Journal of Marine Science and Engineering* 8.6 (2020), p. 431.

[4] Claude Bathias and André Pineau. *Fatigue of Materials and Structures: Fundamentals*. John Wiley & Sons, 2013.

[5] Elzbieta M Bitner-Gregersen and Alessandro Toffoli. "Uncertainties of wind sea and swell prediction from the Torsethaugen spectrum". In: *International Conference on Offshore Mechanics and Arctic Engineering*. Vol. 43420. 2009, pp. 851–858.

[6] Michael Borg et al. "Technical definition of the tetraspar demonstrator floating wind turbine foundation". In: *Energies* 13.18 (2020), p. 4911.

[7] Lucas HS Carmo and Alexandre N Simos. "On the complementarity of the slender-body and Newman's approximations for difference-frequency second-order wave loads on slender cylinders". In: *Ocean Engineering* 259 (2022), p. 111905.

[8] CR Chaplin, AE Potts, and A Curtis. "Degradation of wire rope mooring lines in SE Asian waters". In: *Offshore Asia Conf., Kuala Lumpur*. 2007.

[9] DNV. "Floating offshore wind: the next five years". In: (Mar. 2022). URL: https://www.dnv.com/focus-areas/floating-offshore-wind/floating-offshore-wind-the-next-five-years.html.

[10] Emma C Edwards et al. "Evolution of floating offshore wind platforms: A review of at-sea devices". In: *Renewable and Sustainable Energy Reviews* 183 (2023), p. 113416.

[11] E. Fontaine et al. "Industry Survey of Past Failures, Pre-emptive Replacements and Reported Degradations for Mooring Systems of Floating Production Units". In: *Day 4 Thu, May 08, 2014* (May 2014). DOI: 10.4043/25273-ms. URL: http://dx.doi.org/10.4043/25273-ms.

[12] Robert B Gordon, Martin G Brown, and Eric M Allen. "Mooring integrity management: a state-of-the-art review". In: *Offshore technology conference*. OnePetro. 2014.

[13] Andrew J Goupee et al. "Additional wind/wave basin testing of the DeepCwind semi-submersible with a performance-matched wind turbine". In: *International Conference on Offshore Mechanics and Arctic Engineering*. Vol. 45547. American Society of Mechanical Engineers. 2014, V09BT09A026.

[14] Manuel Herduin et al. "Abrasion process between a fibre mooring line and a corroded steel element during the transit and commissioning of a marine renewable energy device". In: *Engineering Failure Analysis* 60 (2016), pp. 137–154.

[15] Leo H Holthuijsen. *Waves in oceanic and coastal waters*. Cambridge university press, 2010.

[16] SA Hsu, Eric A Meindl, and David B Gilhousen. "Determining the power-law wind-profile exponent under near-neutral stability conditions at sea". In: *Journal of Applied Meteorology and Climatology* 33.6 (1994), pp. 757–765.

[17] Wei-ting Hsu et al. "Snap loads on mooring lines of a floating offshore wind turbine structure". In: *International Conference on Offshore Mechanics and Arctic Engineering*. Vol. 45530. American Society of Mechanical Engineers. 2014, V09AT09A036.

[18] INNOSEA. *Review of the state of the art of mooring and anchoring designs, technical challenges and identification of relevant DLCs*. Tech. rep. D2.1. Feb. 2020. URL: https://corewind.eu/wp-content/uploads/files/publications/COREWIND-D2.1-Review-of-the-state-of-the-art-of-mooring-and-anchoring-designs.pdf.

[19] J.M.J. Journée and W.W. Massie. *OFFSHORE HYDROMECHANICS*. 1st ed. TU Delft, Jan. 2001. URL: https://ocw.tudelft.nl/wp-content/uploads/Introduction_Offshore_Hydromechanics.pdf.

[20] Ellen Jump. *MOORING AND ANCHORING SYSTEMS - MARKET PROJECTIONS*. Oct. 2021. URL: https://ore.catapult.org.uk/wp-content/uploads/2021/12/PN000413-RPT-003-Rev-2-Mooring-and-Anchoring-Market-Projections_Formatted.pdf.

[21] Jichuan Kang, Liping Sun, and C Guedes Soares. "Fault Tree Analysis of floating offshore wind turbines". In: *Renewable energy* 133 (2019), pp. 1455–1467.

[22] J Knappett et al. "A review of anchor technology for floating renewable energy devices and key design considerations". In: *Frontiers in Offshore Geotechnics III* (May 2015), pp. 887–892. DOI: 10.1201/b18442-127. URL: http://dx.doi.org/10.1201/b18442-127.

[23] Junho Lee and Charles P Aubeny. "Multiline Ring Anchor system for floating offshore wind turbines". In: *Journal of Physics: Conference Series*. Vol. 1452. 1. IOP Publishing. 2020, p. 012036.

[24] Haixiao Liu, Kui Xu, and Yanbing Zhao. "Numerical investigation on the penetration of gravity installed anchors by a coupled Eulerian–Lagrangian approach". In: *Applied Ocean Research* 60 (2016), pp. 94–108.

[25] Erling N Lone et al. "Influence of mean tension on mooring line fatigue life". In: *International Conference on Offshore Mechanics and Arctic Engineering*. Vol. 84324. American Society of Mechanical Engineers. 2020, V02AT02A053.

[26] Kai-Tung Ma et al. *Mooring system engineering for offshore structures*. Gulf Professional Publishing, 2019.

[27] Kai-tung Ma et al. "Mooring Designs for Floating Offshore Wind Turbines Leveraging Experience From the Oil & Gas Industry". In: *International Conference on Offshore Mechanics and Arctic Engineering*. Vol. 85116. American Society of Mechanical Engineers. 2021, V001T01A031.

[28] Ravi K Nalla et al. "On the in vitro fatigue behavior of human dentin: effect of mean stress". In: *Journal of dental research* 83.3 (2004), pp. 211–215.

[29] "Offshore wind in Europe". In: (2019). URL: https://windeurope.org/wp-content/uploads/files/about-wind/statistics/WindEurope-Annual-Offshore-Statistics-2019.pdf.

[30] SENOL OZMUTLU. *HARNESSING OFFSHORE MOORING EXPERIENCE AND ANCHORING TECHNOLOGY FOR THE FLOATING RENEWABLE ENERGY SYSTEMS*.

[31] Qi Pan, Mohammad Youssef Mahfouz, and Frank Lemmer. "Assessment of mooring configurations for the IEA 15MW floating offshore wind turbine". In: *Journal of Physics: Conference Series*. Vol. 2018. 1. IOP Publishing. 2021, p. 012030.

[32] João Pessoa and Nuno Fonseca. "Second-order low-frequency drift motions of a floating body calculated by different approximation methods". In: *Journal of Marine Science and Technology* 20 (2015), pp. 357–372.

[33] C Qiao, AT Myers, and SR Arwade. "Characteristics of hurricane-induced wind, wave, and storm surge maxima along the US Atlantic coast". In: *Renewable Energy* 150 (2020), pp. 712–721.

[34] Mohamed I Ramadan, Stephen D Butt, and Radu Popescu. "Offshore anchor piles under mooring forces: centrifuge modeling". In: *Canadian geotechnical journal* 50.4 (2013), pp. 373–381.

[35] IML Ridge, RE Hobbs, and J Fernandez. "Predicting the torsional response of large mooring chains". In: *Offshore technology conference*. OnePetro. 2006.

[36] Amy Robertson et al. *Definition of the semisubmersible floating system for phase II of OC4*. Tech. rep. National Renewable Energy Lab.(NREL), Golden, CO (United States), 2014.

[37] Alfred Roubos et al. "Partial safety factors for berthing velocity and loads on marine structures". In: *Marine Structures* 58 (2018), pp. 73–91.

[38] T Russell. "Floating Wind: Changing Gear". In: (July 2019). URL: https://www.4coffshore.com/news/floating-wind--changing-gear-nid13899.html.

[39] Mahmood Shafiee. "Failure analysis of spar buoy floating offshore wind turbine systems". In: *Innovative Infrastructure Solutions* 8.1 (2023), p. 28.

[40] American Bureau of Shipping. *SELECTING DESIGN WAVE BY LONG TERM STOCHASTIC METHOD*. Tech. rep. Oct. 2016. URL: https://ww2.eagle.org/content/dam/eagle/rules-and-guides/current/offshore/238_Guidance_Notes_on_Selecting_Design_Wave_by_Long_Term_Stochastic_Method/Long_Term_Design_Wave_GN_e.pdf.

[41] Robert Spong et al. "Mooring integrity issues and lessons learned database-DeepStar® project 20401". In: *Offshore Technology Conference*. OnePetro. 2022.

[42] Jeffrey Thomas et al. "Application of human factors in reducing human error in existing offshore facilities". In: (2002).

[43] Apostolos Tsouvalas. "Underwater noise emission due to offshore pile installation: A review". In: *Energies* 13.12 (2020), p. 3037.

[44] J Tule et al. "Red hawk project polyester soil ingress testing". In: *Offshore Technology Conference*. OnePetro. 2005.

[45] Chenglin Zhang et al. "Effects of mooring line failure on the dynamic responses of a semisubmersible floating offshore wind turbine including gearbox dynamics analysis". In: *Ocean Engineering* 245 (2022), p. 110478.

A

Appendix - Results

The subsequent tables supplement Case 3 illustrated in Table 5.11 from Section 5.2.4. They provide further detail on fatigue accumulation in the mooring chain for the remaining three cases, presenting damage accumulation for both broken-line and intact-line scenarios.

Table A.1: Fatigue accumulation comparison Case 1

	Broken-line	**Intact-line**	**Unit**
F_m	650	975	kN
S_m	37.5	56.3	MPa
ΔF	300	150	kN
ΔT	17.3	8.66	MPa
ΔT_{gerber}	17.4	8.73	MPa
N	92752.9	300342.9	Cycles/year
N_k	20668509.5	163085120.7	Cycles to failure
Damage	0.00449	0.00184	Damage fraction

Table A.2: Fatigue accumulation comparison Case 2

	Broken-line	**Intact-line**	**Unit**
F_m	837.5	950	kN
S_m	48.4	54.9	MPa
ΔF	625	200	kN
ΔT	36.1	11.5	MPa
ΔT_{gerber}	36.3	11.6	MPa
N	128718.4	300342.9	Cycles/year
N_k	2269215.2	68888167.2	Cycles to failure
Damage	0.0567	0.00436	Damage fraction

Table A.3: Fatigue accumulation comparison Case 4

	Broken-line	**Intact-line**	**Unit**
F_m	525	1000	kN
S_m	30.3	57.7	MPa
ΔF	250	200	kN
ΔT	14.4	11.5	MPa
ΔT_{gerber}	14.5	11.6	MPa
N	66391.6	525600.0	Cycles/year
N_k	35851921.4	68712728.7	Cycles to failure
Damage	0.00185	0.00765	Damage fraction